Binary Chromophore Electro-Optic Materials: Synthesis and Optical Characterizations

賈, 越

https://doi.org/10.15017/1398547

出版情報：九州大学, 2013, 博士（工学）, 課程博士
バージョン：
権利関係：全文ファイル公表済

Binary Chromophore Electro-Optic Materials: Synthesis and Optical Characterization

Yue Jia

Institute for Materials Chemistry and Engineering

Kyushu University

2013

Abstract

Polymeric Electro-Optic (EO) materials incorporating nonlinear optical (NLO) chromophores have shown a commercial potential as the active media in high-speed broadband waveguides for optical switches, optical sensors, and information processors. The most striking advantage of poled polymers results from their unique EO mechanism, unlike inorganic ferroelectric crystals, where the EO response is dominated by acoustic-phonon and optical-phonon contributions, the EO effect in poled polymers arises mainly from electronic excitations in individual nonlinear molecules and molecular units. This thesis discusses the design, synthesis and characterization of polymer matrix that simultaneously exhibit azobenzene substitutes. The synthesized polymer matrix containing three different classification, azobenzene dyes side chain polymers, poly(2-(2-bromoisobutyryloxy)ethyl methacrylate) (PBIEM) cylindrical polymer brushes, norbornene dicarboximide (NDI) cylindrical polymer brushes. These polymer matrixes' applications have been shown in binary chromophore systems which represent a very promising class of organic second-order nonlinear optical materials. Finally, EO coefficient have been measured with different guest chromophores with Teng-Man measurement at 1310nm.

Key words: organic electro-optic material, polymer matrix, polymer brush, electro-optic coefficient

Contents

Chapter 1 General Introduction

1.1 Application of EO materials

1.1.1 Background

Operation of polymeric electro-optic (EO) modulator frequencies of greater than 100 GHz has been demonstrated. The total insertion loss of polymeric EO modulators has been reduced to values as low as 5dB, which is much lower than inorganic EO materials. Polymeric EO modulators can be operated for long periods of time at temperature on the order of 100 ^{o}C. Techniques have been developed for integrating polymeric EO circuitry with passive low loss optical circuitry and with very large scale integration semiconductor electronics. These advances have created a considerable interest in the commercialization of polymeric EO materials. Polymeric EO materials are now being evaluated for applications such as phased array radar, satellite and fiber telecommunications, backplane interconnects for high speed computers, spatial light modulators [1]. The large second order nonlinear susceptibilities of the organic molecules and molecular units arise principally from π-electron conjugated systems substituted by electron donor and acceptor groups. The most striking advantage of poled polymers results from their unique EO mechanism. Unlike inorganic ferroelectric crystals, where the EO response is dominated by acoustic-phonon and optical-phonon contributions, the EO effect in poled polymers arises mainly from

electronic excitations in individual nonlinear molecules and molecular units [2]. As a result, the poled polymers exhibit relatively large EO coefficients of 10-40 pm/V [3], with little dispersion from dc to optical frequencies, and 18-40 GHz optical intensity modulators have been demonstrated using the poled polymers [4][5].

Nonlinear optical effect belongs to glare optics research, derived from molecular nonlinear polarization from optical beam irradiation [6][7]. When an external forcing field is applied to a material, it causes a displacement of the charges in molecules and atoms. In case of a low-intensity field, this induced polarization (P) is linearly proportional to the field strength (E). However, under sufficiently intense fields, the relationship is no longer linear, and the polarization can be expressed as a power series expansion. Thus, the molecular polarization p can be written as [8]:

$$p = \alpha E + \beta EE + \gamma EEE + \cdots , \qquad \text{(Eq . 1-1)}$$

where α is the molecular polarizability, whereas β, γ, and so forth are the molecular hyperpolarizabilities of the first order, second order, and so forth, corresponding to second-, third-, and higher- order nonlinearities, respectively. On a macroscopic scale, the polarizability can be expressed as:

$$p = \chi^{(1)}E + \chi^{(2)}EE + \chi^{(3)}EEE + \cdots , \qquad \text{(Eq . 1-2)}$$

where χ^{s} are the macroscopic susceptibilities.

EO activity can be thought of as control of the index of refraction of a material by application of a finite dc or ac voltage. As the refractive index relates with the speed of the light transiting a material, EO activity can be defined as a voltage-controlled

phase shift of light. Therefore, the application of an electric field will cause a change in the charge distribution of the material and thus, alter the speed of light propagating through the material. If all chromophores are pointing in the direction of the applied field, then the effect of individual chromophores will simply be additive and the electro-optic activity of the material is given by

$$r_{33} = \frac{2N\beta f(\omega)\langle \cos^3\theta \rangle}{n^4} \qquad \text{(Eq . 1-3)}$$

where N is the chromophore number density, $f(\omega)$ is the local optical field correction factor from the dielectric nature of the environment surrounding the chromophore, n is the refractive, and $<cos^3\theta>$ is the order parameter. Therefore, to achieve the maximum EO activity, the product $<cos^3\theta>N$ has to be optimized. Unfortunately, due to strong interchromophores electrostatic interactions N and $<cos^3\theta>$ are not independent [9]. As the density of the highly dipolar chromophores increases, the average distance between them decreases and strong dipole-dipole interactions begin to compete with ordering forces such as the poling filed [10][11][12]. Great progress has been made in enhancing r_{33} through the use of coupled quantum and statistical mechanical modeling to guide the improvement of both β and $<cos^3\theta>N$ [13].

1.1.2 Application

In optical application, 10GHz bandwidth have been widely used, 40GHz bandwidth also been induced. This research have been enlarged to 80, 100, even

160GHz. Based on these advances, several devices incorporating polymeric EO materials have been made for different types of applications, including electrical to optical signal generation, optical beam steering, backplane interconnections for high-speed personal computers, or wavelength division multiplexing. Among all these devices, EO modulators play a fundamental role in many growing areas of broadband telecommunication and to increase the diffusion of multimedia services such as high-quality cable television, telephone, real-time videoconferencing, telemedicine, distance learning, video-on-demand, and ultra-fast internet.

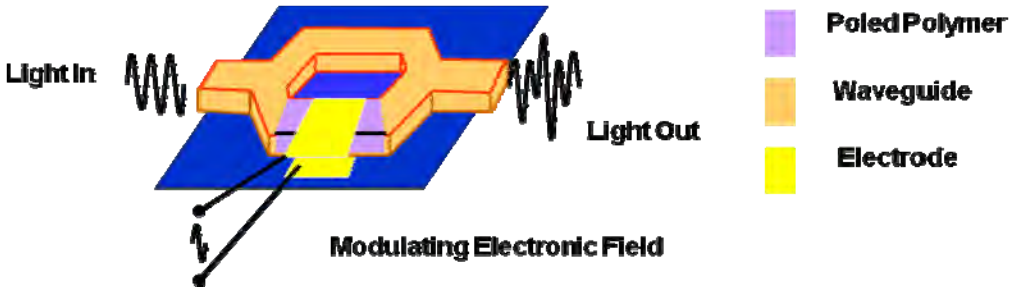

Fig. 1-1 Schematic representation of a MZ modulator

The Mach-Zehnder (MZ) interferometer, which acts as an electrical to optical switch (Fig. 1-1) is a simple device, configuration for light modulation based on a second-order NLO phenomenon.

If no electric field is applied, the input light is split into two beams propagating in separated arms of the MZ modulator to then recombine at the end of Y-junction ("on"-position). By applying an electric field of a proper intensity to one arm, the refractive index of this channel will change, resulting in a phase retardation of π relative

to the signal traversing the order arm and thus to destructive interference ("off"-position). Using this principle, the MZ modulator can transduce the applied electrical signal onto the optical beam as an amplitude modulation.

The phase retardation of light transiting a material to which an electric field has been applied is given by Equation 1.4, where n is the material refractive index, r is its EO coefficient, L is the propagation length, E is the strength of the applied electric field, and λ is the operation wavelength.

$$\Delta\varphi = \frac{\pi n^3 rLE}{\lambda} \qquad \text{(Eq . 1-4)}$$

The minimum voltage required for a π-phase shift, called half-wave voltage Vπ, can be expressed as:

$$V\pi = \frac{\lambda h}{n^3 rL\Gamma} \qquad \text{(Eq . 1-5)}$$

where h is the electrode spacing and Γ is the overlap integral of the electrical and optical wave.

1.2 Material requirements — chromophore design

Generally EO materials can be considered as dipolar chromophores non-centrosymmetrically aligned in poled polymers. The chromophore has an electron donor coupled to an electron acceptor through a π-electron bride. Therefore, the most intuitive way of achieving a bulky EO response is by optimizing the molecular first hyperpolarizability β of the active component. For organic molecules, β is generally

determined in solution, using methods such as electric field-induced second harmonic generation or hyper-Rayleigh scattering. For a chromophore to be useful for EO applications, it must not exhibit significant optical absorption at anticipated operating wavelengths, and chromophores must be thermally robust enough to withstand temperatures encountered in electric field poling and subsequent processing of EO materials [14].

1.3 Material requirements — polymer matrix design

1.3.1 Guest-Host systems

The first investigated EO systems are the guest-host systems, because they can be easily obtained by simply dissolving an EO chromophore in a compatible amorphous polymeric matrix, to form a solid solution. The advantages of polymer host should have a good optical transparency, high thermal stability, easy controllability of chromophore, and good solubility in spin-casting solvents. Dalton group put high μβ CLD chromophore in PMMA get a kind of guest-host material. They measured this material, the result showed when chromophore loading density getting to 30 wt%, the EO coefficient catched the maximum 85 pm/V, optical loss only showed 0.8 dB/cm [15]. In order to obtain a high EO response, the chromophore should be able to dissolve in the polymer matrix at high loadings, without phase separation to occur.

1.3.2 Side-Chain systems

In the side-chain polymers, which is different from that for guest-host systems, chromophores are covalently attached to the polymer backbone on one side. These systems have the advantage that high chromophore loadings (and therefore, high NLO responses) can be obtained, without phase separation, crystallization, or chromophore sublimation. In general, the glass transition temperatures of side-chain polymers are considerably higher than of a guest-host system with comparable chromophore loading, no plasticization effect occurs [16]. Therefore, an improved thermal and temporal stability of the poled order is observed, because the chromophore rotational freedom is restricted by the chemical connection to the polymer. Many kinds of NLO chromophore functionalized polymers have been investigated, including polymethacrylates, polystyrenes, polyethers, and polyamides [17][18].

1.3.3 Main-Chain systems

In the main-chain polymer systems, in which the chromophores are chemically incorporated in the polymer backbone itself, rather than being attached as pendant groups. The main difference between the main-chain and the side-chain approach is that large segmental motion of the polymer backbone is needed for poling and relaxation [19]. Main-chain NOL polymers can be divided into three categories: ⑴ head-to-tail [20]; ⑵ random [21], where the chromophore dipole moments are pointing along the polymer backbone; ⑶ accordion polymers [22], where the dipole

moments are nearly perpendicular to the main chain.

Sreekumar etc. induced chromophore to chiral polyester main chain, and final got chiral structure main chain EO materials. All the polymers have Tg higher than 100 ^{o}C, SHG efficiency is between 0.35-1.22, and β is (2.72-21.7)×10^{-30}esu. A wide variety of main-chain chromophoric polymers have been investigated, with the purpose of improving processability, thermal stability, and alignment stability, including polyurethanes [23], polyimides [24], polyamides [25], carbazoles [26], and polyesters [27]. Most main-chain polymers show relatively poor processabilities or low NLO responses and the choice of the chromophores suitable for main-chain incorporation is limited and high loadings are difficult to achieve.

1.3.4 Dendritic systems

Dalton and Jen et al have prepared various series of NLO dendrimers and dendronized polymers, and their work confirmed that the dendritic structure is a very promising molecular topology for the next generation of highly efficient NLO materials [28][29]. Other groups also have synthesized some NLO dendrimers with good performance successesfully [30][31]. In Zhen Li's group, NLO hyperbranched polymers and dendrimers, prepared through click chemistry, showed that the triazole rings formed in the click chemistry reaction could act as suitable isolation groups to boost the NLO effects of the resultant polymer as high as possible. Accompanied by the increasing of loading density of the chromophore moieties in NLO dendrimers,

the tested NLO effects were going higher, indicating that the frequently observed asymptotic dependence of EO activity on chromophore number density may be overcome through rational design [32].

1.3.5 Binary chromophore systems

From the summary above, the poled polymers may be grouped into two systems: ⑴ guest-host systems, where the nonlinear optical organic molecules (guests) are dissolved in a polymer host; ⑵ substituted systems, where the organic molecular units are covalently bound to a polymer backbone. Binary chromophore systems originate from combining the last two system, using the substituted systems as host and mixing in guest host system with other chromophore. Binary chromophore systems represent a new and very promising class of organic second-order nonlinear optical (electro-optic) materials [33], where favorable intermolecular electrostatic interactions lead to significantly enhanced electro-optic coefficients and other favorable physical properties such as low optical loss and high stability.

1.4 Teng-Man method — method for characterizing of EO activity

Single-beam reflection ellipsometry which is called Teng-Man method [34][35] is a simple and efficient method to characterization of the relevant bulk material EO coefficients r_{33}. Fig. 1-2 shows the schematic of a modified Teng-Man method [36].

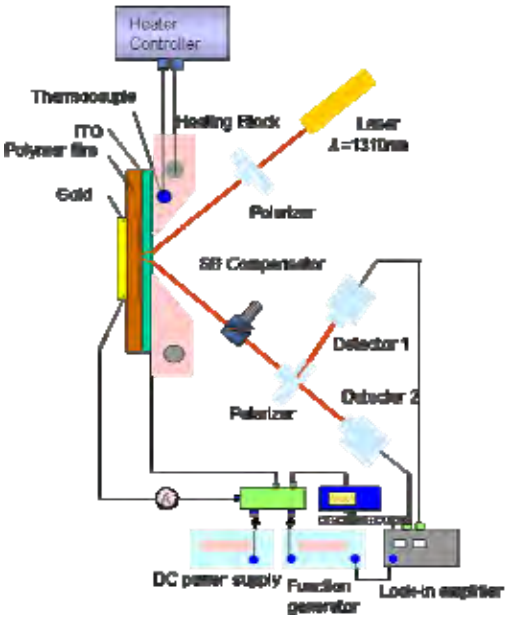

Fig. 1-2 The modified reflection ellipsometry (Teng-man method)

In this experimental real-time measurement during the poling process can be obtained. In this system, temperature and electric poling are controllable, and the resulting current flow and r_{33} are recorded. Poling is the alignment of NLO chromophore under electric field from random orientation to acentric symmetry through heating the stage to the material glass transition temperature (Tg) [37]. Such a system enable us to precisely control the temperature and poling voltage to optimize the r_{33}, on the other hand, it also provide detail information which macroscopically reflects the alignment of chromophore [38].

The formula for r_{33} is obtained according the equation as follow:

$$r_{33} = \left(\frac{3\lambda}{4\pi n^2}\right)\frac{\mathrm{Im}}{IcVm}\frac{\left(n^2-\sin^2\theta\right)^{\frac{1}{2}}}{\sin^2\theta} \qquad \text{(Eq . 1-6)}$$

where θ, n and Vm are the incident angle of laser, refractive index at 1310nm, and AC electric modulation field respectively. Im is the amplitude of modulation, Ic is the

half intensity point.

It is convenient to evaluate r_{33} during the poling process through Teng-Man method and it is useful to confirm that a sample has been poled.

1.5 Aim and scope of this study

The aim of the research presented in this thesis is to exploit high r_{33} EO materials through synthesis a serious of polymer matrixes, then utilized as host in EO materials to find the best matches during application.

One of the simplest and most practically amenable EO polymer approaches for device fabrication is the guest-host, as it is chemically simple and easy to scale. In this approach a high molecular hyperpolarizability chromophore serves as the active guest, this is mixed in intimately with a passive host polymer with a high glass transition temperature (Tg). When an optimum chromophore loading is found, the EO coefficient is greatly amplified by the polymer medium. An alternative approach, which can avoid this limitation is the side chain-type EO polymer. Here a chromophore molecule is modified and attached directly to a passive polymer backbone. An attractive means of avoiding such problems is to change the design of the polymer host, thus enabling higher chromophore loading and little aggregation in host-guest systems. In the rational design of an alternative polymer host we must prepare a material with a high chromophore miscibility, good optical transparency, thermal stability, and a suitable Tg for the poling process.

This paper contains six chapters. The first chapter is "General introduction". The second to the fifth chapter are elaborated different kinds of polymer matrix attached pigments in the backbone. The sixth chapter is "General Conclusion".

In **Chapter 2**, free radical polymerization will be utilized in preparing side chain polymer containing pigment in the side chain, then these polymer will be used in host-guest system to form binary chromophore EO materials to measure EO coefficients. After these free radical polymerization to make side chain polymer, optimization synthesis route will be proposed, Reversible Addition Fragmentation Chain Transfer Polymerization (RAFT) will be applied during synthesizing to control the polydispersity (PDI) and molecular weight (Mw).

In **Chapter 3**, a cylindrical polymer brush will be synthesized in this part, atom transfer radical polymerization (ATRP) will be selected during synthesizing polymer brush. First macro initiators $PBIFM_{450}$ will be made from 2-(trimethylsilyloxy)ethyl 2-oxopropanoate (HEMA-TMS), then use this macro initiator to prepare polymer brush, N,N,N′,N″,N″-pentamethyldiethylenetriamine (PMDETA) as ligand, CuBr as catalyst. EO coefficients of these polymer brushes accomplished guest FTC chromophore will be detected.

In **Chapter 4**, to enhance the polymer brush physical properties, a rigid macro initiator will be selected and synthesized from N-phenol-norbornene-5,6-dicarboximide. Then use this macro initiator to prepare norbornene-dicarboximide derived polymer brush capable of both ROMP and ATRP. Measurement of the r_{33}

polymer brush and FTC chromophores **C2**, **C3**, **C4** will use in-situ poling *via* the Teng-Man reflection technique.

In **Chapter 5**, to investigate the application of the polymer brush using in EO materials, twelve polymer brushes containing three different pendent azobenzene moieties were prepared and employed in EO materials. We will change the substituent of this moiety to include three different groups, methoxy, cyano and nitro. The refractive index of the materials was measured at both 1310 and 1550 nm with a view to their utilization in current EO waveguide applications. Polymer brush will mix with FTC chromophore in cyclopentanone solvent to make films to measure r_{33}.

In **Chapter 6**, a summary of this thesis including some prospects for future research topics will be introduced.

1.6 References

[1] L. R. Dalton. *J*. Advances in Polymer Science. 158 (2002).

[2] Y. Shuto, M. Amano, T. Kaino. *J*. Jpn. J. Appl. Phys. 30 (1991) 320.

[3] E.V. Tomme, P. P. V. Daele, R. G. Baets, P. E. Lagasse. *J*. IEEE J. Quantum Electron. QE-27 (1991) 778.

[4] D. G. Girton, S. L. Kwiatkowski, G. F. Lipscomb, R. S. Lytel. *J*. Appl. Phys. Lett. 58 (1991) 1730.

[5] W. Wang, D. Chen, H. Fetterman, Y. Shi, W. H. Steier, L. R. Dalton. *J*. Appl. Phys. Lett. 65 (1994) 929.

[6] P. N. Prasad and D. J. Williams. Introduction to nonlinear optical Effects in Molecules and polymers. John Wiley & Sons, Inc. New York. 2010.

[7] R. W. Boyd. Nonlinear Optics. Academic Press. San Diego, CA. 1992.

[8] M.Faccini, D. N. Reinhoudt, W. Verboom. Photochemistry and Photophysics of

Polymer Materials. 2010 John Wiley & Sons, Inc.

[9] L. R. Dalton, P. A. Sullivan, D. H. Bale. *J*. Chem. Rev. 110 (2010) 25-55.

[10] L. R. Dalton, A. W. Harper, B. H. Robinson. *J*. Proc. Natl. Acad. Sci. U.S.A. 94 (1997) 4842.

[11] B. H. Robinson, L. R. Dalton. *J*. Phys. Chem. A 104 (2000) 4785.

[12] L. R. Dalton, B. H. Robinson, A. K. Y. Jen, W. H. Steier, R. Neilsen. *J*. Opt. Mater. 21 (2003) 19.

[13] P. A. Sullivan, H. Rommel, Y. Liao, B. C. Olbricht, A. J. P. Akelaitis, K. A. Firestone, J. W. Kang, etc. *J*. Am. Chem. Soc. 129 (2007) 7523.

[14] C. A. Barrios, M. Lipson. *J*. Optics Express. 13 (2005) 10092-10101.

[15] Y. Shi, C. Zhang, H. Zhang, J. H. Bechtel, L. R. Dalton, B. H. Robinson, W. H. Steier. *J*. Science. 288 (2000) 199.

[16] C. Samyn, T. Verbiest, and A. Persoons. Macromol. Rapid Commum. 21 (2010) 1-15.

[17] F. Kajzar, K. S. Lee, and A. K. Y. Jen. *J*. Adv. Polym. Sci. 161 (2003) 1-85.

[18] C. C. Chang, C. P. Chen, C. C. Chou, W. J. Kuo, and R. J. Jeng. *J*. Macromol. Sci. Polym. Rev. 45 (2005) 125-170.

[19] M. E. Wright, S. Mullick, H. S. Lackritz, and L. Y. Liu. *J*. Macromolecules. 27 (1994) 3009-3015.

[20] F. Fuso, A. B. Padias, and H. K. HallJr. *J*. Macromolecules. 24 (1991) 1710-1713.

[21] C. Xu, B. Wu, L. R. Dalton, P. M. Ranon, Y. Shi, W. H. Steier. *J*. Macromolecules. 25 (1992) 6716-6718.

[22] G. A. lindsay, J. D. Stenger-Smith, R. A. Henry, J. M. Hoover, R. A. Nissan, K. J. Wynne. *J*. Macromolecules. 25 (1992) 6075-6077.

[23] Z. Li, S. Dong, G. Yu, Z. Li, Y. Liu, C. Ye, J. Qin. *J*. Polymer. 48 (2007) 5520-5529.

[24] N. Tsutsumi, M. Morishima, W.Sakai. *J*. Macromolecules. 31 (1998) 7764-7769.

[25] M. Dobler, C. Weder, O. Ahumada, P. Neuenschwander, U. W. Suter, S. Follonier, C. Bosshard, P. Gunter. *J*. Macromolecules. 29 (1996) 1569-1573.

[26] G. Sheeren, A. Persoons, H. Bolink, M. heylen, M. Vanbeylen, C. Samyn. *J*. Eur. Polym. 29 (1993) 981-986.

[27] F. Kajzar, K. S. Lee, and A. K. Y. Jen. *J*. Adv. Polym. Sci. 161 (2003) 1-85.

[28] J. M. J. Frechet. Proc. Natl. Acad. Sci. U. S. A. 99 (2002) 4782-4787.

[29] M. J. Cho, D. H. Choia, P. A. Sullivan, A. J.-P. Akelaitis, L. R. Dalton. *J*. Prog. Polym. Sci. 33 (2008) 1013-1058.

[30] J. D. Luo, S. Liu, M. Haller, L. Liu, H. Ma, A. K.-Y. Jen. *J*. Adv. Mater. 14 (2002) 1763-1768.

[31] Y. Okuno, S. Yokoyama, S. Mashiko. *J*. Phys. Chem. B 105 (2001) 2163-2169.

[32] Z. Li, Q. Zeng, G. Yu, Z. Li, C. Ye, Y. Liu, J. Qin. *J*. Macromol. Rapid Commum. 29 (2008) 136-141.

[33] Y. V. Pereverzev, K. N. Gunnerson, O. V. Prezhdo, P. A. Sullivan, Y. Liao, B. C. Olbricht, A. J. P. Akelaitis, A. K.-Y. Jen, L. R. Dalton. *J*. J. Phys. Chem. C. 112 (2008) 4355-4363.

[34] C. C. Teng, H. T. Man. *J*. Appl. Phys. Lett. 56 (1990) 1734.

[35] J. S. Schildkraut. *J*. Appl. Opt. 29 (1900) 2839.

[36] Y. Shuto, M. Amano. *J*. Appl. Phys. Lett. 77 (1995) 4632-4638.

[37] C. A. Walsh, D. M. Burland, V. Y. Lee, R. D. Miller, B. A. Smith, R. J. Tweig. *J*. Macromolecules. 39 (2006) 7566.

[38] X. Piao, Y. Mori, X, Zhang, S. Inoue, S. Yokoyama. *J*. Proc. of SPIE. 7599 (2010) 75990G-1.

Chapter 2 Synthesis Azobenzene Side-Chain Electro-Optic Polymer Hosts and Optimize These Polymer Hosts via RAFT

2.1 Introduction

Development of organic electro-optic (EO) materials has attracted extensively interest, due to the advantaged properties easily processing and low power consumption in device etc, which is superior to conventional inorganic materials [1][2]. There is a growing momentum for developing ultrahigh speed, energy saving optical modulators using EO polymers. The production of devices based on high performance materials is also being researched. The EO polymer technology would bring significant benefits to existing technologies.

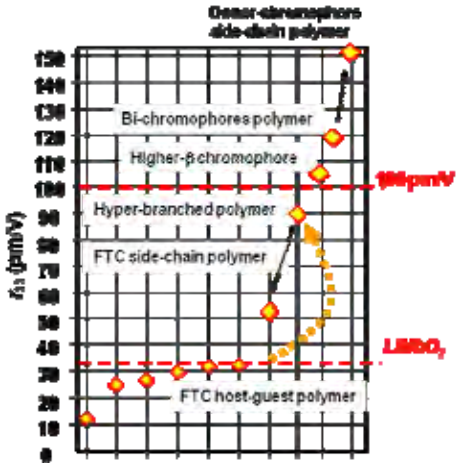

Fig. 2-1 Comparison between EO polymers developed by the author and LN in EO characteristics

The development of EO materials significantly not only depends on the designing and synthesis of high performance nonlinear optics (NLO) chromophore but also depends on the exploiting and synthesis of stable and special polymer matrix during poling [3]. Compares EO coefficients for lithium niobate (LN), which is practical used in modulators for optical communication, and EO polymers, which are being developed by the author, in EO characteristics.

At present, the most commonly applied model of EO polymers for devices is the guest-host system. In this chapter, we synthesized various kinds of side chain polymers host containing azobenzene pigments as suspended substitutional group used in binary chromophore system to enhance the EO coefficients then used for the application of EO devices.

By introducing large group azobenzene pigments can increase the interaction between intramolecular and intermolecular at the same time improve Tg of the polymer. It has been shown that the relaxation time of NLO chromophores is strongly related to the Tg of the polymer matrix. Increasing the Tg results in an improved poled-order stability and the temperature window at which the relaxation is much retarded will be expanded to a large extent. In guest-host NLO polymeric materials, the dipolar NLO chromophores loading level beyond which the poling-induced polar order considerably decreases due to the strong intermolecular electrostatic interactions. Thus, the research efforts have been focused on increasing the chromophore loading density, and at the same time maintaining the high poling efficiency. The target is to

increase the chromophore loading density without causing electrostatic effect, and eventually to enhance the electro-optic properties for the EO device application.

2.2 Experimental details

2.2.1 Materials

p-Nitroaniline, 4-cyanoaniline, 4-methoxyaniline, 2-(N-ethylanilino) ethanol, methacrrloyl chloride (stabilized with MEHQ) were bought from Tokyo Chemical Industry Co., LTD and used without further purification. Monomer methylmethacrylate (MMA) was distilled under reduced pressure on 40 ^{o}C with drier CaH_2. Triethylamine was dried by KOH. Methylene chloride, Anhydrous dioxane, anhydrous toluene, hexane, methanol, cyclopentanone, ethanol were commercialized solvents and used as received. 2-cyano-2-propyl dodecyl trithiocarbonate (97%, Aldrich), 2,2′ -azobis-isobutyronitrile (AIBN, 99%, Aldrich), sodium nitrite, and hydrochloride were bought from Kanto Chemical Co., INC.

2.2.2 Measurements

Thermogravametric analysis (TGA) and differential scanning calorimetry (DSC) were performed using an SII-TG/DTA 6200 instrument under a nitrogen atmosphere at a heating rate of 5 °C /min. DSC was performed using a SII-DSC 6220 under a nitrogen atmosphere at a heating rate of 5 °C /min. The molecular weights (Mw) and

polydispersity (PDI) of the polymers were determined by size-exclusion chromatography (SEC) using a Shodex GPC K-804L column on a JASCO LC2000 liquid chromatography system with $CHCl_3$ as the eluent. This system was calibrated using a narrow PDI Shodex SM-105 polystyrene standards. UV absorption spectra were recorded using a Shimadzu UV–vis spectrometer 1240.

2.2.3 Synthesis azobenzene pigments

2.2.3.1 Synthesis nitro substitutional group azobenzene pigment

p-Nitroaniline (6.9g, 50mmol) was dissolved in 18% hydrochloride solution (30ml) and diazotized with sodium nitrite (3.4g in 5ml of H_2O, 50mmol) at 0~5^oC. The mixture was then added dropwise to N-ethyl-N-(2-hydroxyethyl) aniline (8.3g, 50mmol) in concentrated hydrochloride solution (25mL) at 0~5 ^oC. The mixture was stirred for another 1h, and saturated sodium acetate solution was then added to neutralize the mixture. The deep red precipitate was collected and washed several times with water. Recrystallization from ethanol gave compound and the product was confirmed by nuclear magnetic resonance (^1H NMR), synthesis route as shown in Scheme 2-1.

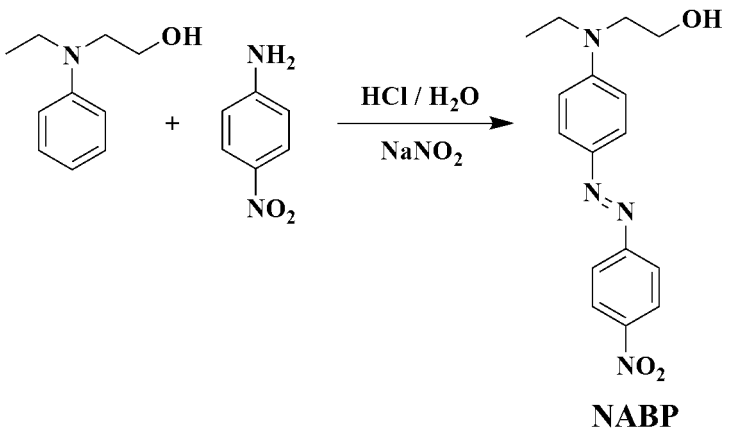

Scheme 2-1 Synthesis route of NABP

2.2.3.2 Synthesis cyano substitutional group azobenzene pigment

p-Cyanoaniline (6.9g, 50mmol) was dissolved in 18% hydrochloride solution (30ml) and diazotized with sodium nitrite (3.4g in 5ml of H_2O, 50mmol) at 0~5 ^oC. The mixture was then added dropwise to N-ethyl-N-(2-hydroxyethyl)aniline (8.3g, 50mmol) in concentrated hydrochloride solution (25mL) at 0~5 ^oC. The mixture was stirred for another 1h, and saturated sodium acetate solution was then added to neutralize the mixture. The deep red precipitate was collected and washed several times with water. Recrystallization from ethanol gave compound and the product was confirmed by ^1H NMR, synthesis route as shown in Scheme 2-2.

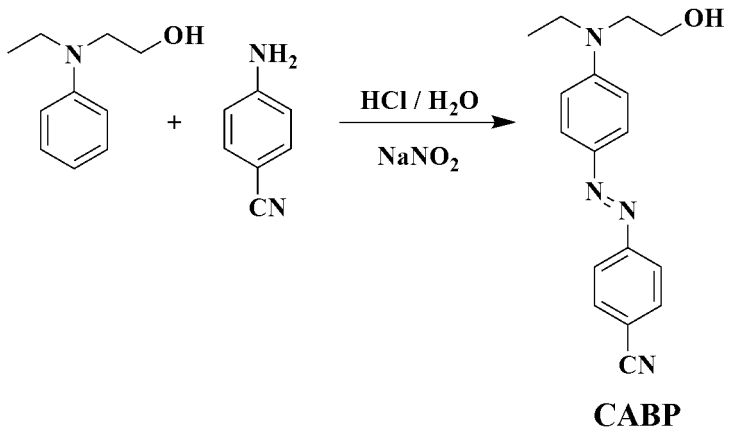

CABP

Scheme 2-2 Synthesis route of CABP

2.2.3.3 Synthesis methoxyl substitutional group azobenzene pigment

p-Methoxyaniline (6.9g, 50mmol) was dissolved in 18% hydrochloride solution (30ml) and diazotized with sodium nitrite (3.4g in 5ml of H_2O, 50mmol) at 0~5 ^oC. The mixture was then added dropwise to N-ethyl-N-(2-hydroxyethyl)aniline (8.3g, 50mmol) in concentrated hydrochloride solution (25mL) at 0~ 5^oC. The mixture was stirred for another 1h, and saturated sodium acetate solution was then added to neutralize the mixture. The deep red precipitate was collected and washed several times with water. Recrystallization from ethanol gave compound and the product was confirmed by ^1H NMR, synthesis route as shown in Scheme 2-3.

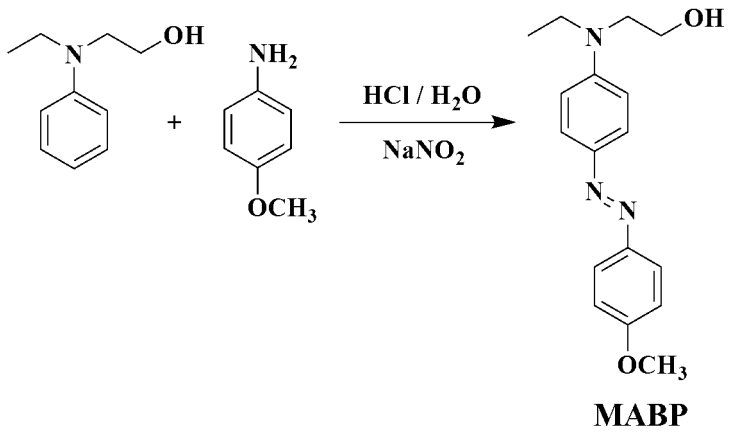

Scheme 2-3 Synthesis route of MABP

2.2.4 Synthesis azobenzene pigments methacrylate

2.2.4.1 Synthesis nitro substitutional group azobenzene pigment methacrylate

To the solution of dye (6.00g, 18.1mmol) in dry methylene chloride (20mL) was added triethylamine (2.7mL) then cooled to 0 ^{o}C, and distilled methyacryloyl chloride (1.77mL, 1.90g, 18.1mmol) was added dropwise while stirring, the resulting mixture was stirred at 0 ^{o}C for 2 h then at room temperature for 16h. The methylene chloride solution was extracted with water to remove water-soluble impurities. The crude pigment methacrylate monomer product was purified by silica gel chromatography eluting with hexane/methylene chloride (1:1 to 1:3) to afford a red solid (4.85g, 70%), and was confirmed by ^{1}H NMR, synthesis route as shown in Scheme 2-4.

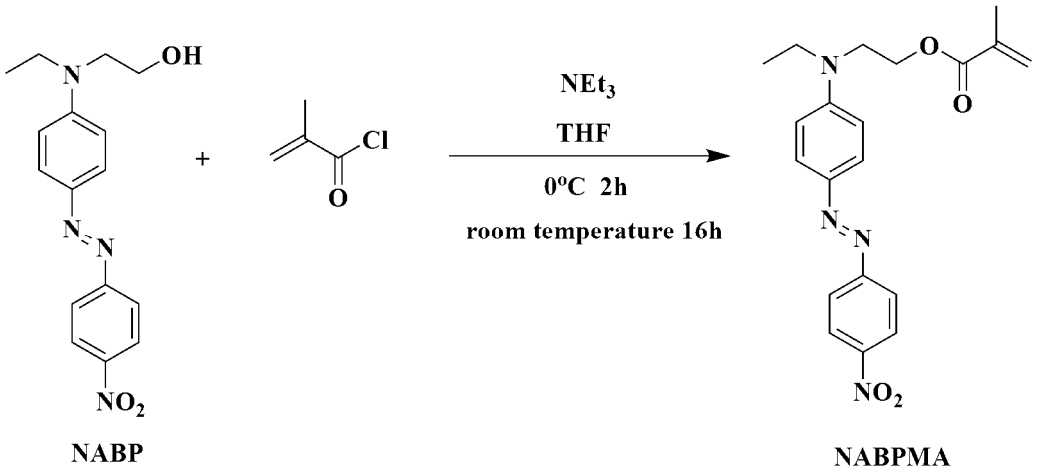

Scheme 2-4 Synthesis route of NABPMA

2.2.4.2 Synthesis cyano substitutional group azobenzene pigment methacrylate

Triethylamine (2.7mL) was added to the solution of dye (6.00g, 18.1mmol) in dry methylene chloride(20mL) then the mixture was cooled to 0^{o}C. Distilled methyacryloyl chloride (1.77mL, 1.90g, 18.1mmol) was added dropwise while stirring, the resulting mixture was stirred at 0 ^{o}C for 2 h then at room temperature for 16h. The methylene chloride solution was extracted with water to remove water-soluble impurities. The crude pigment methacrylate monomer product was purified by silica gel chromatography eluting with hexane/methylene chloride (1:1 to 1:3) to afford a red solid (4.85g, 70%), and was confirmed by ^{1}H NMR, synthesis route as shown in Scheme 2-5.

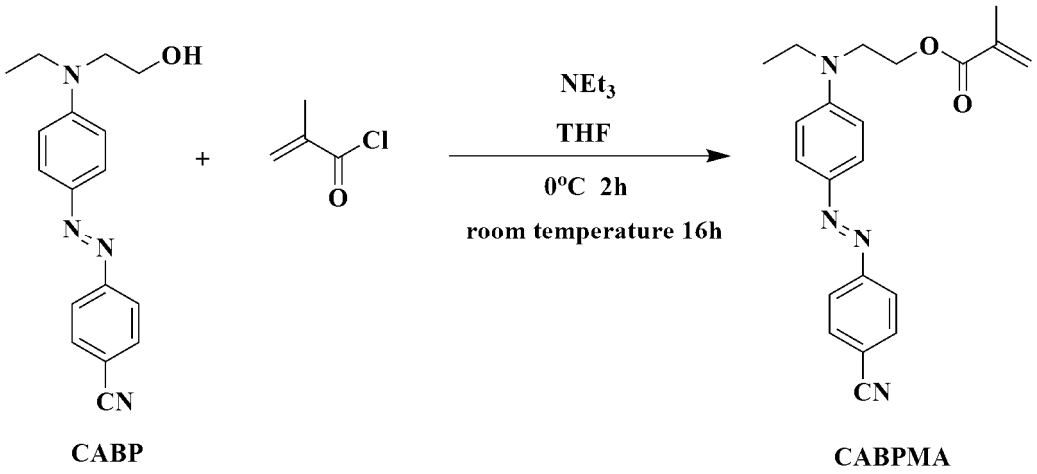

Scheme 2-5 Synthesis route of CABPMA

2.2.4.3 Synthesis methoxyl substitutional group azobenzene pigment methacrylate

To the solution of dye (6.00g, 18.1mmol) in dry methylene chloride (20mL) was added triethylamine (2.7mL) then cooled to 0 ^{o}C. Distilled methyacryloyl chloride (1.77mL, 1.90g, 18.1mmol) was added dropwise while stirring, the resulting mixture was stirred at 0 ^{o}C for 2 h then at room temperature for 16h. The methylene chloride solution was extracted with water to remove water-soluble impurities. The crude pigment methacrylate monomer product was purified by silica gel chromatography eluting with hexane/methylene chloride (1:1 to 1:3) to afford a red solid (4.85g, 70%), and was confirmed by ^{1}H NMR, synthesis route as shown in Scheme 2-6.

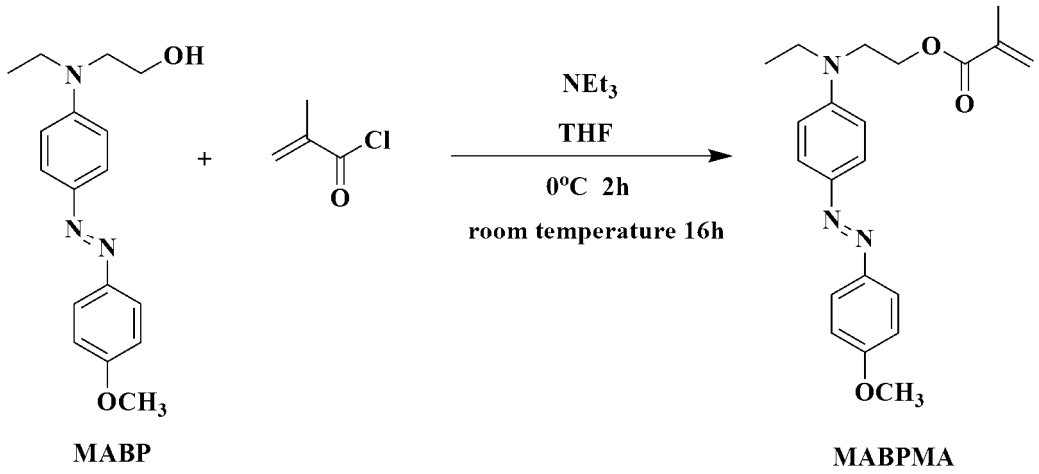

Scheme 2-6 Synthesis route of MABPMA

2.2.5 Free radical polymerization to prepare side chain polymers

Typically, the copolymerization was carried out in a mole ratio of MMA/ABPMA 95/5~75/25 in 20 ml of dioxane solution to get PMMA-co-ABPMA, under nitrogen atmosphere at 65 °C in the presence of 1 wt% of 2,2'-azobisisobutyronitrile (AIBN) for 24 h. The resulting copolymer solution was cooled, precipitated with methanol, filtered and finally dried under reduced pressure overnight, synthesis route as shown in Scheme 2-7.

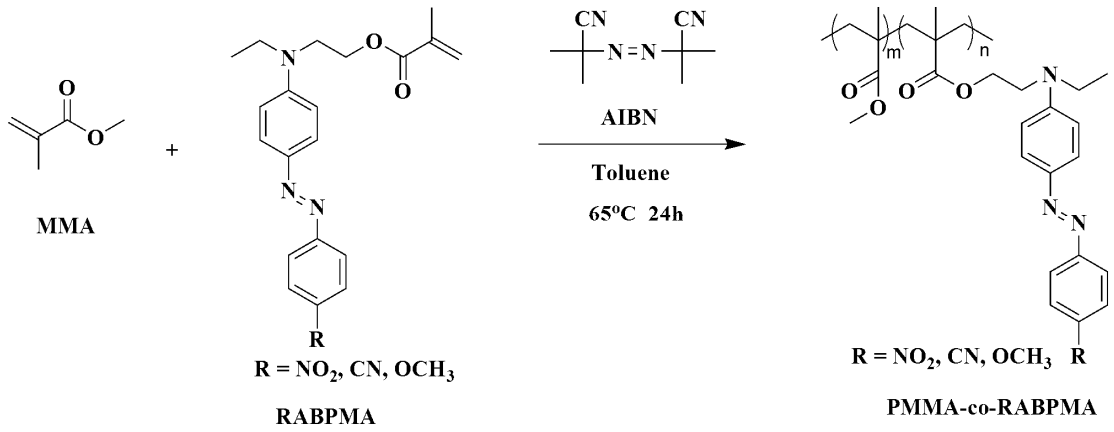

Scheme 2-7 Synthesis route of PMMA-co-RABPMA

2.2.6 RAFT to prepare side chain polymers

The monomer MMA, ABPMA and RAFT agent in a mole ratio of 200/1/1 were dissolved in nitrogen degassed anhydrous toluene (10mL) and stirred at room temperature for 10 minutes. The initiator 1wt% AIBN was quickly added in the previous mixture then the mixture through deoxygenization operation was stirred with nitrogen bobbling at room temperature for half an hour. The reaction was carried at 65^{o}C for 24 hour under nitrogen atmosphere. The resulting polymer solution was cooled and poured into methanol to precipitate the polymer. The precipitated polymer was filtered, redissolved and reprecipitated, filtered, and finally dried at 60 ^{o}C under reduced pressure overnight, synthesis route as shown in Scheme 2-8.

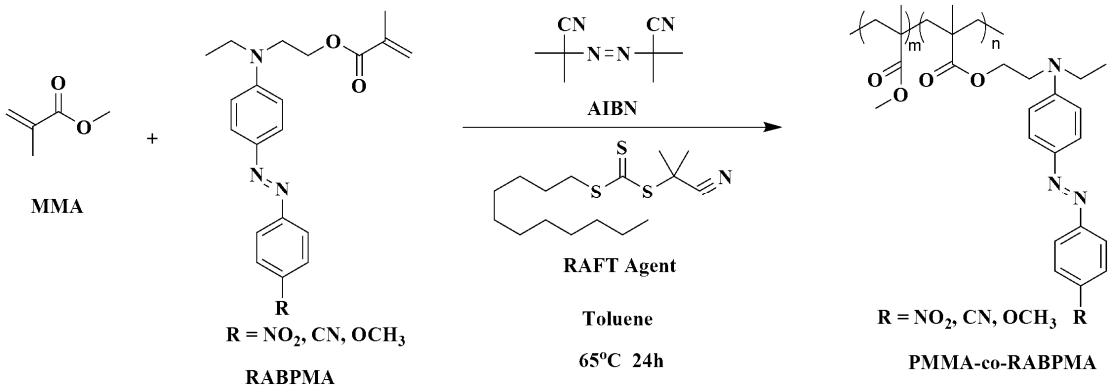

Scheme 2-8 Synthesis route of PMMA-co-RABPMA

2.2.7 Synthesis of chromophore (C1)

The chromophore investigated in this study belong to the FTC structural family and is shown in the Fig. 2-2. The detailed synthesis and characterization of the

molecules has been reported extensively elsewhere [4][5][6].

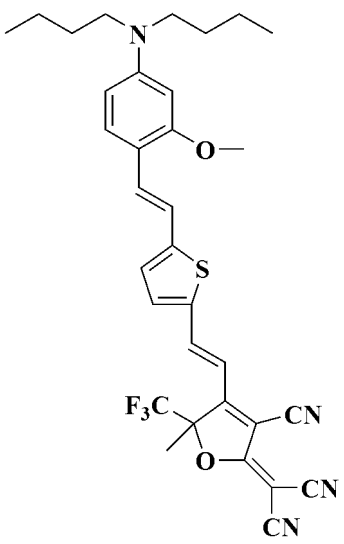

Fig. 2-2 Molecular structure of guest chromophore (**C1**)

2.2.8 Thin films preparation

The FTC chromophore (**C1**) was mixed with the host polymer at 15 wt% in cyclopentanone and stirred at room temperature for 12 hours. After this dispersion phase, the resulting solution was filtered through a 0.2 μm filter and spin coated onto an indium tin oxide (ITO) glass substrates, to produce thin films. After a short pre-baking (20 min) on a hotplate at 90 ^{o}C and then under vacuum at 85 ^{o}C (2 days) to remove the residual solvent, the measured thickness was 2.5 μm (Surface profiler - DEKTAK3). A thin gold layer (~ 50 nm) was sputtered directly onto the film to act as the electrode, the process as shown in Fig. 2-3.

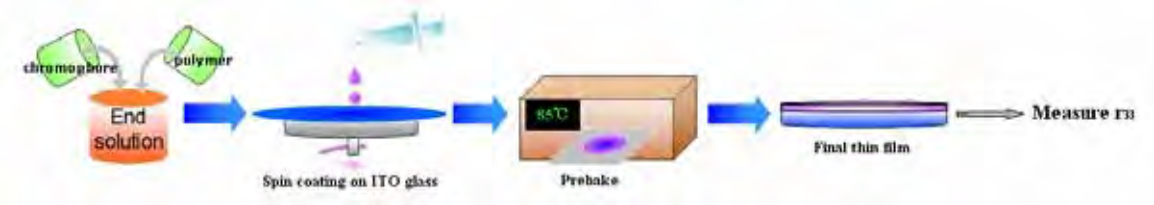

Fig. 2-3 Film-making process

2.3 Results and discussion

2.3.1 Synthesis and chracterization

2.3.1.1 Resultant of azobenzene pigments

p-Nitroaniline was diazotized with sodium nitrite in 18% hydrochloride solution at 0~5 ^{o}C. The mixture was then added drop wise to N-ethyl-N-(2-hydroxyethyl) aniline in concentrated hydrochloride solution, then neutralized by saturated sodium acetate solution. The deep red precipitate was collected and washed several times with water. Recrystallization from ethanol gave the product, yield 95%. ^{1}H NMR spectrum of pure product NABP is showed in Fig. 2-4, ^{1}H NMR (δ, $CDCl_3$): 8.32 (2H, d), 7.91 (4H, t), 6.80 (2H, d), 3.89 (2H, m), 3.63 (2H, m), 1.56 (2H, s), 1.26 (3H, t) ppm.

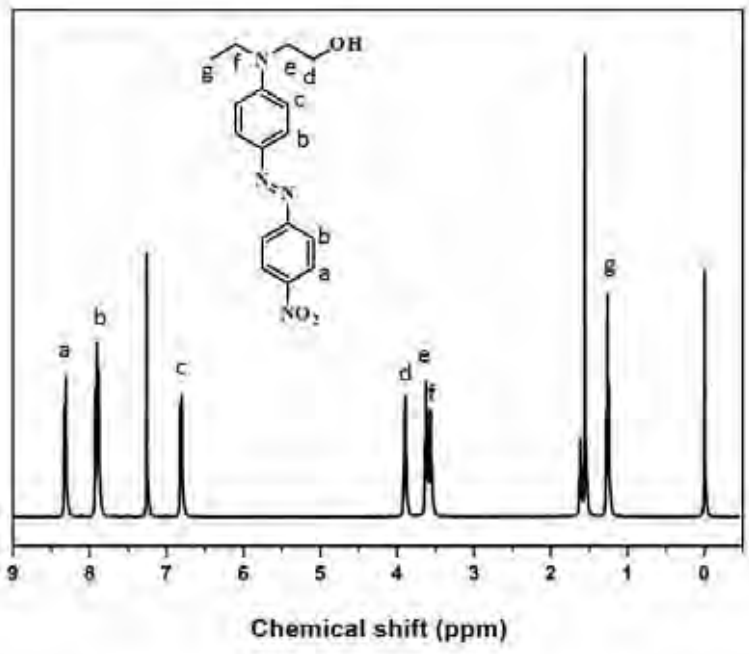

Fig. 2-4 ^{1}H NMR spectrum of NABP

p-Cyanoaniline was diazotized with sodium nitrite in 18% hydrochloride solution at 0~5 ^{o}C. The mixture was then added drop wise to N-ethyl-N-(2-hydroxyethyl) aniline in concentrated hydrochloride solution, then neutralized by saturated sodium acetate solution. The deep red precipitate was collected and washed several times with water. Recrystallization from ethanol gave the product, yield 89%. ^{1}H NMR spectrum of pure product CABP is showed in Fig. 2-5. ^{1}H NMR (δ, $CDCl_3$): 7.87 (4H, m), 7.76 (2H, d), 6.82 (2H, d), 3.89 (2H, m), 3.61 (2H, m), 3.45 (2H, m), 1.25 (3H, t) ppm.

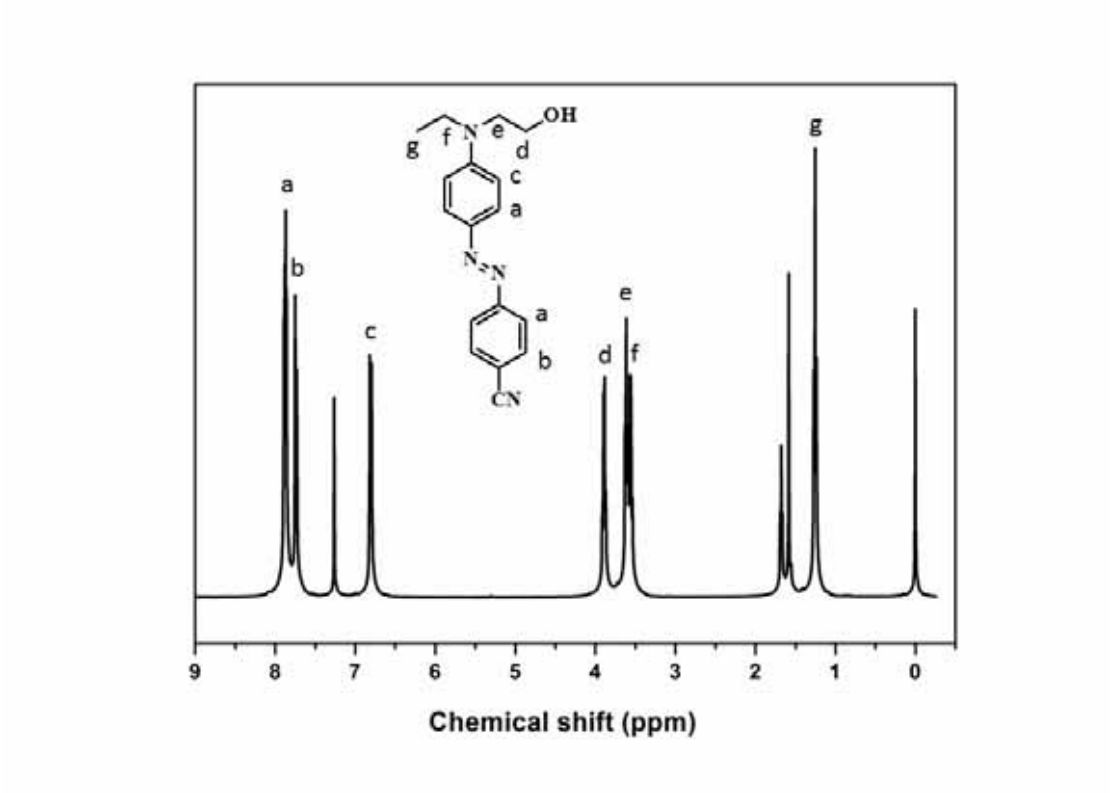

Fig. 2-5 ^{1}H NMR spectrum of CABP

p-Methoxyaniline was diazotized with sodium nitrite in 18% hydrochloride solution at 0~5 ^{o}C. The mixture was then added drop wise to N-ethyl-N-(2-hydroxyethyl) aniline in concentrated hydrochloride solution, then

neutralized by saturated sodium acetate solution. The deep red precipitate was collected and washed several times with water. Recrystallization from ethanol gave the product, yield 85%. ^{1}H NMR spectrum of pure product MABP is showed in Fig. 2-6, ^{1}H NMR (δ, $CDCl_3$): 7.82 (4H, t), 6.98 (2H, d), 6.78 (2H, d), 3.87 (3H, s), 3.80 (2H, t), 3.56 (2H, t), 3.48 (2H, m), 1.21 (3H, t) ppm.

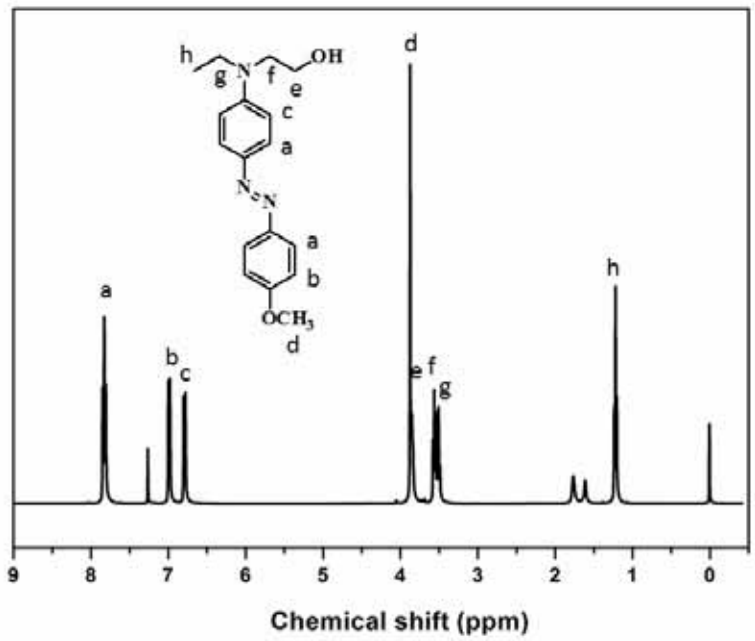

Fig. 2-6 ^{1}H NMR spectrum of MABP

2.3.1.2 Resultant of azobenzene pigments methacrylate

Pigment and triethylamine in dry methylene chloride were cooled to 0 ^{o}C, and distilled methyacryloyl chloride was added dropwise while stirring, the resulting mixture was stirred at 0 ^{o}C for 1 h then at room temperature for 16 h. The methylene chloride solution was extracted with water and the crude pigment methacrylate monomer product was purified by silica gel chromatography eluting with

hexane/methylene chloride to afford a red solid, yield 64%. ^{1}H NMR spectrum of pure product NABPMA is showed in Fig. 2-7, ^{1}H NMR (δ, $CDCl_3$): 8.32 (2H, d), 7.91 (4H, t), 6.82 (2H, d), 6.10 (1H, s), 5.59 (1H, s), 4.38 (2H, m), 3.72 (3H, t), 3.54 (2H, t), 1.94 (3H, s), 1.26 (3H, t) ppm.

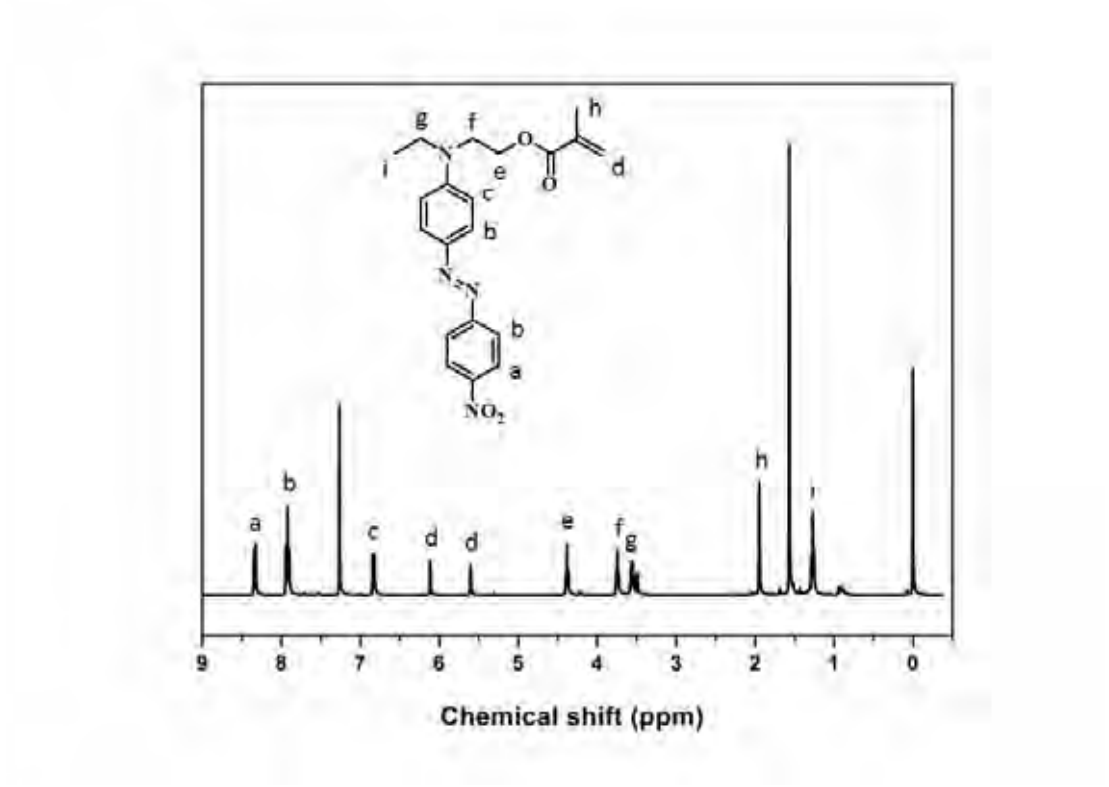

Fig. 2-7 ^{1}H NMR spectrum of NABPMA

Pigment and triethylamine in dry methylene chloride were cooled to 0 ^{o}C, and distilled methyacryloyl chloride was added dropwise while stirring, the resulting mixture was stirred at 0 ^{o}C for 1 h then at room temperature for 16 h. The methylene chloride solution was extracted with water and the crude pigment methacrylate monomer product was purified by silica gel chromatography eluting with hexane/methylene chloride to afford a red solid, yield 59%. ^{1}H NMR spectrum of pure

product CABPMA is showed in Fig. 2-8, ^{1}H NMR (δ, $CDCl_3$): 7.87 (4H, d), 7.75 (2H, d), 6.80 (2H, d), 6.10 (1H, s), 5.59 (1H, s), 4.38 (2H, t), 3.73 (2H, t), 3.55 (2H, m), 1.94 (3H, s), 1.26 (3H, t) ppm.

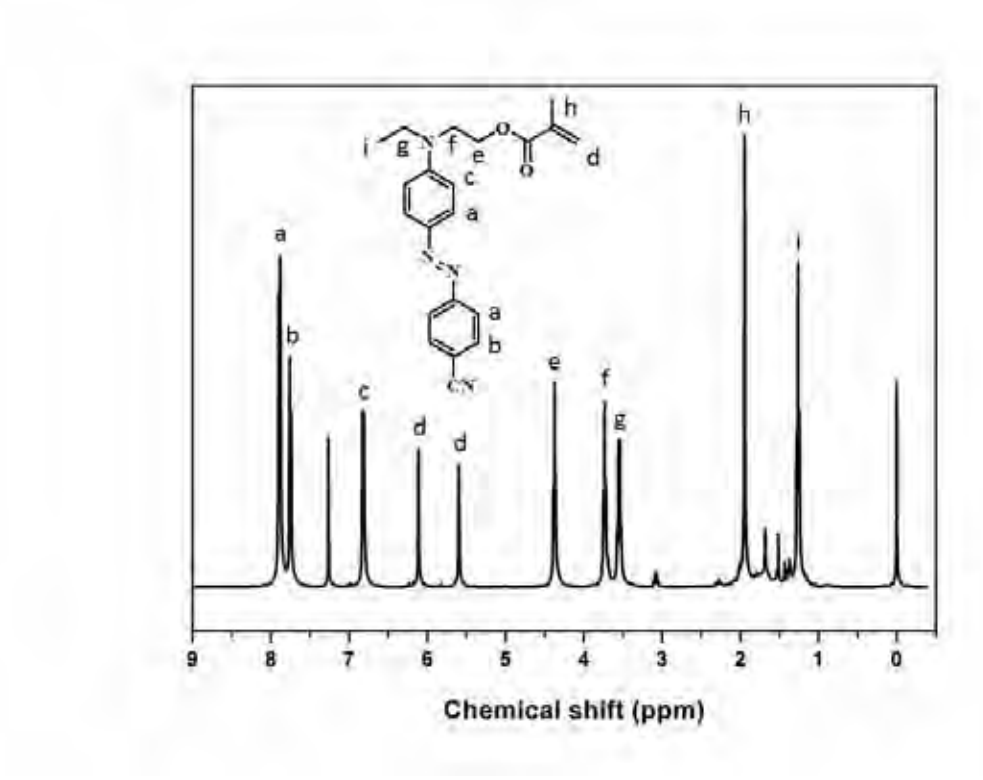

Fig. 2-8 ^{1}H NMR spectrum of CABPMA

Pigment and triethylamine in dry methylene chloride were cooled to 0 ^{o}C, and distilled methyacryloyl chloride was added dropwise while stirring, the resulting mixture was stirred at 0 ^{o}C for 1 h then at room temperature for 16 h. The methylene chloride solution was extracted with water and the crude pigment methacrylate monomer product was purified by silica gel chromatography eluting with hexane/methylene chloride to afford a red solid, yield 61%. ^{1}H NMR spectrum of pure product MABPMA is showed in Fig. 2-9, ^{1}H NMR (δ, $CDCl_3$): 8.83 (4H, d), 6.97 (2H, d), 6.78 (2H, d), 6.10 (1H, s), 5.8 (1H, t), 4.35 (2H, m), 3.87 (3H, s), 3.69 (2H, t), 3.50

(2H, m), 1.94 (3H, s), 1.25 (3H, t) ppm.

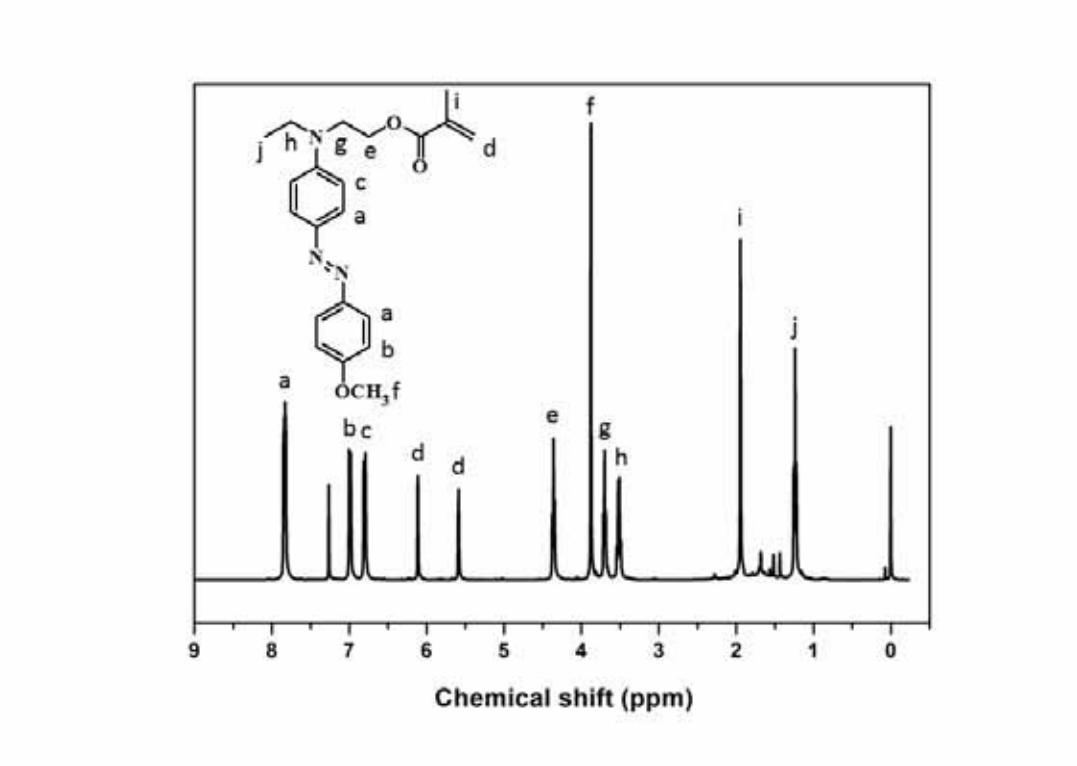

Fig. 2-9 ^{1}H NMR spectrum of MABPMA

2.3.1.3 Physical properties of side chain polymers made by Free Radical Polymerization

Three different substituent group side-chain azobenzene polymers, including nitro, cyano, methoxyl substituent, were synthesized through Free Radical Polymerization. The copolymerizations were carried out in a different mole ratio of MMA/ABPMA from 95/5 to 75/25 in dioxane solvent to get a serious PMMA-co-ABPMA, under nitrogen atmosphere at 65 ^{o}C in the presence of 1 wt% of 2,2′ -Azobis-isobutyronitrile (AIBN) for 24 h. The resulting copolymer solutions were cooled, precipitated in methanol, filtered and finally dried under reduced pressure overnight. The polymers physical properties are showed in Table 3-1.

Table 2-1 Characterization of polymers

	Chromophore desity (mol%)	Chromophore desity [b] (wt%)	Mn [d] (k)	Mw [d] (k)	PDI [d]	Tg [a] (°C)	Td [a] (°C)	λmax [c] (nm)
PMMA-co-NABPMA$_5$	5	14.4	21	27	1.28	110	263	471
PMMA-co-NABPMA$_{15}$	15	30.8	13	20	1.46	106	268	472
PMMA-co-NABPMA$_{25}$	25	47.2	14	22	1.63	103	270	471
PMMA-co-MABPMA$_5$	5	13.1	12	13	1.61	110	258	407
PMMA-co-MABPMA$_{15}$	15	32.2	14	20	1.53	104	252	407
PMMA-co-MABPMA$_{25}$	25	44.7	15	26	1.72	114	254	408
PMMA-co-CABPMA$_5$	5	13.0	14	20	1.47	103	265	443
PMMA-co-CABPMA$_{15}$	15	31.5	16	27	1.74	101	259	444
PMMA-co-CABPMA$_{25}$	25	44.3	13	21	1.59	105	260	443
PMMA	—	—	29	34	1.90	104	255	—

[a] Thermogravametric analysis (TGA) and differential scanning calorimetry (DSC) were performed using an SII-TG/DTA 6200 instrument under a nitrogen atmosphere at a heating rate of 5 °C /min.

[b] UV absorption spectra were recorded using a Shimadzu UV–vis spectrometer 1240.

[c] Electro-Optic (EO) coefficient measured at 1.31μm, unit of r_{33} is pm/V, unit of PE is $(nm/V)^2$.

[d] The molecular weights (Mw) and polydispersity (PDI) of the polymers were determined by size-exclusion chromatography (SEC) using a Shodex GPC K-804L column on a JASCO LC2000 liquid chromatography system with $CHCl_3$ as the eluent. This system was calibrated using a narrow PDI Shodex SM-105 polystyrene standards.

2.3.1.4 Physical properties of side chain polymers made by RAFT

Follow the previous work, I used Reversible Addition-Fragmentation Chain Transfer Polymerization (RAFT) to prepare three different substituent group side-chain

azobenzene polymers, including nitro, cyano, methoxyl. RAFT is a kind of controlled polymerization, so it will get more ideal polymers. The monomer MMA, ABPMA and RAFT agent in a mole ratio of 200/1/1 was dissolved in nitrogen degassed anhydrous toluene and stirred at room temperature. The initiator 1 wt% 2,2'-azobisisobutyronitrile (AIBN) was added. The mixture was stirred at room temperature for one hour and at 65^{o}C for 24 hour under nitrogen atmosphere. The resulting polymer solution was precipitated from methanol three times, and finally dried at 60 ^{o}C under reduced pressure overnight. And at the same time, free radical polymerization also been taken in the same feed ratio as compare. Fig. 2-10~ Fig. 2-12 show the GPC trace of side chain polymers with nitro, cyano, methoxyl substituent, red lines are made from RAFT and black line are prepared from free radical polymerization (FRP). All the polymers made through RAFT have obvious narrow PDI.

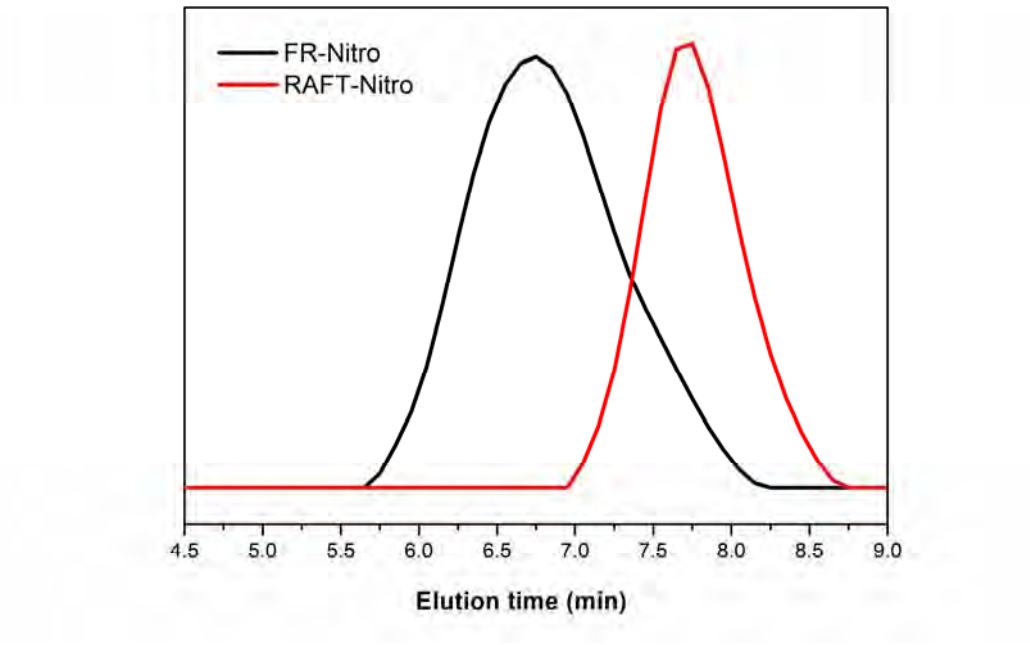

Fig. 2-10 GPC trace of nitro substitution polymer using FR and RAFT

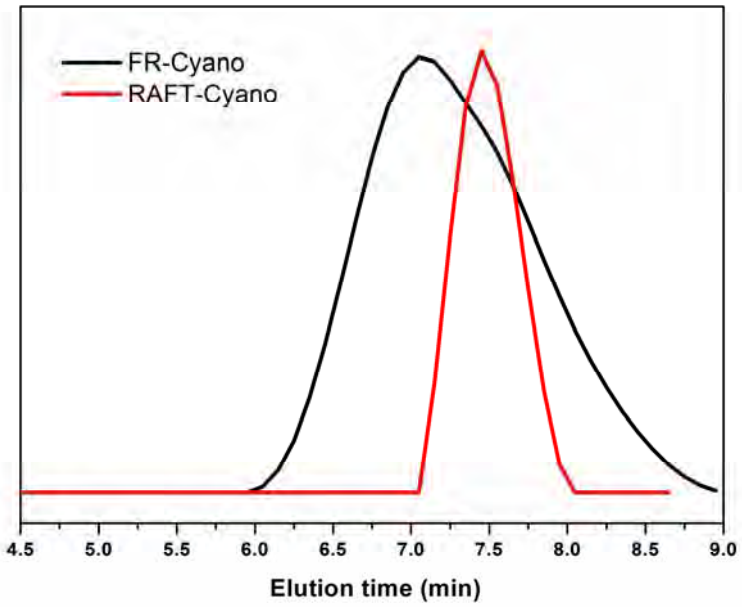

Fig. 2-11 GPC trace of cyano substitution polymer using FR and RAFT

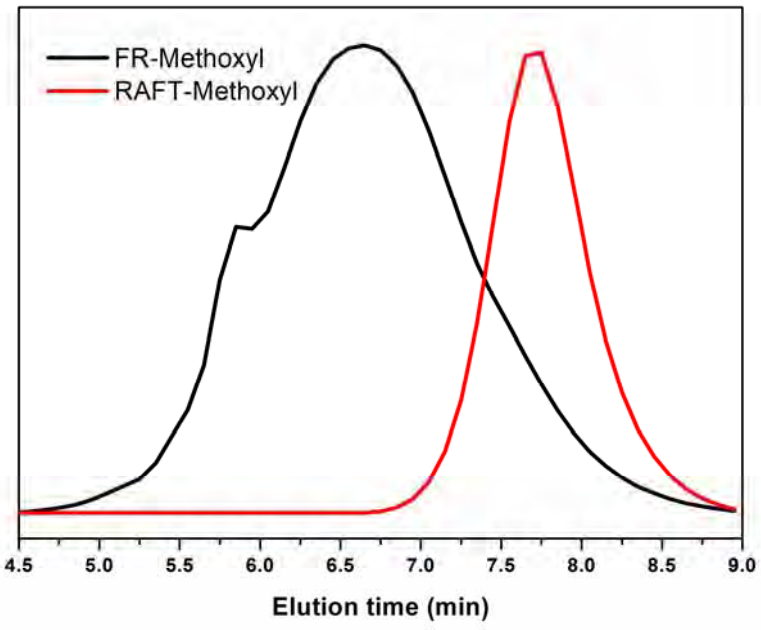

Fig. 2-12 GPC trace of methoxyl substitution polymer using FR and RAFT

From the GPC data of these three polymers, Mn are nearly 40,000, PDI are around

2.00 using the first way, and Mn are 10,000, PDI are around 1.30 using RAFT, all react conditions are 24 hours, toluene as solvent, 65 ^{o}C. The polymers made from RAFT get narrow PDI, but the molecular weight are low, this because the feed ratio of monomer MMA and RAFT agent are low, though increase the molecular weight through enhance the feed ratio of monomers and RAFT agent. The molecular weights (Mw) and polydispersity (PDI) of the polymers were determined by size-exclusion chromatography (SEC) using a Shodex GPC K-804L column on a JASCO LC2000 liquid chromatography system with $CHCl_3$ as the eluent. This system was calibrated using a narrow PDI Shodex SM-105 polystyrene standards. All the definite physical data are showed in Table 2-2.

Table 2-2 Physical properties of polymers prepared both from FR and RAFT

	Mn [a]	Mw [a]	Mz [a]	PDI [a]	Tg [b]	Td [b]
FR-Nitro	39684	69432	104433	1.74	110	263
RAFT-Nitro	10882	14443	18481	1.32	113	260
FR-Cyano	18650	38110	60819	2.04	105	258
RAFT-Cyano	6864	7696	8564	1.11	108	269
FR-Methoxy	41971	99776	168834	2.37	103	265
RAFT-Methoxy	10491	14411	18688	1.37	111	270

[a] The molecular weights (Mw) and polydispersity (PDI) of the polymers were determined by size-exclusion chromatography (SEC) using a Shodex GPC K-804L column on a JASCO LC2000 liquid chromatography system with $CHCl_3$ as the eluent. This system was calibrated using a narrow PDI Shodex SM-105 polystyrene standards.

[b] Thermogravametric analysis (TGA) and differential scanning calorimetry (DSC) were performed using an SII-TG/DTA 6200 instrument under a nitrogen atmosphere at a heating rate of 5 °C /min.

2.3.2 EO properties

Three different substituent group side-chain azobenzene polymers, including nitro, cyano, methoxyl substituent, were synthesize through free radical polymerization. These side chain polymers were used as host and **C1** as guest accomplished binary chromophore system, to measure the EO coefficients by Teng-Man measurement at 1310nm. All the data are listed in Table 2-3. We have found that an optimum PMMA-co-CABPMA$_5$ contained a 5 mol% cyano substituent on the azobenzene moiety and furthermore that the r_{33} was maximized by incorporation of 15 wt% of C1 chromophore into the polymer host. In this ideal system a high r_{33} of 63 pm/V was achieved.

Table 2-3 EO coefficient of side chain polymers preparing by Free Radical Polymerization

	Chromophore desity	Chromophore desity [a]	none guest chromophore		guest C1	
	(mol%)	(wt%)	Max r_{33} [b]	Final r_{33} [b]	Max r_{33} [b]	Final r_{33} [b]
PMMA-co-NABPMA$_5$	5	14.4	3	2	46	35
PMMA-co-NABPMA$_{15}$	15	30.8	16	13	43	27
PMMA-co-NABPMA$_{25}$	25	47.2	30	12	35	20
PMMA-co-MABPMA$_5$	5	13.1	13	5	77	58
PMMA-co-MABPMA$_{15}$	15	32.2	16	8	51	25
PMMA-co-MABPMA$_{25}$	25	44.7	17	2	39	26

PMMA-co-CABPMA$_5$	5	13.0	13	2	103	63
PMMA-co-CABPMA$_{15}$	15	31.5	14	3	41	17
PMMA-co-CABPMA$_{25}$	25	44.3	26	5	35	23
PMMA	—	—	—	—	33	20

[a] UV absorption spectra were recorded using a Shimadzu UV–vis spectrometer 1240.

[b] Electro-Optic(EO) coefficient measured at 1.31 μm, unit of r_{33} is pm/V, unit of PE is $(nm/V)^2$.

Three different substituent group side-chain azobenzene polymers, including nitro, cyano, methoxyl substituent, have also been optimized through RAFT. Size-exclusion chromatography (SEC) trace shows Mw 14k, PDI under 1.3 with THF as the eluent. From the polymers themselves have been optimized on controlling the molecular weight and PDI, but the physical properties didn't change through this way, Tg and Td are 110 ^oC and 260 ^oC similar as the side chain polymer gotten from Free Radical Polymerizations. And using cyano substituent side chain polymer get from RAFT accomplished with 15 wt% **C1** the maximum r_{33} is 120 pm/V, final r_{33} is 65 pm/V.

Figure. 2-13 to Figure. 2-16 show the conditions during poling about sample which is cyano substituent side chain polymer getting from RAFT and accomplished with 15 wt% **C1** chromophore.

In a general experiment, the sample was fixed on the poling stage and the temperature was increased in several minutes up to around Tg. The poling field was then applied to the sample at a ramping rate 8 V/min. During the poling process, the electric current was monitored to optimize poling efficiency and to control local

electrical breakdown in the films. As shown in Figure. 2-15, the current grew rapidly with the ramping of poling field, and maximized at 205 μA when the poling field climbed to 165 V/μm. Generally, the breakdown of the electric field through the polymeric film is accompanied by an abrupt overflow of the electric current. Thus, the ramping of the poling field ceased and maintained at 165 V/μm and temperature rise to 110 ^{o}C, when the second increasing trend of the current flow appeared in Figure. 2-15. The current dropped slowly after peaking, and even the poling field maintained a constant value. Figure. 2-16 indicates that the r_{33} varied simultaneously with the applied voltage and reached its maximum of 120 pm/V at the poling filed of 165 V/μm. The sample was then cooled to room temperature with the poling field maintained. During the rapid cooling process, there was a notable relaxation phenomenon of the molecular ordering as the total EO signal deceased by 45%. Eventually, r_{33} of 65 pm/V was realized at room teperature for the poled EO film after removing the poling field.

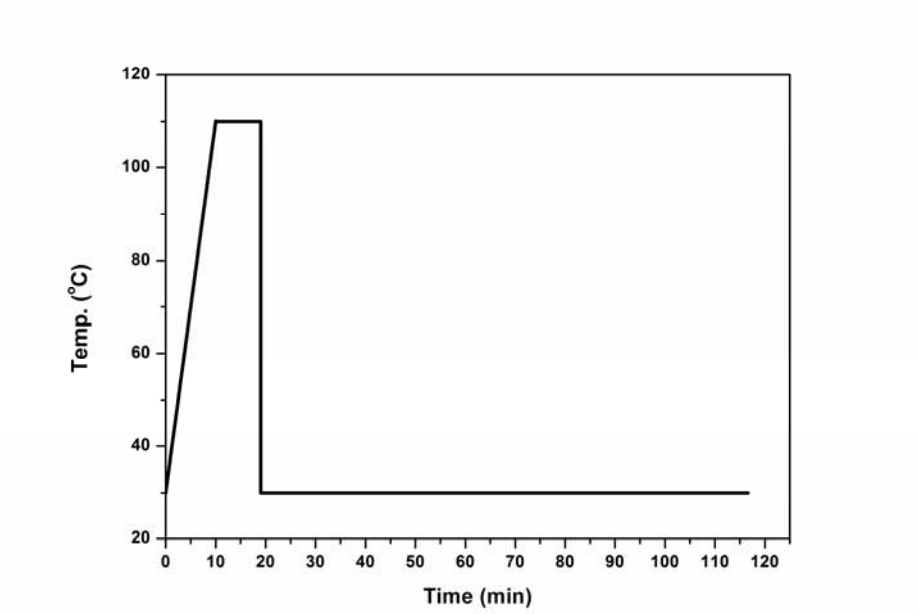

Fig. 2-13 Typical poling process on cyano substituent side chain polymer get from RAFT as host 15 wt% C1 as guest, Temperature are plotted during the poling process.

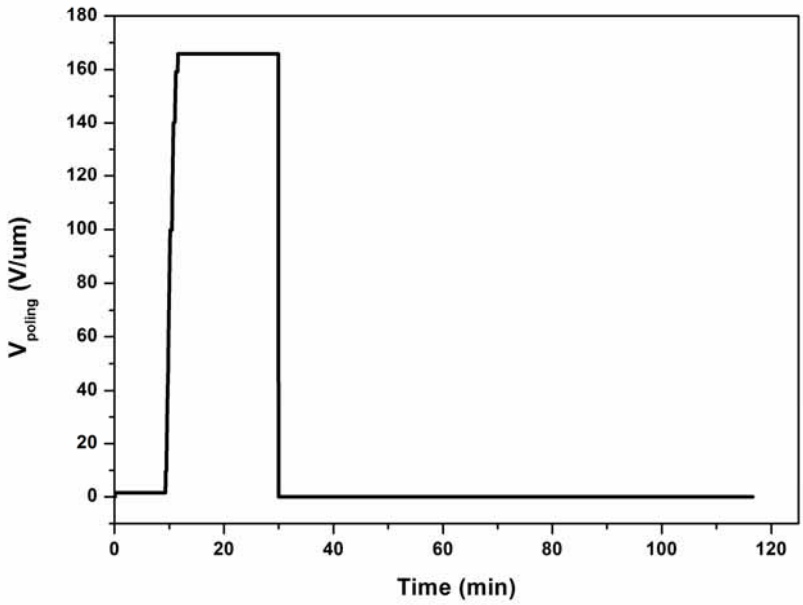

Fig. 2-14 Typical poling process on cyano substituent side chain polymer get from RAFT as host 15 wt% C1 as guest, applied field are plotted during the poling process.

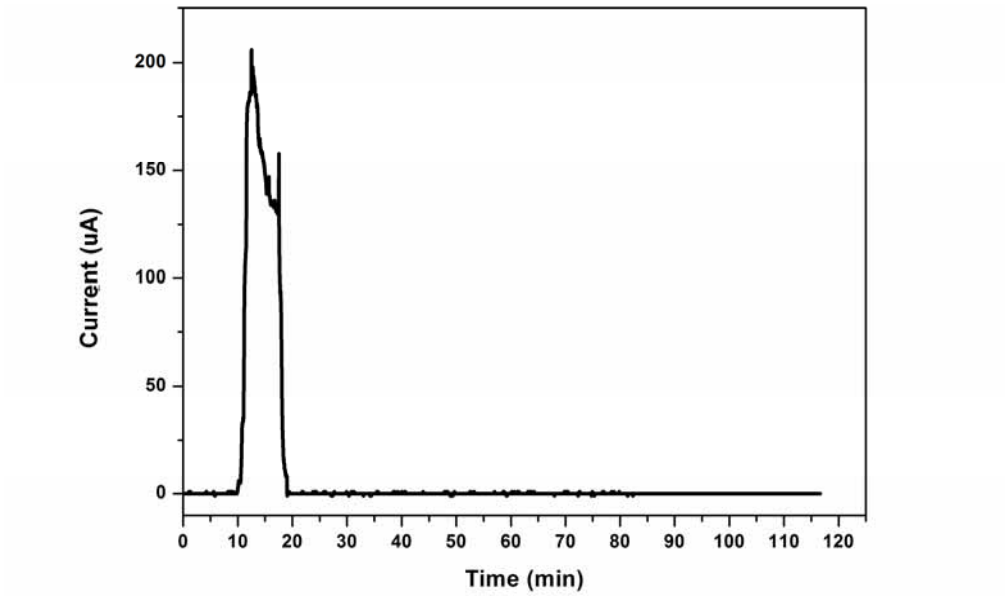

Fig. 2-15 Typical poling process on cyano substituent side chain polymer get from RAFT as host 15 wt% C1 as guest, flowing current are plotted during the poling process.

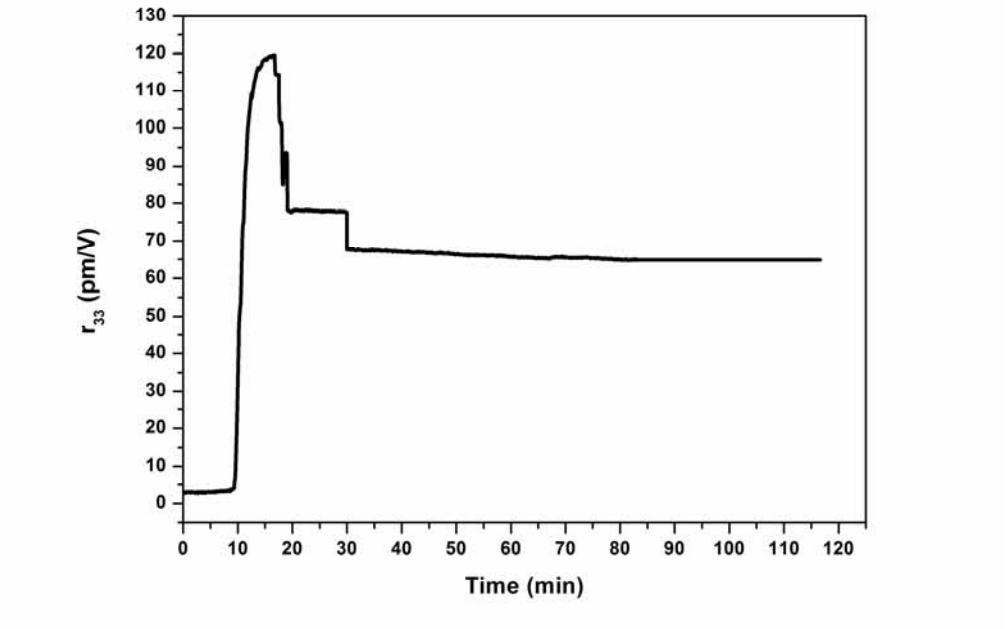

Fig. 2-16 Typical poling process on cyano substituent side chain polymer get from RAFT as host 15 wt% C1 as guest, r_{33} are plotted during the poling process.

2.4 Conclusions

Nine azobenzene side chain polymers were prepared through Free Radical Polymerization which containing three different pendent azobenzene moieties, nitro, cyano, methoxy. The chemical structures of the nine azobenzene derivatives were confirmed by NMR, UV absorption and the GPC traces. These polymers displayed a large molecular weight Mw 20 k, PDI 1.3 ~ 1.7, and glass transition temperature of nearly 110 ^{o}C. The macroscopic electro-optic coefficients of these polymer were measured using Teng-Man measurement at 1310nm. We have found that an optimum PMMA-co-CABPMA$_5$ contained a 5 mol% cyano substituent on the azobenzene moiety and furthermore that the r_{33} was maximized by incorporation of 15 wt% of C1 chromophore into the polymer host. In this ideal system a high r_{33} of 63 pm/V was achieved.

Three different substituent group side-chain azobenzene polymers, including nitro, cyano, methoxyl substituent, have been optimized through RAFT. Size-exclusion chromatography (SEC) trace shows Mw 14k, PDI under 1.3 with THF as the eluent. From the polymers themselves have been optimized on controlling the molecular weight and PDI, but the physical properties didn't change through this way, Tg and Td are 110 ^{o}C and 260 ^{o}C similar as using Free Radical Polymerizations gotten the side chain polymers. And using cyano substituent side chain polymer get from RAFT accomplished with 15 wt% **C1** the maximum r_{33} is 120 pm/V, final r_{33} is 65 pm/V.

2.5 References

[1] Y. Shi, C. Zhang, H. Zhang, J. H. Bechtel, L. R. Dalton, B. H. Robinson, and W. H. Steier. *J*. Science. 199 (2000) 288.

[2] M. Lee, H. E. Katz, C. Erben, D. M. Gill, P. Gopalan, J. D. Heber, and D. J. McGee. *J*. Science. 298 (2002) 1401.

[3] L. R. Dalton, P. A. Sullivan and D. H. Bale. *J*. Chem. Rev. 110(1) (2010) 25.

[4] X. Piao, X. Zhang, S. Inoue, S. Yokoyama, H. Miki, I. Aoki, A. Otomo, H. Tazawa. *J*. Organic Electronics. 12 (2011) 1093-1097.

[5] X. Piao, X. Zhang, Y. Mori, M. Koishi, A. Nakaya, S. Inoue, I. Aoki, A. Otomo, S. Yokoyama. *J*. Journal of Polymer Science: Part A: Polymer Chemistry. 49 (2011) 47-54.

[6] X. Zhang, I. Aoki, X. Piao, S. Inoue, H. Tazawa, S. Yokoyama, A. Otomo. *J*. Tetrahedron Letters, 51 (2010) 5873-5876.

Chapter 3 The Synthesis and Characterization of Electro-Optic Material Based on Novel Polymer Brush

3.1 Introduction

Organic second-order nonlinear optical (electro-optic, EO) materials represent a potentially transformative technology around which next generation computing, telecommunications, sensing, medical/security imaging, and other industries may be constructed. Binary chromophore system EO materials which are made up of chromophore containing polymer matrix and guest chromophore in simple guest-host system represent a recently developed class of EO materials that shows great promising. Compared to their individual components, the remarkably large EO activity displayed by binary chromophore material systems, is thought to arise from one important effect, the increased glass transition temperature and molecular weight of the dipolar chromophore containing polymer matrix may enhance the macroscopic EO coefficients of the binary chromophore EO material systems.

Cylindrical polymer brush possessing densely grafted side chains on a linear polymer main chain, ideally every monomer unit of the main chain carries one side chain [1]. This type of structure has also been given the very intuitive name molecular bottlebrush. Cylindrical polymer brushes are interesting because of the expectation that their unique structure may result in unusual properties [2]. Because of the regular

multibranched structure, they have the following characteristics in comparison with the corresponding linear polymers of the same molecular weight: (1) a small and compact molecular dimension, (2) an extended wormlike conformation resulting from the steric repulsion between densely grafted side chains, and (3) many chain ends per molecule enhancing the chain-end effects [3].These virtues of polymer brushes may enhance the Tg of polymer matrix, improve the loading density of chromophore, and increase chromophore regular arrangement. Our major effects have been focused on developing chromophore containing polymer brush to use as polymer matrix in binary chromophore EO materials.

Three main strategies for preparing molecular brushes: grafting through [4][5]— the polymerization of macro monomers, grafting onto [6][7]— the addition of previously prepared side chains to a backbone, and grafting from [8]— the polymerization of side chains from a macroinitiator backbone.

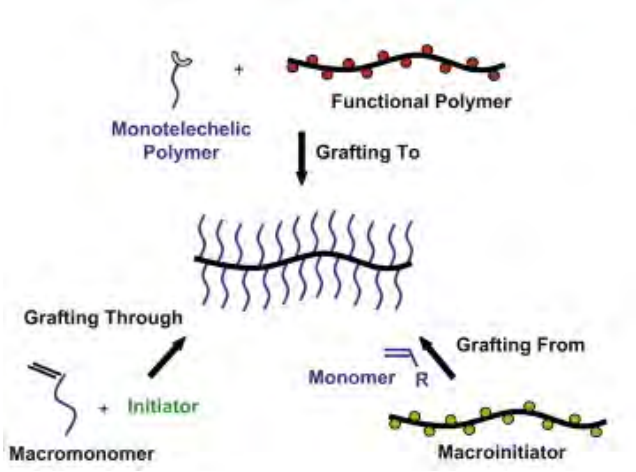

Fig. 3-1 Three main strategies for preparing molecular brushes: grafting through, grafting onto, and grafting from.

Grafting from has received much attention recently as a new pathway for the

preparation of well-defined cylindrical polymer brushes. This technique is based on the growth of side chains from polymeric backbone bound initiating groups. With the grafting from method, cylindrical polymer brushes with high grafting density and well defined backbones and side chains have been prepared. In particular, the purification of the resulting polymer brush is much simpler in comparison with the other two methods because the resulting polymer brush is the only polymeric product [9].

In this report, nonlinear optics azobenzene polymer brushes were synthesized as the following steps: (1) the synthesis of a well defined macro initiator, PBIEM, by the esterification of poly(2-hydroxyethyl methacrylate) (PHEMA), which was synthesized via RAFT of silyl-protected HEMA; (2) ATRP of MMA, Disperse Red 1 Methacrylate (DR1-MA) initiated by the pendant α-bromoester groups of PBIEM, yielding cylindrical brushes with PMMA and PDR1-MA side chain. Well defined polymer brushes were confirmed by gel permeation chromatography (GPC) and nuclear magnetic resonance spectroscopy (^{1}H NMR). Mn of the polymer brush are around 2,000k, narrow PDI 1.30~1.34, Tg =120 ^{o}C. The macroscopic EO coefficient of these polymer brushes are nearly 5 pm/V using Teng-Man measurement, indicating through ATRP can get chromophore containing polymer brush to use in binary chromophore EO materials as polymer matrix.

3.2 Experimental details

3.2.1 Materials

2-Cyanopropan-2-yl-4-fluorobenzodithioate (CPFDB) was prepared according to the literature [10]. CuBr was prepared according to the literature [11]. Anisole was stirred over CaH_2 overnight and distilled under reduced pressure. Tetrahydrofuran (THF) was distilled over CaH_2 prior to use. 2-Bromoisobutyryl bromide (98%, Aldrich), N,N,N′,N″,N″-pentamethyldiethylenetriamine (PMDETA, 99%, Aldrich), and other reagents were commercialized chemicals and used as received. Potassium fluoride, tetrabutylammonium fluoride and trimethylchloro silicane were bought from Tokyo Chemical Industry Co., LTD and used without further purification. Monomer methylmethacrylate (MMA) was distilled under reduced pressure with drier CaH_2. Methylene chloride was stirred over CaH_2 overnight. Triethylamine was dried by KOH. 2-Hydroxyethyl methacrylate (HEMA), magnesium sulfate ($MgSO_4$), 2,2′-Azobis-isobutyronitrile (AIBN, 99%, Aldrich), Methanol, cyclopentanone and hexane commercialized solvents and used as received.

3.2.2 Measurements

Thermogravametric analysis (TGA) and differential scanning calorimetry (DSC) were performed using an SII-TG/DTA 6200 instrument under a nitrogen atmosphere at a heating rate of 5 ^{o}C /min. DSC was performed using a SII-DSC 6220 under a nitrogen

atmosphere at a heating rate of 5 ^{o}C /min. The molecular weights (Mw) and polydispersity (PDI) of the polymer brushes were determined by size-exclusion chromatography (SEC) using a Shodex GPC K-804L column on a JASCO LC2000 liquid chromatography system with $CHCl_3$ as the eluent. This system was calibrated using narrow PDI Shodex SM-105 polystyrene standards. UV absorption spectra were recorded using a Shimadzu UV–vis spectrometer 1240.

3.2.3 Synthesis of HEMA-TMS

Dry HEMA (40 mL, 0.33 mol), NEt_3 (78 mL, 0.56 mol) and 600 mL dehydrate ether were added in 1000 mL flask, after well-distributed trimethylchloro-silicane (52 mL, 0.41 mol) splash into slowly at 0 ^{o}C, then warm to room temperature, stirred 12h. The resulted crude product was filtered then dissolved in ether and washed by water three times, following dried by $MgSO_4$. Reduced pressure distillation get the final product. Monomer conversion was determined by the ^{1}H NMR spectrum, synthesis route as shown in Scheme 3-1.

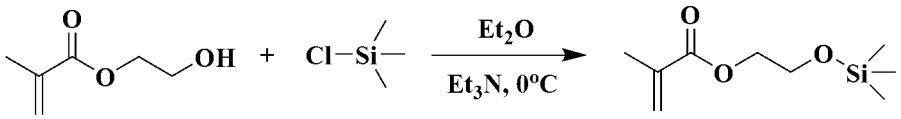

Scheme 3-1 Schematic illustration of the synthesis of HEMA-TMS

3.2.4 Synthesis of P(HEMA-TMS)

Bulk polymerization of HEMA-TMS was performed in a sealed ampule equipped

with a stir bar under vacuum. A typical procedure was as follows: CPFDB (13.8 mg, 5.8×10^{-2} mmol), AIBN (1.9 mg, 1.2×10^{-2} mmol) and HEMA-TMS (14.0 g, 69.3 mmol) were added into a 20 mL glass ampule, dehydrate THF as solvent. The mixture was degassed through four freeze-evacuate-thaw cycles, and then the ampule was sealed under vacuum.

The polymerization was carried out in an oil bath at 90 ^{o}C for 1 h. The reaction was terminated by cooling reaction the mixture with an ice bath. The resulted crude product was purified by precipitating into a large amount of methanol and water mixture (7:3 volume ratio) three times. Monomer conversion was determined by the ^{1}HNMR spectrum, synthesis route as shown in Scheme 3-2.

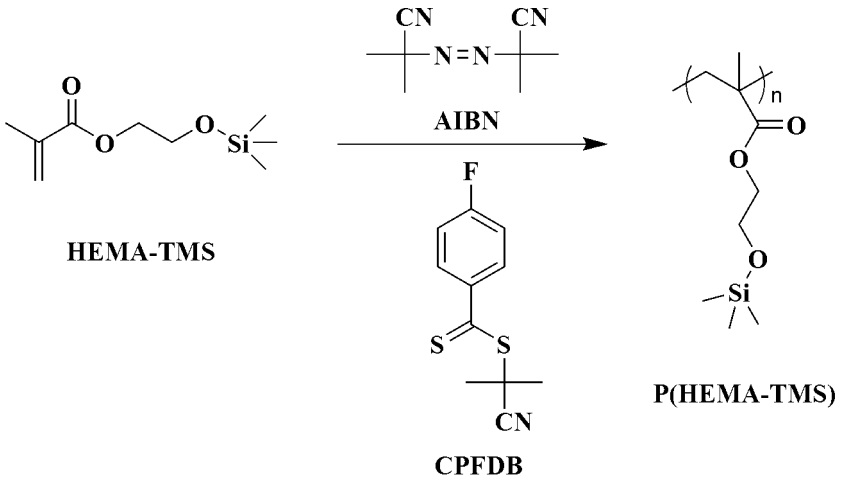

Scheme 3-2 Schematic illustration of the synthesis of P(HEMA-TMS)

3.2.5 Synthesis macro initiator PBIEMn

P(HEMA-TMS) (3.17 g, 15.7 mmol) was dissolved in dry THF (30 mL) under

nitrogen. Potassium fluoride (2.18 g, 37.5 mmol) was added followed by slow addition of tetrabutylammonium fluoride (82 mg, 0.31 mmol) in THF. 2-Bromoiso-butyryl bromide (4.74 mL, 37.6 mmol) was added dropwise over the course of 20 min. The reaction mixture was stirred at room temperature for 36 h and afterward precipitated from THF into methanol/ice (50/50 v/v). The isolated polymer was reprecipitated three times in hexane and dried under vacuum at 30 ^{o}C for 24 h, synthesis route as shown in Scheme 3-3.

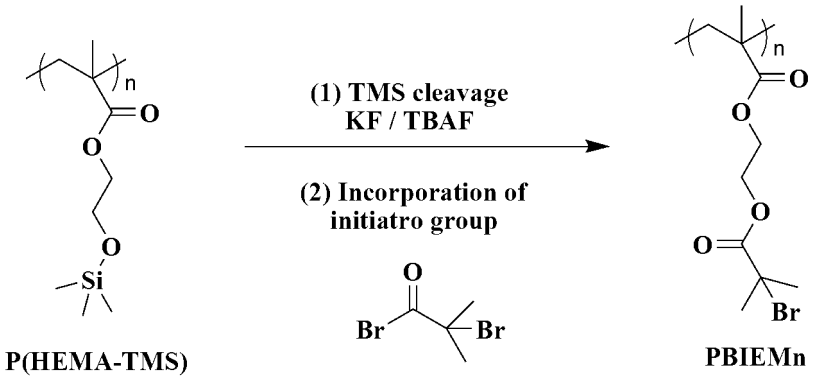

Scheme 3-3 Schematic illustration of the synthesis of PBIEMn

3.2.6 Synthesis polymer brush PBIEM-g-PMMA-g-PNABPMA-Br

Initiator $PBIEM_{450}$ (0.0140 g, 0.05 mmol), PMDETA (2.5 μL, 0.0125 mmol), MMA (1.01 g, 10 mmol), monomer DR1 (0.48 g, 1.25 mmol), and anisole (3 mL) were added into a 20 mL flask. The mixture was degassed by three freeze-evacuate-thaw cycles, and then the CuBr (1.8 mg, 0.0125 mmol) was added into the flask. The flask was sealed under vacuum after evacuated and backfilled with nitrogen twice. The polymerization was carried out in an oil bath at 90 °C for 4 h. The resulted crude

product was passed through a column filled with neutral alumina and purified by precipitating into a large amount of methanol three times. After precipitating, weighing method to calculate monomer rate of conversion, synthesis route as shown in Scheme 3-4.

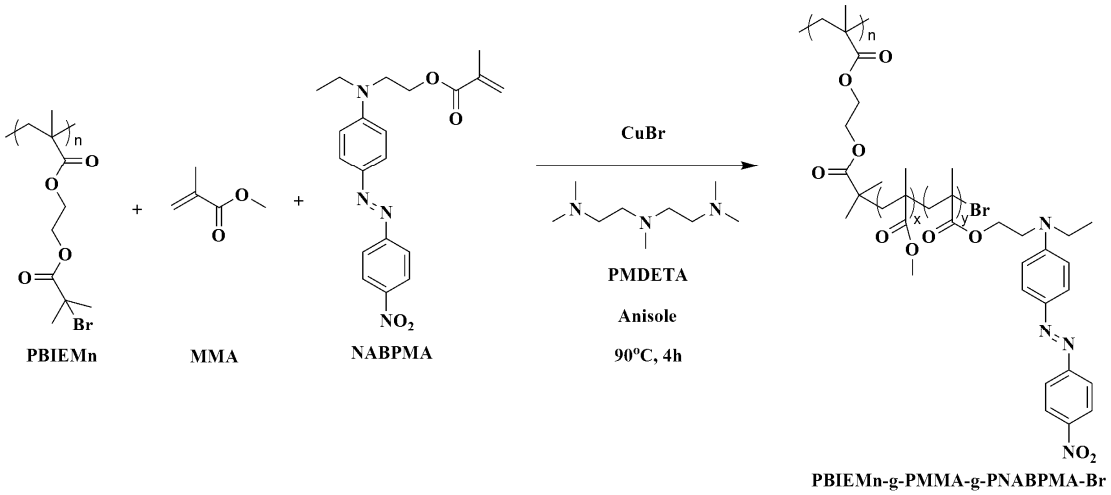

Scheme 3-4 Schematic illustration of the synthesis of PBIEMn-g-PMMA-g-PNABPMA-Br

3.2.7 Synthesis of chromophore (C4)

The chromophore investigated in this study belong to the FTC structural family and is showed in the Fig. 3-2. The detailed synthesis and characterization of this molecules has been reported extensively elsewhere [12]. Such molecules incorporate the accepter moiety, Ph-CF_3-TCF (2-dicyanomethylen-3-cyano-4-trimethyl-5-trifluoromethyl-5-phenyl-2,5-dihydrofuran.

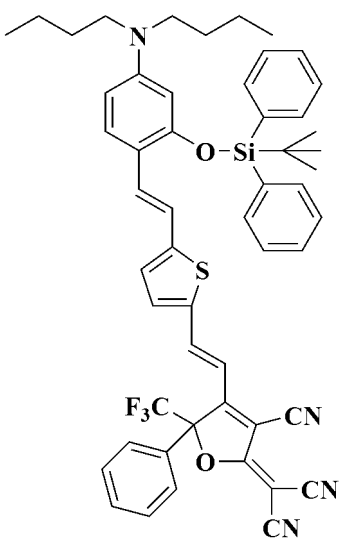

Fig. 3-2 Molecular structure of guest chromophore (**C4**)

3.2.8 Thin films preparation

The FTC chromophore (**C4**) was mixed with the host polymer brushes at 15 wt% in cyclopentanone and stirred at room temperature for 12 hours. After this dispersion phase, the resulting solutions were filtered through a 0.2 μm filter and spin coated onto an indium tin oxide (ITO) glass substrate, to produce thin films. After a short pre-baking (20 min) on a hotplate at 90 °C and then under vacuum at 85 °C (2 days) to remove the residual solvent, the measured thickness was 3.2 μm (Surface profiler - DEKTAK3). A thin gold layer (~ 50 nm) was sputtered directly onto the film to act as the electrode.

3.3 Results and discussion

3.3.1 Synthesis and characterization

3.3.1.1 Resultant of HEMA-TMS

Due to the solvent-sensitive both in polar and nonpolar solvent, this is a good property in the following synthesis steps, HEMA-TMS was choosen and prepared by hydroxyethyl methacrylate and trimethyl chlorosilane halogenating reaction, during reaction all the agent and flask need dehydrate, avoiding byproduct. After purification the final product HEMA-TMS was obtained, yield 95%. ^{1}H NMR spectrum of pure product HEMA-TMS shows in Fig. 3-3, ^{1}H NMR (δ, $CDCl_3$): 6.14 and 5.56 ppm (2H, C**H**$_2$=CHCH$_3$), 4.20 ppm (2H, COOC**H**$_2$CH$_2$), 3.82 ppm (2H, COOCH$_2$C**H**$_2$), 1.95 ppm (3H, CH$_2$=CHC**H**$_3$), 0.12 ppm (9H, OSi(C**H**$_3$)$_3$), and integral ratio is $I_{6.14}$:$I_{5.56}$:$I_{4.20}$:$I_{3.82}$: $I_{1.95}$:$I_{0.12}$ = 1:1:2:2:3:9. This certificated that we have gotten pure HEMA-TMS product, it can be use in the next step.

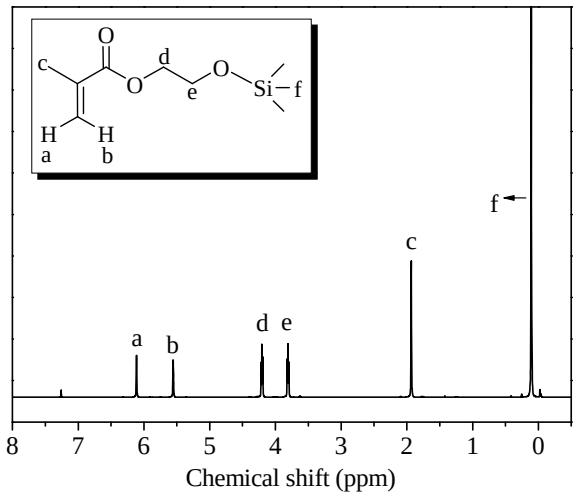

Fig. 3-3 ^{1}H NMR spectrum of the HEMA-TMS in $CDCl_3$

3.3.1.2 Resultant of PHEMA-TMS

Bulk polymerization of HEMA-TMS was performed in a typical procedure was as follows: $[HEMA\text{-}TMS]_0$:$[CPFDB]_0$:$[AIBN]_0$ = 1200:1:0.2 were added into a glass ampule. The polymerization was carried out in an oil bath at 90 °C for 1 h. Conversion ratio is 50% confirmed by ^{1}H NMR, we get a single peak in SEM, $M_{n,SEC}$ =119 Kg/mol, PDI = 1.23. The resulted crude product was purified by precipitating into a large amount of methanol and water mixture (7:3 volume ratio) three times. Azeotropy with toluene to remove water, dry in oven to get pink solid product. Monomer was determined by the ^{1}H NMR spectrum, peaks a, b, come from the protons of methylene near ester bond, and peak f come from the proton of methyl near the silicon. Integral area is a:b:c=2:2:9, indicate we get goal product PHEMA-TMS , degree of polymerization (DP) = 450, as shown in Fig. 3-4.

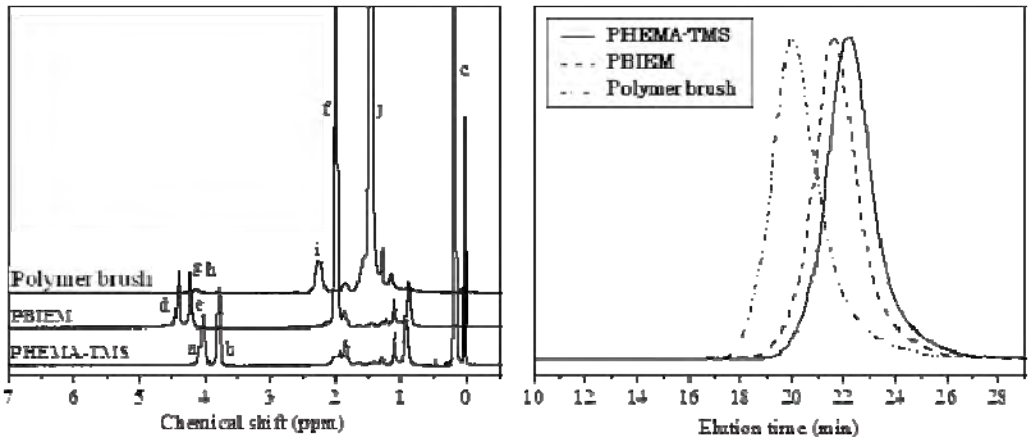

Fig. 3-4 ^{1}H NMR spectra recorded in $CDCl_3$ and DMF SEC traces recorded for PHEMA-TMS , PBIEM and PBIEM-g-PtBA.

3.3.1.3 Resultant of macro initiator Poly(2-(2-bromoisobutyryloxy)ethyl methacrylate) PBIEM$_{450}$

ATRP initiation point -Br is gotten from removing the protection group -TMS of PHEMA-TMS and introducing 2-bromoisobutyrylbromide in every repeat units, finally the macro initiator PBIEMn was obtained. ^{1}H NMR spectrum (Fig. 3-5) shows peak f chemical shift 2.0 belong the proton of methoxy near bromide. Integral ratio d:e:f=1:1:3 shows all the TMS group are instead by 2-Bromoisobutyrylbromide. SEC spectrum the elution time become fast and molecular get large, this confirm that the reaction is succeed.

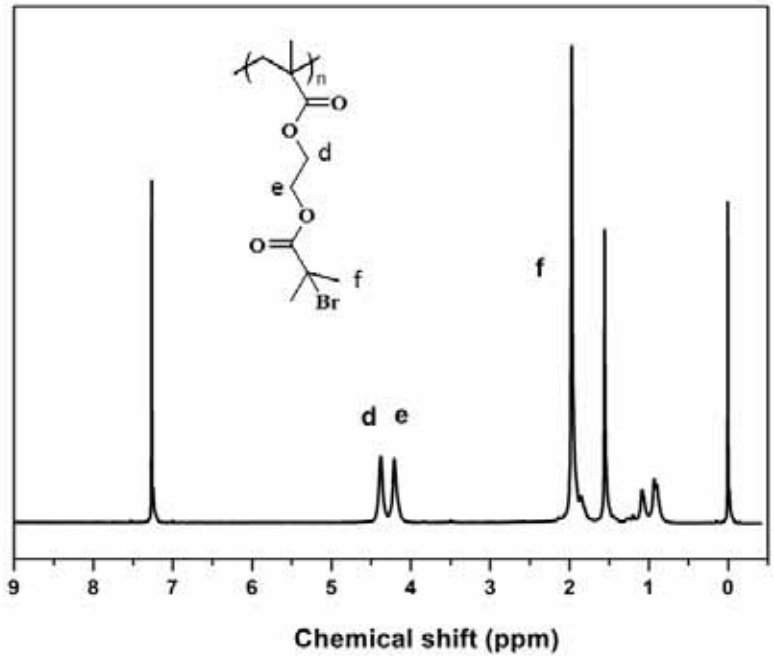

Fig. 3-5 ^{1}H NMR spectrum of macro initiator PBIEM$_{450}$

3.3.1.4 Resultant of polymer brush PBIEM-g-PMMA-PNABPMA-Br

ATRP was chosen to synthesize polymer brush $PBIEM_{450}$-g-PMMA-PNABPMA-Br due to its well control over molecular weight and chain uniformity, as shown in Scheme 3-4.

"Grafting from" way to make the polymer brush, $PBIEM_{450}$ as macro initiator, PMDETA/CuBr as catalyst, MMA and NABPMA as monomer, to put into raw materials into production ratio is as follow: $[PBIEM]_0$: $[PMDETA]_0$: $[CuBr]_0$: $[MMA]_0$: $[NABPMA]_0$= 1: 0.2: 0.2: 70: 1. The polymerization was carried out in an oil bath at 60 °C for 4 h, anisole as solvent, after three times precipitating, weighing method to calculate monomer rate of conversion is 14.3%.

^1H NMR spectrum of $PBIEM_{450}$-g-PMMA-PNABPMA-Br is demonstrated in Fig. 3-6. The peak labeled as “h” is from the protons of MMA group, and peak labeled as “g” can be assigned to the corresponding protons as depicted in the structure of monomer DR1. By comparing the peak areas of “h” (-OCH_3 protons from MMA group at 3.54 ppm) and “g” (protons on azobenzene group in monomer DR1 at 8.32 ppm), $PBIEM_{450}$-g-PMMA-PNABPMA-Br was determined to contain 64 MMA units and 8 DR1 units using percent conversion 32%, can get a number average molecular weight $M_{n,NMR}$ =1,401,840.

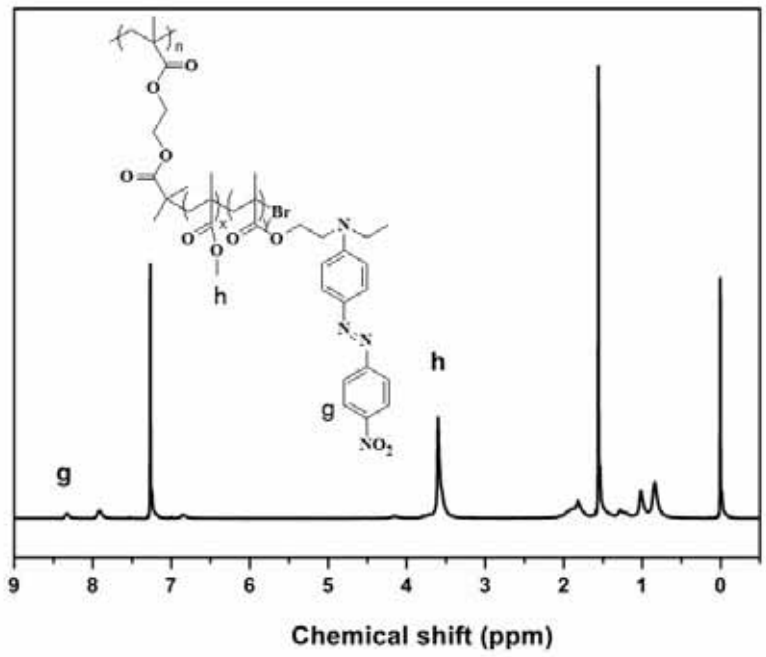

Fig. 3-6 ^{1}H NMR spectrum of azobenzene polymer brush PBIEM$_{450}$-g-PMMADR1

The gel permeation chromatography traces of the initiator PBIEM$_{450}$ and azobenzene polymer brushes PB-A, PB-B, PB-C, PB-D given by size exclusive chromatography (SEC) with standard PS calibration with a RI detector were monitored with low molecular weight distribution (Mw/Mn), 1.13 and 1.30~1.33, respectively, as shown in Fig. 3-7. The molecular weight from GPC analysis which is calibrated with linear PS standards is in accordance with by the end group analysis using ^{1}H NMR spectra.

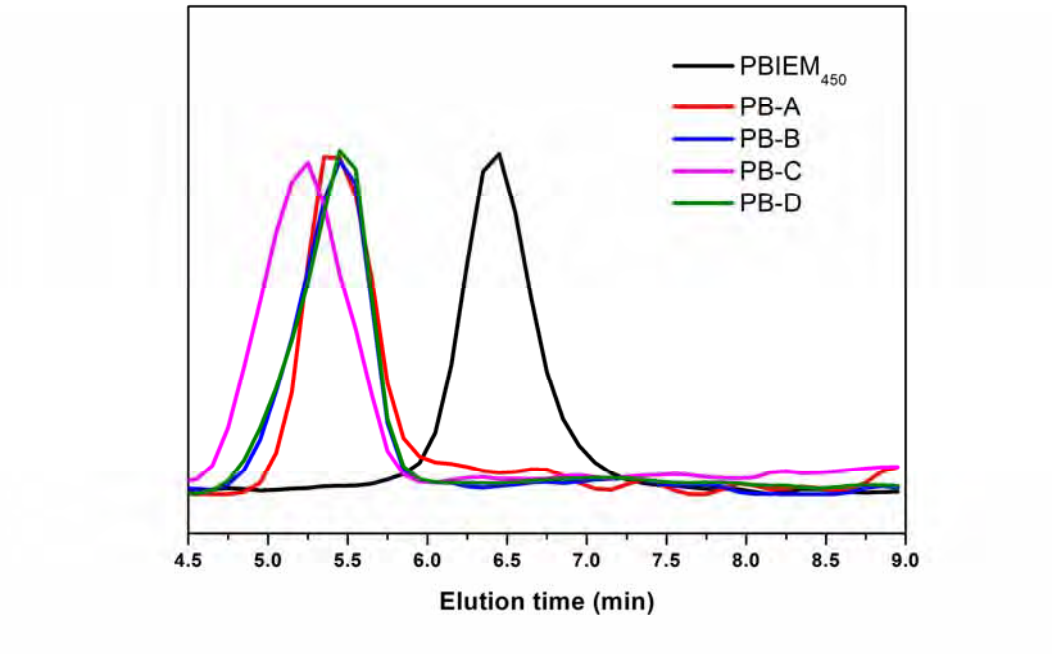

Fig. 3-7 GPC curves of $PBIEM_{450}$ and $PBIEM_{450}$-g-PMMA-PNABPMA-Br

Fig. 3-8 shows the UV absorption of DR1-MA and PB-A, PB-B, PB-C, PB-D in chloroform, from these UV absorption we can get the azobenzene dye DR1 inducing ratio, PB-A, PB-B, PB-C, PB-D respectively contain 31.51, 25.15, 23.01, 20.14 wt% DR1.

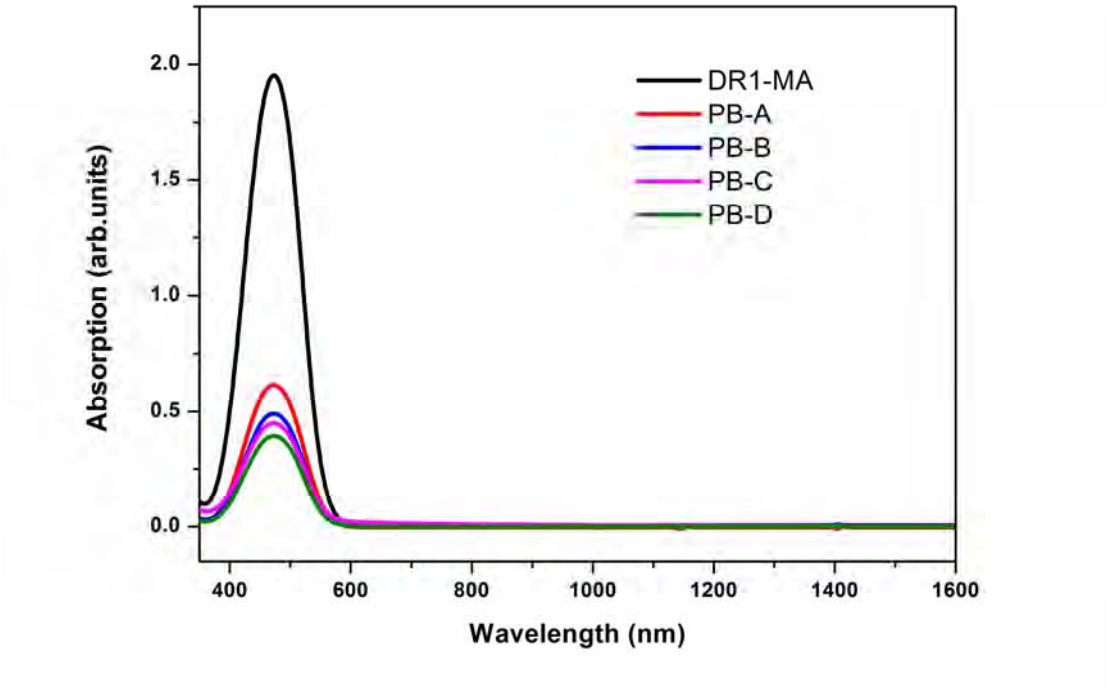

Fig. 3-8 The UV-vis absorption spectra of the DR1-MA

and polymer brushes PB-A, PB-B, PB-C, PB-D

Tg of $PBIEM_{450}$ is 53.4 ^{o}C and Tg of polymer brushes are around 120 ^{o}C, Tg spectrum of $PBIEM_{450}$ and PB-A, PB-B, PB-C, PB-D are showed in Fig. 3-9.

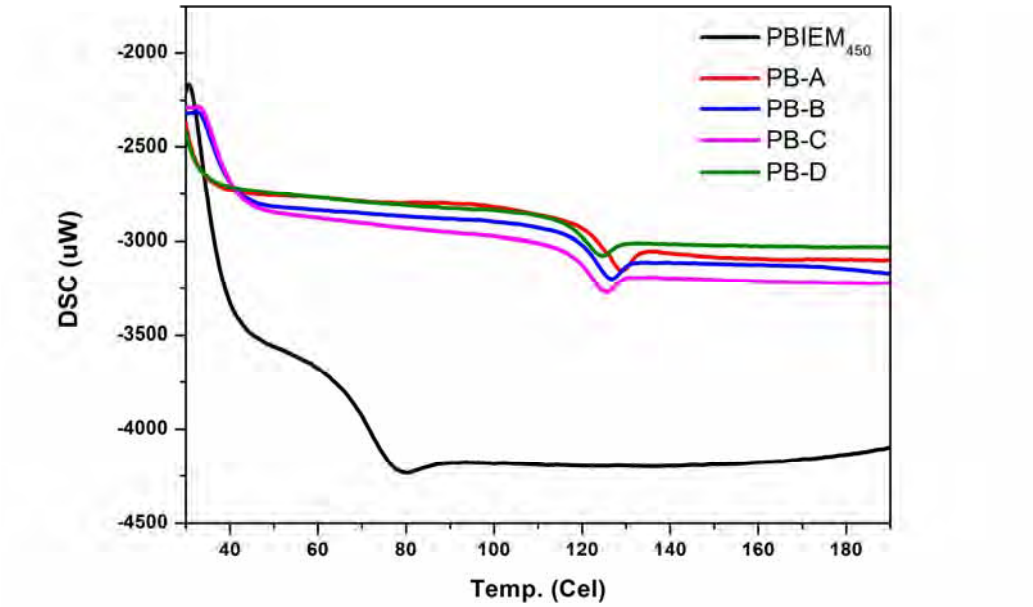

Fig. 3-9 The Tg of the $PBIEM_{450}$ and polymer brushes PB-A, PB-B, PB-C, PB-D

Td of $PBIEM_{450}$ is 283.3 ^{o}C and Td of polymer brushes are around 320 ^{o}C, Fig. 3-10 shows the Td spectrum of $PBIEM_{450}$ and PB-A, PB-B, PB-C, PB-D.

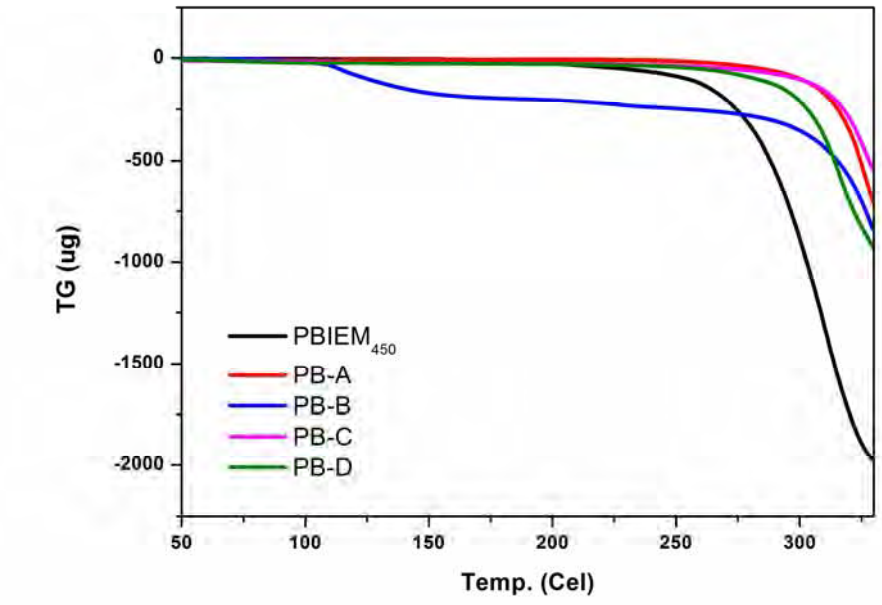

Fig. 3-10 The Td of the $PBIEM_{450}$ and polymer brushes PB-A, PB-B, PB-C, PB-D

Table 3-1 shows physical properties of the synthesized polymer brushes PB-A, PB-B, PB-C, PB-D and PMMA, including the glass transition temperature (Tg), thermal decomposition temperature (Td), molecular weight (Mn) and polydispersity Index (PDI). These polymer brushes displayed a large molecular weight, narrow PDI ~1.3, and glass transition temperature (Tg) of nearly 120 ^{o}C.

Table 3-1 Physical properties of polymer brushes

	Chromophore density UV absorption [a] (wt%)	Mn [b] ╳10^3	Mw [b] ╳10^3	PDI [b]	Tg [c] ℃	Td [c] ℃
$PBIEM_{450}$	0	69	85	1.24	53.4	283.3
PB-A	31.51	1050	1398	1.33	120.4	312.0
PB-B	25.15	1517	2028	1.34	120.2	302.3
PB-C	23.01	1973	2556	1.30	119.5	319.3
PB-D	20.14	1450	2556	1.34	119.8	317.5
PMMA	0	29	34	1.90	104.2	255.2

[a] UV absorption spectra were recorded using a Shimadzu UV–vis spectrometer 1240.

[b] The molecular weights (Mw) and polydispersity (PDI) of the polymers were determined by size-exclusion chromatography (SEC) using a Shodex GPC K-804L column on a JASCO LC2000 liquid chromatography system with $CHCl_3$ as the eluent. This system was calibrated using a narrow PDI Shodex SM-105 polystyrene standards.

[c] Thermogravametric analysis (TGA) and differential scanning calorimetry (DSC) were performed using an SII-TG/DTA 6200 instrument under a nitrogen atmosphere at a heating rate of 5 °C /min.

3.3.2 EO properties

These polymer brushes have DR1 pigment in the brush side, this invent EO effect in these materials, and after films preparation EO coefficient r_{33} of these polymer brushes were measured using Teng-Man method at 1310nm. These EO polymer brushes also acted as polymer matrix and accomplished with C4 at a function of loading concentration 15 wt% to compose EO materials, then to measure the EO coefficient r_{33}. And EO material which consist PMMA as host and loading concentration 15 wt% **C4** as guest was measured as compare. The EO coefficient r_{33} were listed in Table 3-2. Contact poling was processed with the poling voltage of 150 V/μm at glass trasition temperature, and got the final r_{33} 58 pm/V, which is higher than the chromophore in PMMA host. The EO coefficient of this polymer brush is nearly 10 pm/V by using Teng-Man measurement [13].

Table 3-2 EO coefficient of polymer brushes

	Chromophore desity	Chromophore density UV absorption [a]	none guest chromophore		guest C4	
	(mol%)	(wt%)	Max r_{33} [b]	Final r_{33} [b]	Max r_{33} [b]	Final r_{33} [b]
$PBIEM_{450}$	5	0	3	2	46	35
PB-A	15	31.51	16	13	43	27
PB-B	25	25.15	30	12	35	20
PB-C	5	23.01	13	5	77	58
PB-D	15	20.14	16	8	51	25
PMMA	-	0	-	-	33	20

[a] UV absorption spectra were recorded using a Shimadzu UV–vis spectrometer 1240.

[b] Electro-Optic(EO) coefficient measured at 1.31μm, unit of r_{33} is pm/V, unit of PE is $(nm/V)^2$.

In this work, the EO properties of the novel polymer brushes were enhanced through ATRP, this study indicated its important for the developing various well-controlled chromophore containing polymer brushes and further to prepare EO polymer matrix devices.

Figure. 3-11 to Figure. 3-14 show the conditions during poling about sample PB-C and accomplished with 25 wt% C4 chromophore.

In a general experiment, the sample was mounted on the poling stage and the temperature was increased in several minutes up to around Tg. The poling field was then applied to the sample at a ramping rate 8 V/min. During the poling process, the electric current was monitored to optimize poling efficiency and to control local electrical breakdown in the films. As shown in Figure. 3-13, the current grew rapidly with the ramping of poling field, and maximized at 140 μA when the poling field climbed to 160 V/μm. Generally, the breakdown of the electric field through the polymeric film is accompanied by an abrupt overflow of the electric current. Thus, the ramping of the poling field ceased and maintained at 160V/μm and temperature rise to 115 ^{o}C, when the second increasing trend of the current flow appeared in Figure. 3-13. The current dropped slowly after peaking, and even the poling field maintained a constant value. Figure. 3-14 indicates that the r_{33} varied simultaneously with the applied voltage and reached its maximum of 100 pm/V at the poling filed of 160

V/μm. The sample was then cooled to room temperature with the poling field maintained. During the rapid cooling process, there was a notable relaxation phenomenon of the molecular ordering as the total EO signal deceased by 42%. Eventually, r_{33} of 58 pm/V was realized at room teperature for the poled EO film after removing the poling field.

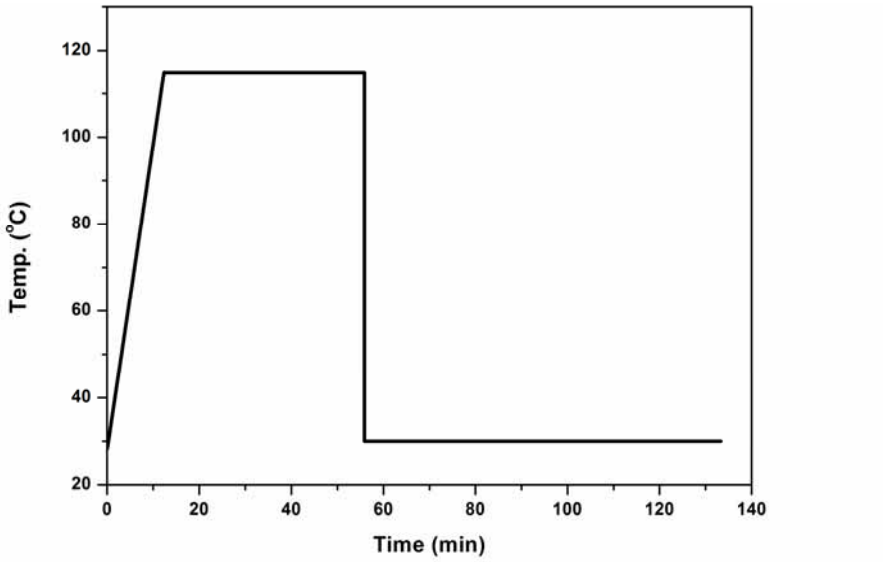

Fig. 3-11 Typical poling process on PB-C as host 15 wt% C4 as guest,

temperature are plotted during the poling process.

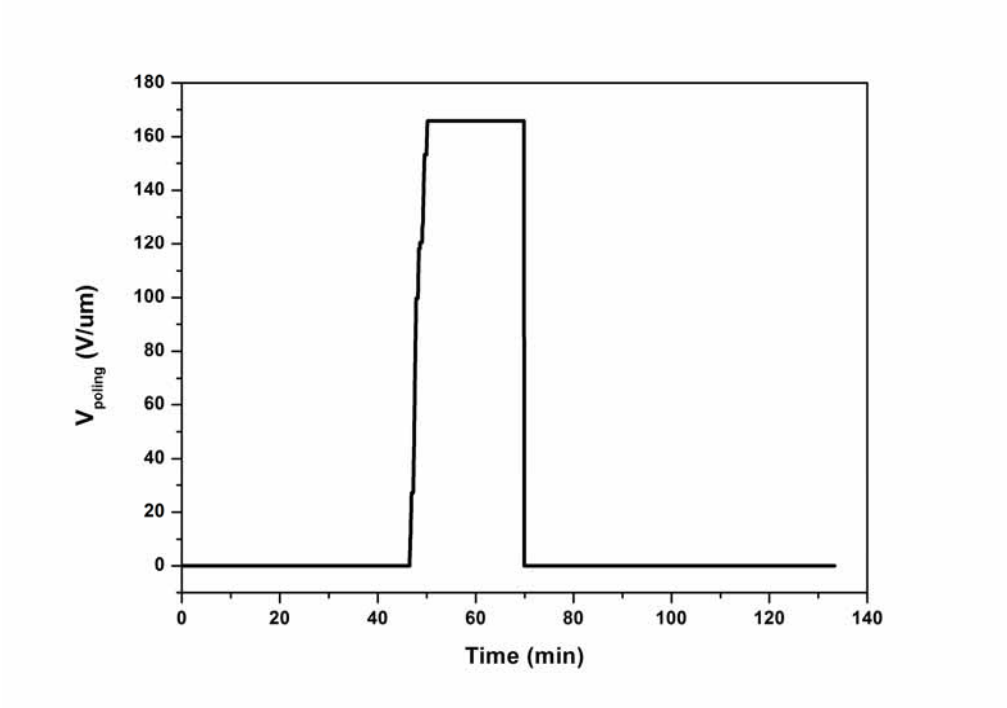

Fig. 3-12 Typical poling process on PB-C as host 15 wt% C4 as guest,

applied field are plotted during the poling process.

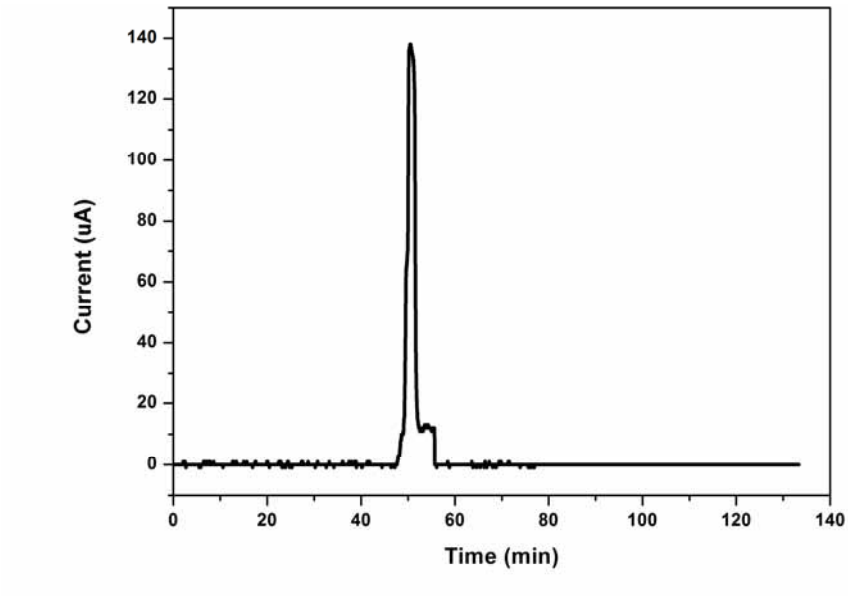

Fig. 3-13 Typical poling process on PB-C as host 15 wt% C4 as guest,

flowing current are plotted during the poling process.

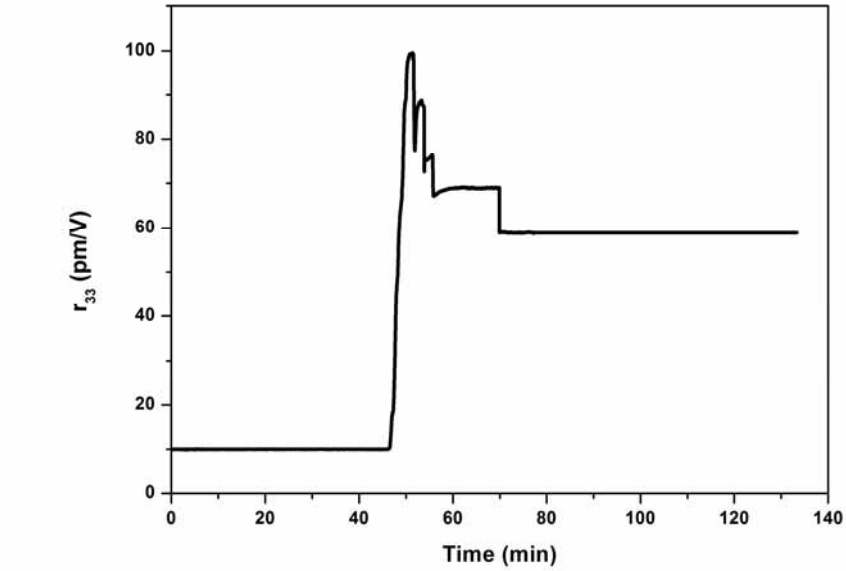

Fig. 3-14 Typical poling process on PB-C as host 15 wt% C4 as guest, r_{33} are plotted during the poling process.

3.4 Conclusions

Azobenzene polymer brushes PB-A, PB-B, PB-C, PB-D were prepared by ATRP grafting MMA and DR1-MA from a macro initiator Poly(2-(2-bromoisobutyryloxy)ethyl methacrylate) ($PBIEM_{450}$) bears bromoisobutyryl species. The reactivity ratios of the two monomers were determined to be close during the reaction, and chromophore DR1 without decomposition. Chemical structures of the four polymer brushes were confirmed by NMR, UV absorption and the GPC traces. These polymer brushes displayed a large molecular weight Mw 2000 k, PDI 1.30 ~ 1.34, and glass transition temperatures are nearly 120 ^{o}C, decompose temperature are around 310 ^{o}C. The macroscopic electro-optic coefficient of these polymer brushes were

measured using Teng-Man measurement at 1310nm. We have found that an optimum PB-C contained a cyano substituent on the brush and the r_{33} was maximized by incorporation of 25 wt% FTC chromophore into the polymer brush. In this ideal system a high r_{33} of 58 pm/V was achieved. This result may be important for developing various well-controlled chromophore containing polymer brushes and to prepare EO polymer matrix objects.

3.5 References

[1] Matyjaszewski et al. Prog. in Polym. Sci. 33 (2008) 759-789.

[2] Y. M. Chen, X. Q. Xiong. *J*. Chem. Commun. 46 (2010) 5049–5060.

[3] Zhang, M.; Mueller, A. H. E. *J.* Polym. Sci., Part A: Polym. Chem. 43 (2005) 3461-3481.

[4] Y. Xia, J. A. Kornfield, R. H. Grubbs. *J*. Macromolecules 42 (2009) 3761-3766.

[5] S. Rajaram, J. M. Frechet. *J*. J. Am. Chem. Soc. 129 (2007) 9619-9621.

[6] H. Gao, K. Matyjaszewski. *J*. Am. Chem. Soc. 129 (2007) 6633.

[7] B. Helms, J. M. J. Frechet, et al. *J.* Am. Chem. Soc. 126 (2004) 15020.

[8] A. Nese, K. Matyjaszewski. *J*. Macromolecules. 43 (2010) 4016-4019.

[9] G. Cheng, A. H. E. Müller, et al. *J*. Macromolecules. 34 (2001) 6883-6888.

[10] M. Benaglia, E. Rizzardo, A. Alberti, M. Guerra. *J*. Macromolecules. 38 (2005) 3129.

[11] G. Cheng, A. Boker, M. Zhang, G. Krausch, and A.E. Muller. *J*. Macromolecules. 34 (2001) 6883.

[12] X. Piao, X. Zhang, Y. Mori, M. Koishi, A. Nakaya, S. Inoue, I. Aoki, A. Otomo, S. Yokoyama. *J*. Polym. Sci., Part A: Polym. Chem. 49 (2011) 47.

[13] C.C. Teng, H.T. Man. *J*. Appl. Phys. Lett. 56 (1990) 1734.

Chapter 4 Electro-Optic Norbornene-2,3-dicarboximide Polymer Brushes by Tandem ROMP and ATRP

4.1 Introduction

Electro-Optic (EO) organic polymers [1][2] are being intensively investigated because of their potential applications in data processing. Such advanced applications include telecommunications, sensing and next generation computing [3]. In all of these cutting-edge technologies a low driving voltage (V π) is essential [4]. Over the last decade polymeric materials have been developed with an increasingly high EO coefficient (r_{33}); at least higher than 100 pm/V at telecommunication wavelengths. This enhanced r_{33} is a crucial requirement for the reduction of V π. The driving voltage may be defined as: $V\pi = \lambda d/(2n^3 r_{33} L\Gamma)$, where λ, d, n, L and Γ are the working wavelength, electrode gap, refractive index, interaction length and overlap integral factor, respectively [5].

The most simple and easy to prepare EO polymer system for exploitation in devices is the guest-host. In such materials, the dipolar EO chromophores have been physically incorporated into the host polymer matrix to obtain their maximum EO response. Unfortunately, there is a practical limit for the chromophore loading density beyond which the poling-induced polar order considerably decreases due to the strong intermolecular electrostatic interactions. Thus, the research efforts have been focused

on increasing the chromophore loading density, and at the same time maintaining the high poling efficiencies. Side chain polymer hosts which incorporate chromophore's appended as a side chains were the next logical step forward in the pursuit of more efficient EO materials [6]. Such systems were a dramatic improvement over simple homopolymer hosts, as the chromophore loading concentration could be increased markedly because of a reduced aggregation [7][8]. As an extension of this technology, the bi-chromophore strategy involves the appending of a small chromophore molecule (usually Disperse Red 1) onto a polymer backbone, thus forming a side chain system. This material was then employed as a host for a more enhanced hyperpolarizability chromophore such as the phenyl vinylene thiophene vinylene (FTC) or phenyl vinylene cyclohex-2-enylidene propenyl (CLD). Bi-chromophore systems have been shown to exhibit an enhanced dielectric constant in the host. This host can in turn enhance the hyperpolarizability of the guest chromophore. Furthermore the appended chromophores of the host polymer enable a large supra-molecular interaction with the guest. These interactions are primarily nuclear repulsive and dipole-dipole electrostatic. Guest-host "coupling" becomes feasible in bi-chromophore systems, which has a large impact on the acentric order under the application of an external electric field. These bi-chromophore systems therefore allow higher loading densities without phase separation because of the strong interaction between guest and host chromophores. Additionally, optical poling may lead to an isomerization of the Disperse Red 1 (DR-1) derivative (trans-cis-trans) which also has been shown to enhance the electro-optic

activity [9]. Also chromophore degradation is known to occur by singlet oxygen chemistry, a high Tg and highly networked material such as polymer brushes may prevent this degradation pathway.

Polymer brushes are known to display a highly compact and regular structure [10][11]. The physical characteristics of the polymer brush are governed by a large degree of steric repulsion between the densely grafted side chains. If used as an EO host, polymer brushes should be able to disperse chromophore molecules to a higher degree than a homopolymer, possibly to the same degree or greater than the side chain. Furthermore a well-controlled synthetic process involving chain growth polymerizations tandem ring opening metathesis polymerization (ROMP) / atom transfer radical polymerization (ATRP) may facilitate optimization of the brush properties, such as backbone / brush length variation. If utilized in an EO device we would expect polymer brushes to exhibit excellent physical stability, which is a paramount requirement in fabrication processes and long-term operation. Furthermore side chain polymer brushes may offer many of the advantages of the bi-chromophore strategy whilst also providing the beneficial physical characteristics of the brush network. The concept is illustrated in Fig. 4-1.

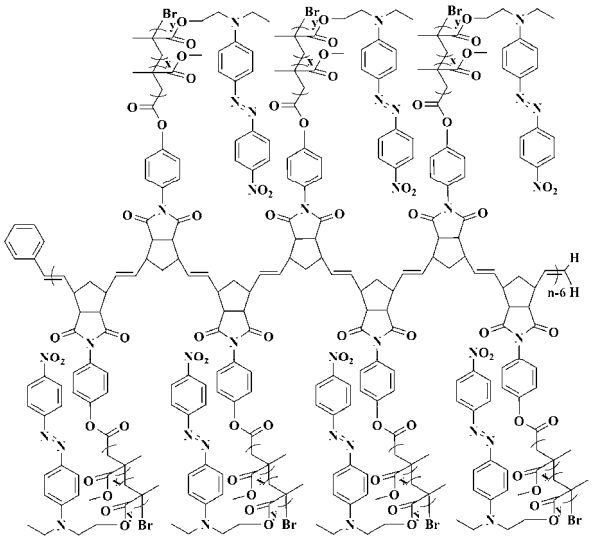

Fig. 4-1 Graphical representation of the polymer brush / bi-chromophore network.

Of the various polymer brush morphologies, the so-called cylindrical polymer brush involves a polymer backbone being densely grafted with many polymeric side chains. Owing to the strong steric repulsion between crowded branches, the main chain is extended greatly and the whole polymer displayed a wormlike morphology. Molecular brushes are branched polymers of which polymeric chains are densely tethered by one end to a linear polymer backbone [12]. Three general strategies have been used to synthesize polymer brushes: “grafting through”— the polymerization of a macro monomer, “grafting onto”— the addition of preformed side chains to a backbone and “grafting from”— the polymerization of side chains from a macromolecular initiator backbone [13][14].

In this investigation we have prepared and characterized a norbornene-dicarboximide (NDI) polymer brush containing the associative chromophore Disperse Red 1 Methacrylate (DR1-MA) in the side chains. We initially

supposed that the addition of this DR1-MA molecule may have numerous beneficial effects, such as increasing the Tg, Td and interacting strongly with other chromophores used as guests by increasing the dielectric constant of the host polymer and the enhancement of supra-molecular interactions between host and guest [15]. Initially the poly(norbornene-dicarboximide) backbone was prepared by the ROMP of NDI monomer (**1**) using Grubbs 1 (**G1**) in chloroform at room temperature. The resulting macro-initiator (**2**) underwent ATRP with DR1-MA and Methyl methacrylate (MMA) to prepare the EO polymer brush as our host. The three FTC chromophores (**C2**, **C3** and **C4**) were prepared according to the literature procedures [16]. These guest chromophores were mixed with the EO polymer brush at a chromophore wt% of 25 in a solvent of cyclopentanone to form EO materials respectively.

4.2 Experimental details

4.2.1 Materials

Anisole, chloroform ($CHCl_3$), tetrahydrofuran (THF) and methylmethacrylate (MMA) were dried over calcium hydride and distilled. N,N,N′,N″,N″-Pentamethyldiethylenetriamine (PMDETA) and **G1** were obtained from TCI and used as received. Copper (I) bromide was purified according to literature procedure [17]. Unfunctionalized DR-1 was obtained from Alfa-Asar and used without further purification.

4.2.2 Techniques

Thermogravametric analysis (TGA) and differential scanning calorimetry (DSC) were performed using an SII-TG/DTA 6200 instrument under a nitrogen atmosphere at a heating rate of 5 °C /min. DSC was performed using a SII-DSC 6220 under a nitrogen atmosphere at a heating rate of 5 °C /min. The molecular weights (Mw) and polydispersity (PDI) of the polymers were determined by size-exclusion chromatography (SEC) using a Shodex GPC K-804L column on a JASCO LC2000 liquid chromatography system with $CHCl_3$ as the eluent. This system was calibrated using a narrow PDI Shodex SM-105 polystyrene standards. UV absorption spectra were recorded using a Shimadzu UV–vis spectrometer 1240.

4.2.3 Synthesis

4.2.3.1 Synthesis of exo-Norbornene-5,6,-dicarboxylic anhydride

Into a solution of maleic anhydride (188.24 g, 1.92 mol) in o-dichlorobenzene (200 mL) at 200 ^{o}C, dicyclopentadiene (128.66 g, 0.96 mol) was added dropwise. The solution was then heated to reflux for 1.5 hours at 250 ^{o}C, then allowed to cool to room temperature. After the reation, if left for a few hours the material will crystallize out of the o-dichlorobenzene, filter off and discard the remaining o-dichlorobenzene, wash the solid with hexanes to remove any yellow coloration. At this stage the exo/endo mixture should be around 50:50. The mixture was then recrystallized from chlorobenzene twice

using a hotplate. The chlorobenzene should contain mostly endo, which is soluble. By repeating this procedure we can obtain pure exo and pure endo. To isolate the endo in the chlorobenzene precipitate into excess hexanes and filter off [18]. Yield = 81 %. ^{1}H-NMR (400 MHz, $CDCl_3$) δ: 6.33 (2H, s), 3.52 (2H, s), 2.96 (2H, s), 1.65 (1H, d), 1.46 (1H, s) ppm, synthesis route as shown in Scheme 4-1.

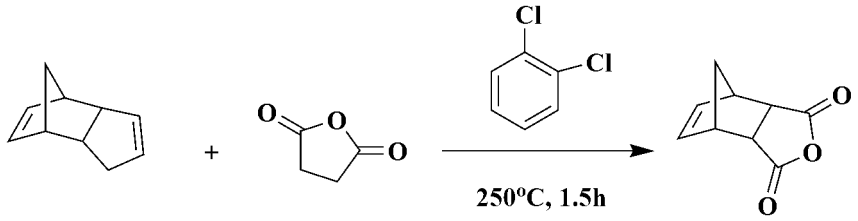

Scheme 4-1 Synthetic route of exo-Norbornene-5,6-dicarboxylic anhydride

4.2.3.2 Synthesis of n-phenol-amic acid

exo-Norbornene-5,6-dicarboxylic anhydride (33.20 g, 202.24 mmol) was dissolved in 200 mL THF. 4-Aminophenol (20.96 g, 192.09 mmol) was added to the stirred solution of exo-norbornene-5,6-dicarboxylic anhydride. The resulting solution was stirred under reflux for 24 hours. The THF was then evaporated in vacuo and the resulting solid was recrystallised from chloroform allowing the isolation of the pure material. The pure product should be a white light powder, yield 78% [19]. ^{1}H-NMR (400 MHz, $CDCl_3$) δ: 9.66 (1H, s), 9.10 (1H, s), 8.30 (2H, d), 7.31 (2H, d), 6.05 (2H, s), 3.46 (2H, d), 2.80 (2H, d), 1.75 (1H, s), 1.56 (1H, s) ppm, synthesis route as shown in Scheme 4-2.

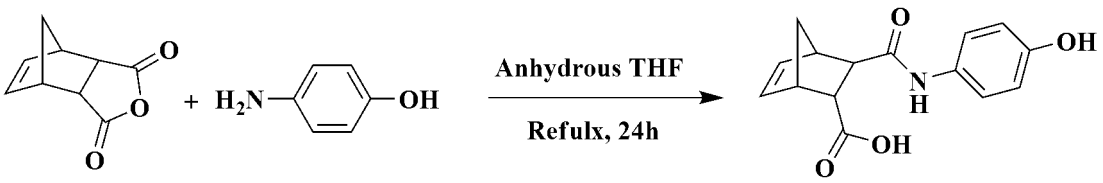

Scheme 4-2 Synthetic route of exo-Norbornene-5,6-dicarboxylic anhydride

4.2.3.3 Synthesis of N-phenol-exo-norbornene-5,6-dicarboximide

n-Phenol-amic acid (16.1 g, 58.9 mmol) and triethylamine (8.94 g, 88.4 mmol) were dissolved in 100 mL DMF and were heated at 120 ^{o}C for 3 hours. After the reaction, the resulting solution was dropped into the water (300 mL) slowly. The white solid which crystalized out was filtered, washed weveral times with water, and dried in a vacuum oven at 50 ^{o}C overnight. Pure compound of N-phenol-exo-norbornene-5,6-dicarboximide was obtained (7.35 g), yield 49% [20]. ^{1}H-NMR (400 MHz, $CDCl_3$) δ: 7.35 (2H, d), 7.20 (2H, d), 6.38 (2H, s), 3.40 (2H, s), 2.85 (2H, s), 1.62 (1H, d), 1.45 (1H, d) ppm, synthesis route as shown in Scheme 4-3.

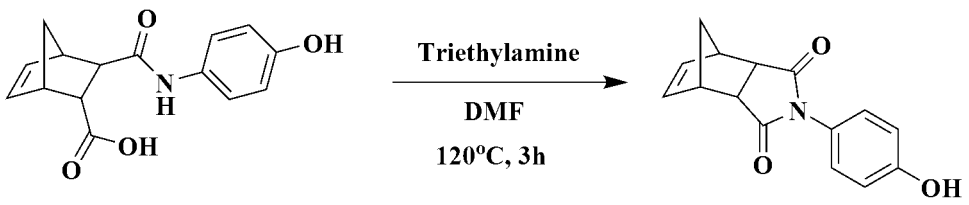

Scheme 4-3 Synthetic route of n-phenol-amic acid

4.2.3.4 Monomer NDI (1) synthesis

The NDI monomer (**1**) was prepared according to a modification of literature procedure [21]. By these methods described, we initially prepared the precursor

N-phenol-norbornene-5,6-dicarboximide. The N-phenol-norbornene-5,6-dicarboximide (4.01 g, 15.90 mmol) was dissolved THF (120 mL). To this stirred solution was added triethylamine (4.5 mL, 23.85 mol). The mixture was cooled to 0 °C, after which a solution of 2-bromoisobutyryl bromide (2.37 mL, 19.08 mmol) in THF (40 mL) was added to the reaction vessel dropwise *via* syringe. The resulting solution was stirred for a further 3 hours at 0 °C and allowed to warm to room temperature overnight. Silica thin layer chromatography (TLC) using a solvent ethyl acetate revealed the complete disappearance of the starting material N-phenol-norbornene-5,6-dicarboximide. The ammonium salt byproduct was filtered off and the solvent removed under reduced pressure to yield a pale-yellow residue that was purified by Si chromatography in a solvent system of ethyl acetate. Yield = 81 %. ^{1}H-NMR (400 MHz, $CDCl_3$) δ: 7.34 (2H, d, J = 9Hz), 7.24 (2H, d, J = 9Hz), 6.36 (2H, m), 2.86 (2H, s), 2.06 (6H, s), 1.62 (1H, d, J = 9Hz), 1.46 (1H, d, J = 9Hz) ppm. ^{13}C-NMR (125 MHz, $CDCl_3$) δ: 177.25, 138.42, 127.83, 122.18, 48.17, 46.19, 43.32, 30.89 ppm. EI-MS: 405 m/z, synthesis route show in Scheme 4-4.

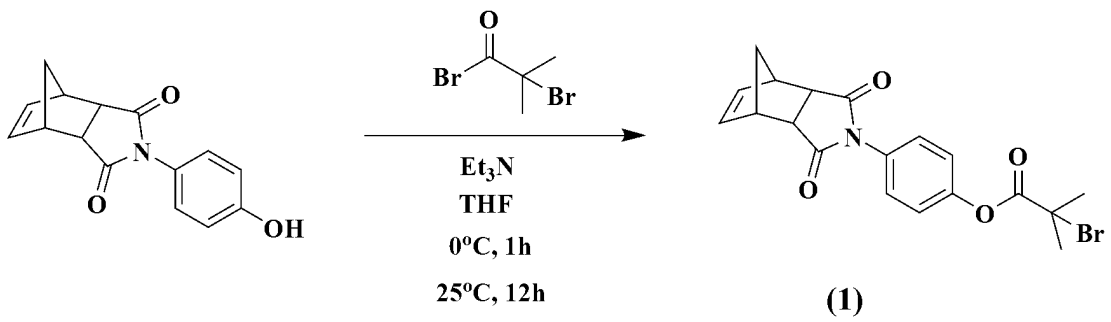

Scheme 4-4 Synthetic route of NDI monomer **(1)**

4.2.3.5 Synthesis of macro-initiator (2)

The NDI monomer (**1**) (3.30 g, 8.16 mmol) was dissolved in nitrogen degassed anhydrous chloroform (30 mL) and stirred at room temperature under nitrogen for 10 minutes. The **G1** initiator (67 mg, 8.16×10^{-5} mmol) was transferred to a separate vessel and also dissolved in nitrogen degassed anhydrous chloroform (1.0 mL). The initiator **G1** was dissolved by agitation on a vortex mixer. This initiator solution was the transferred quickly to the reaction vessel *via* syringe and the polymerization was allowed to proceed at room temperature for 60 minutes. After this time, quenching was achieved by the addition of an excess (8 mL) of degassed ethyl vinyl ether. After stirring for an additional 30 minutes at room temperature the desired polymer was isolated by precipitation into methanol. The pristine polymer was obtained by multiple dissolutions in chloroform and precipitations into methanol. After filtration the polymer (**2**) was dried under vacuum at 30 ^{o}C for 24 hours. Yield = 93 %. ^{1}H-NMR (400 MHz, $CDCl_3$) δ: 7.34 (2 H, d, J = 9 Hz), 7.24 (2 H, d, J = 9 Hz), 5.81 (1.73 H, m)$_{trans}$, 5.57 (0.27 H, m)$_{cis}$, 3.52 (0.28 H, s)$_{cis}$, 3.15 (2 H, s)$_{trans/cis}$, 2.87 (1.72 H, s)$_{trans}$, 2.44-1.29 (2 H, m), 2.06 (6 H, s) ppm. Td (10 % loss) = 263 °C, Tg (2nd scan) = 121°C. Mw = 27,795, PDI = 1.16, Scheme 4-5.

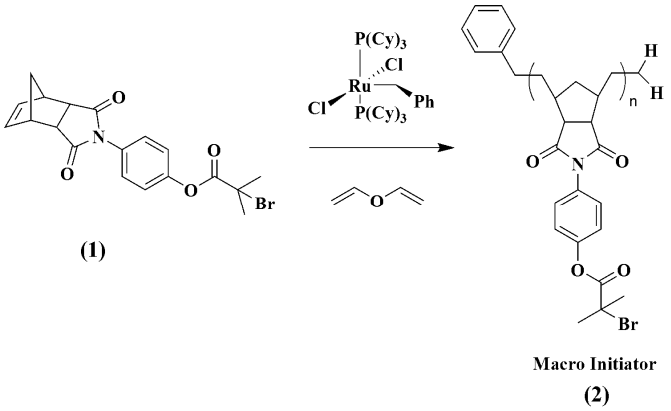

Scheme 4-5 Synthetic route of macro initiator **(2)**

4.2.3.6 Preparation of polymer-brush (3)

The macro-initiator (**2**) (14 mg, 0.05 mmol), PMDETA (2.5 μL, 0.0125 mmol), MMA (1.01 g, 10 mmol), modified DR1 (0.48 g, 1.25 mmol), and anisole (3 mL) were transferred to a Schlenk tube. The materials were thoroughly degassed by using multiple freeze-pump-thaw cycles. After which CuBr (1.8 mg, 0.0125 mmol) was added to the vessel under a nitrogen atmosphere. The polymerization to yield polymer-brush (**3**) was then carried out at 90 °C for 8 hours. The pristine material was purified by passing through a neutral alumina plug and the obtained solution being precipitated into methanol multiple times. Yield = 56 %. Mw = 219,018, PDI = 1.24. Td = 307 °C, Tg = 126 °C, Scheme 4-6.

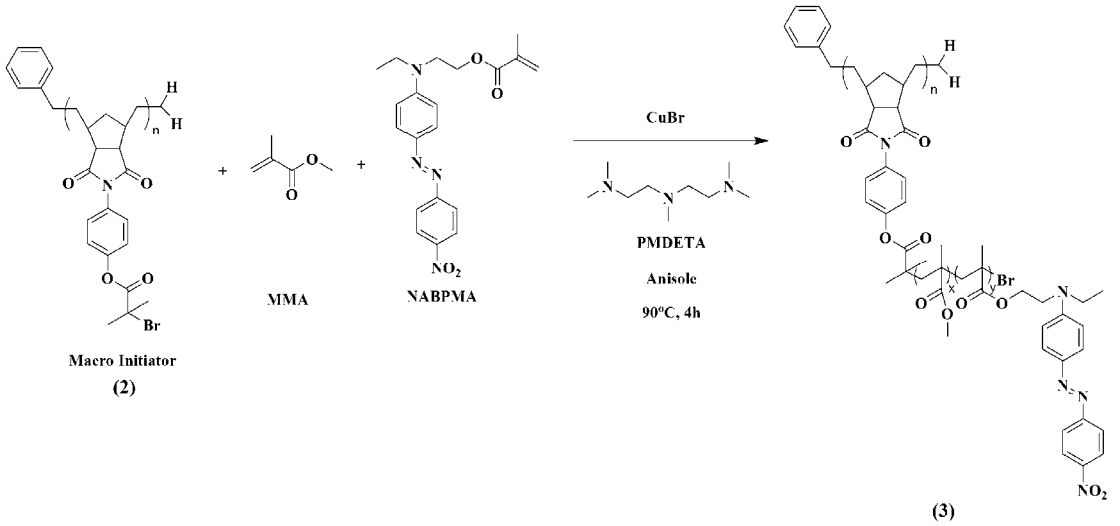

Scheme 4-6 Synthetic route of DR1 containing polymer brush **(P3)**

4.2.3.7 Synthesis of chromophores (C2, C3 and C4)

The chromophores investigated in this study belong to the FTC structural family and are shown in the Fig. 4-2. The detailed synthesis and characterization of these molecules has been reported extensively elsewhere. Such molecules incorporate the accepter moiety, Ph-CF_3-TCF (2-dicyanomethylen-3-cyano-4-trimethyl-5-trifluoromethyl-5-phenyl-2,5-dihydrofuran. **C3** also incorporates the enhanced electron donating phenylmethanol group, which further increases β. Finally the enhanced chromophore **C4**, exhibits the much more strongly donating tert-butyldiphenylsilanol group.

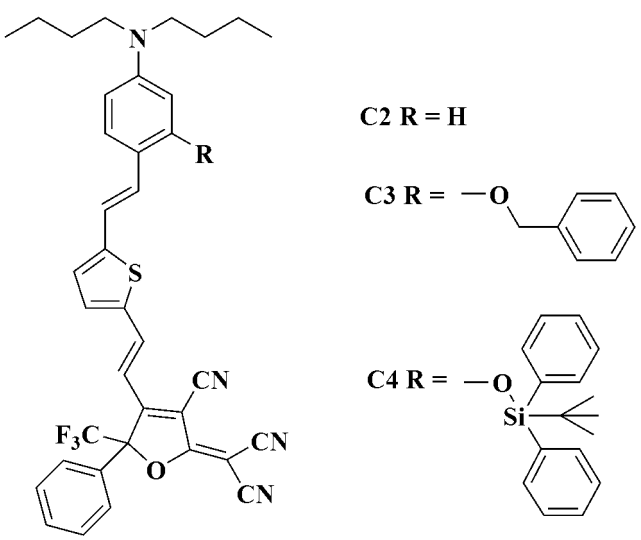

Fig. 4-2 Chromophore structures investigated in **Chapter 4**

4.2.4 Thin film preparation

The three guest chromophores (**C2**, **C3** or **C4**) were mixed with the host polymer-brush (**P3**) at 25 wt% in cyclopentanone and stirred at room temperature for 12 hours. After this dispersion phase, the resulting solution was filtered through a 0.2 μm filter and spin coated onto an indium tin oxide (ITO) glass substrate, to produce films with a thickness of 3 μm (Surface profiler - DEKTAK3). After a short pre-baking (20 min) on a hotplate at 90 ^{o}C and then under vacuum at 85 ^{o}C (2 days) to remove the residual solvent, a gold layer (~ 50 nm) was sputtered as a top electrode.

4.3 Results and discussion

4.3.1 Synthesis and characterization

The NDI monomer (**1**), macro-initiator (**2**) and polymer brush (P**3**) were prepared

according to the Scheme 4-1 ~ Scheme 4-6. NDI monomer (**1**) was synthesized *via* an N-phenol-5-norbornene-2,3-dicarboximide precursor prepared according to the literature. The hydroxyl group of this compound was transformed using 2-bromoisobutyryl bromide to yield the desired NDI monomer (**1**). The monomer was subsequently polymerized *via* ROMP in chloroform using the **G1** initiator at room temperature for 60 minutes. The living polymerization was quenched by the addition of an excess of ethyl vinyl ether. Macro-initiator (**2**) was obtained by filtration and multiple precipitations from chloroform into methanol. In order to prepare the polymer brush (**P3**), the macro-initiator (**2**), PMDETA, MMA and DR1-MA were dissolved in anisole. The addition of a small quantity of CuBr facilitated the ATRP at 50 °C for 8 hours. The polymer brush (**P3**) had a good solubility in a wide range of organic solvents such as THF, DMSO and chloroform. The chemical structure of the macro-initiator (**2**) and polymer brush (**P3**) were confirmed by ^{1}H nuclear magnetic resonance spectra (^{1}HNMR). Brush preparation was also confirmed by the Size Exclusion Chromatography measured Mw increasing from 27,800 for the macro-initiator (**2**) to 219,000 g/mol for the polymer brush (**P3**). The measured Tg of the macro-initiator (**2**) was 121 ^{o}C, upon formation of the brush this increased to 126 ^{o}C, similarly the Td of (**2**) was 263 ^{o}C, increasing to 307 ^{o}C after brush formation. PDI's of the macro-initiator and brush were relatively similar at 1.16 and 1.24 respectively. We would have expected the PDI to increase a little upon brush formation. DR1-MA incorporation into the polymer brush was evaluated using the UV-vis absorption spectra, calculated against pure

DR1-MA standards of a known concentration. By a comparison of the DR1-MA monomer absorption and that of the polymer brush (**P3**) we can calculate the DR1-MA concentration as 4.0 %. TGA analysis (10% loss) shows that the polymer brush (**P3**) did not undergo significant decomposition below 300 ^{o}C, therefore poling at temperature ranges of the polymer Tg (~ 120 ^{o}C) should not have any detrimental effect on the host.

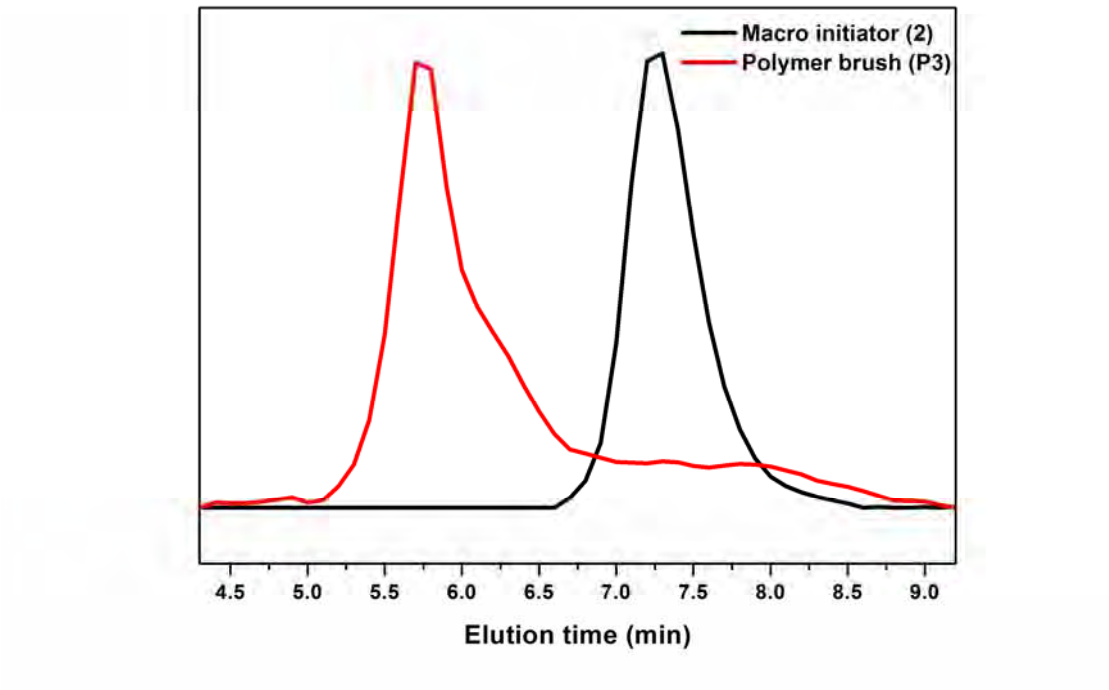

Fig. 4-3 The GPC trace of the macro initiator (**2**) and polymer brush (**P3**)

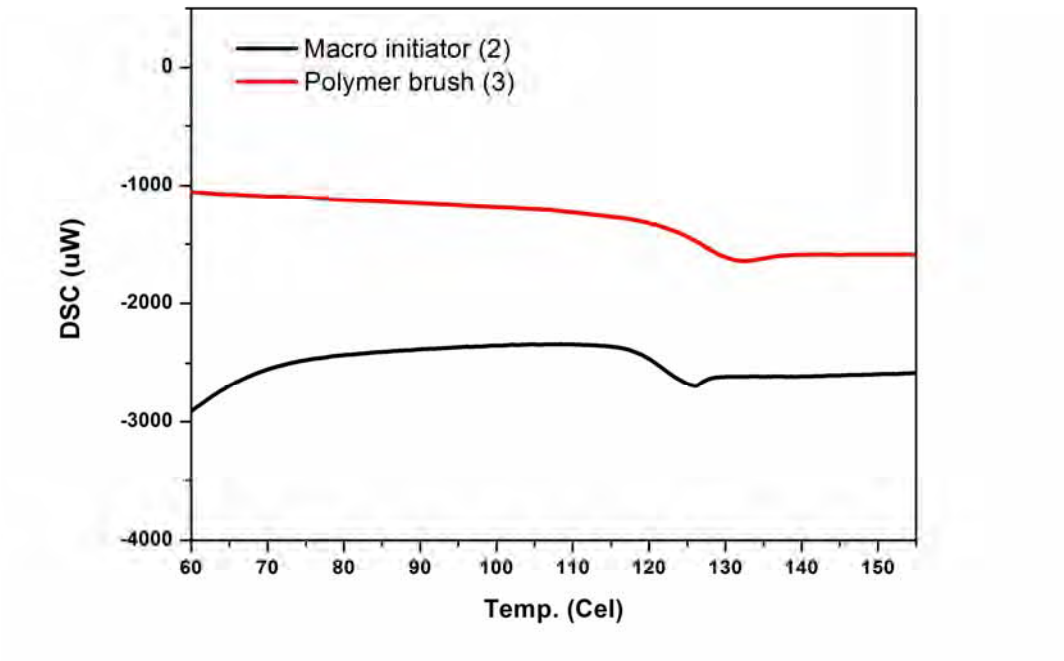

Fig. 4-4 The Tg trace of the macro initiator (**2**) and polymer brush (**P3**)

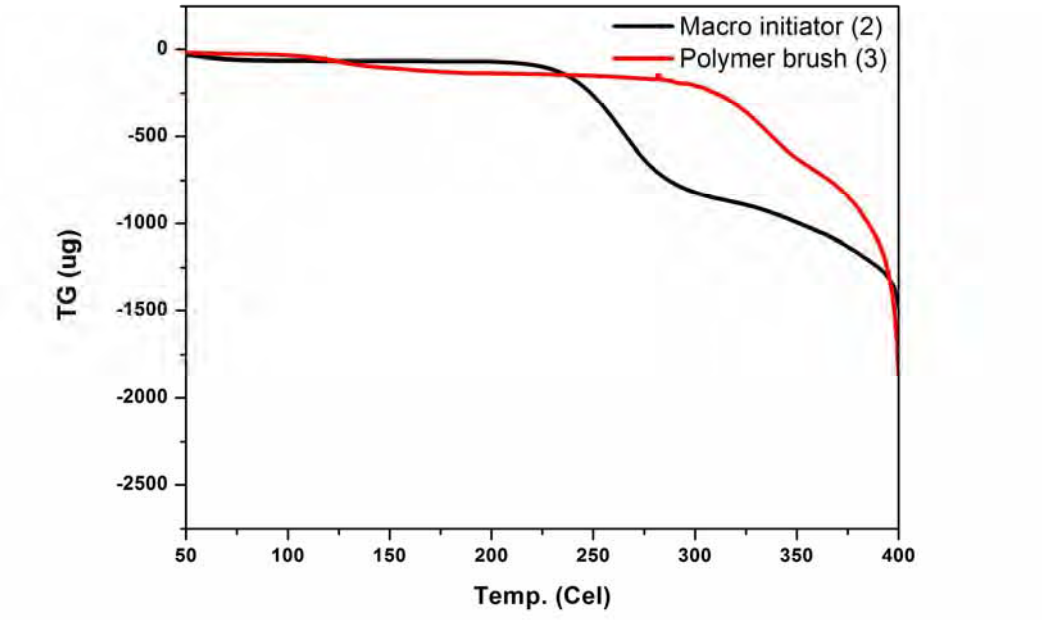

Fig. 4-5 The Td trace of the macro initiator (**2**) and polymer brush (**P3**)

4.3.2 NLO properties

From trial and error experiments we have found that the optimum chromophore (**C2**, **C3**, **C4**) loading density in a simple PMMA host is approximately 25 wt%. This can also be expressed as approximately 10^{20} molecules / cm^3. Consequently the three chromophore's were also dispersed into the polymer brush (P**3**) at this concentration. After preparing the thin films and devices, contact poling was performed using an applied electric field of 100-130 V/μm at elevated temperatures near the glass transition temperature (Tg) of the materials. Diameter of the circular gold electrode was 5 mm. The r_{33} response was measured using a simple reflection method at 1310 nm with a modulation frequency 1000 Hz.

Table 4-1 The chromophore's Td, λ_{max} in film, the r_{33}, the poling efficiency (PE) for both PMMA and polymer brush (P3) and the r_{33} enhancement (Δr_{33}).

chromophore	Td [a] (°C)	λ_{max} [b]	PMMA		P3		Δr_{33} (%)
			r_{33} [c]	PE [c]	r_{33} [c]	PE [c]	
C2	220	766	41	0.51	58	1.03	17
C3	219	823	62	0.63	87	1.28	25
C4	230	827	76	0.70	94	1.37	18

[a] Thermogravametric analysis (TGA) and differential scanning calorimetry (DSC) were performed using an SII-TG/DTA 6200 instrument under a nitrogen atmosphere at a heating rate of 5 °C /min.

[b]UV absorption spectra were recorded using a Shimadzu UV–vis spectrometer 1240.

[c]Electro-Optic(EO) coefficient measured at 1.31μm, unit of r_{33} is pm/V, unit of PE is $(nm/V)^2$.

Using TGA, we have established that chromophore (**C2**, **C3** and **C4**) decomposition under nitrogen occurs at temperatures above 220 ^{o}C. **C4** exhibited the highest Td (230 ^{o}C), possibly a consequence of the bulky tert-butyldiphenylsilane moiety. **C2** and **C3** showed fairly similar Td's at 220 ^{o}C and 219 ^{o}C respectively. (**Table 4-1**) The λ_{max} of the three chromophores was measured in film. We observed that **C4** with the strongly donating tert-butyldiphenylsilane moiety, had the longest λ_{max} (827 nm). **C3** with the less donating phenylmethanol moiety showed a reduced λ_{max} of 823 nm, whilst **C2** with no substituent exhibited the shortest λ_{max} at 766 nm respectively. Furthermore the molecular hyperpolarizability was expected to increases in the order from **C2** to **C3** to **C4**. The λ_{max} of polymer brush (P**3**), which incorporates the DR1-MA molecule, showed a single small absorption at approximately 500 nm. (Fig. 4-6)

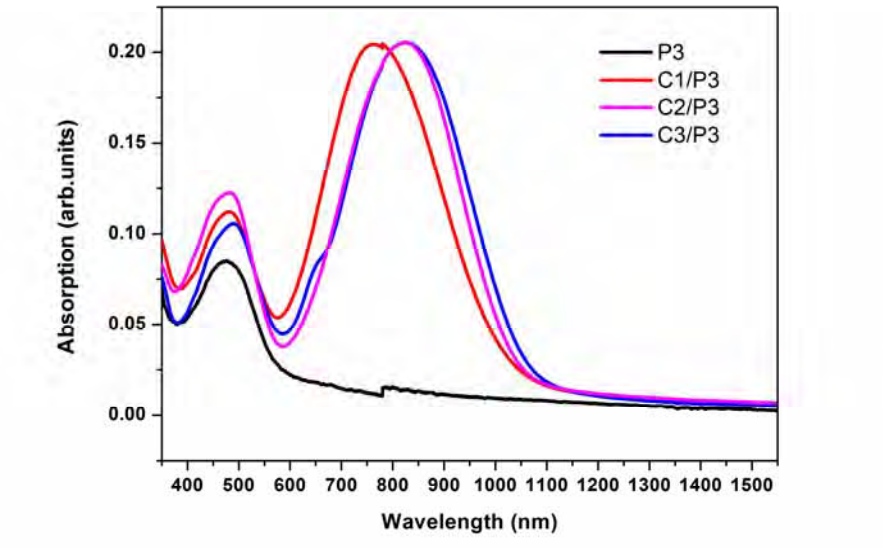

Fig. 4-6 The UV-vis absorption spectra of the polymer brush (P**3**) / chromophore **C2**, **C3** and **C4** thin films and un-doped polymer brush (P**3**).

After film preparation, the r_{33} was measured for the polymer brush / **C2**, **C3**, **C4** host-guests and compared with a benchmark host polymer PMMA. In PMMA, **C4** achieved the highest r_{33} of 76 pm/V, with **C3** giving 62 pm/V and **C2** yielding 41 pm/V (**Table 4-1**). Such a trend can be expected from a consideration of the different chromophore structures and their respective hyperpolarizabilities (β). It seems that the miscibility of all three chromophores are good in PMMA. When considering the results for polymer brush (P**3**) and the three chromophores we can see that in all cases, both the r_{33} and the poling efficiencies are enhanced over our PMMA benchmark. When considering the r_{33} compared to PMMA, **C2** / **P3** exhibits a Δr_{33} of 17, **C3** / **P3** a Δr_{33} of 25 and **C4** / **P3** a Δr_{33} of 18 respectively compared to PMMA. Therefore from **Table 4-1**, we can conclude that in all cases where the polymer brush **P3** is used, the poling efficiency is enhanced over the PMMA host, with values > 1. We can clearly observe that the polymer brush and chromophore **C4** have the highest poling efficiency (1.03), followed by **C3** (1.28) and lastly **C2** (1.37). For PMMA values were always < 1. Chromophore **C4** yielded 0.70, **C3**; 0.63 and **C2**; 0.51. Clearly the optimum chromophore is **C4** for PMMA and **P3**, which is a consequence of the much higher hyperpolarizability of the structure. Furthermore in all cases the **P3 /** chromophore combinations were greatly enhanced compared to the benchmark homopolymer PMMA. The long term thermal stability of the poled polymer films was tested in air at room temperature and at 85^{o}C. At room temperature, more than 95% of the initial r_{33} value remained after 500 hours exposure time for all samples.

Therefore from Table 4-1, for the PE we can conclude that in all cases where the polymer brush P3 is used, the poling efficiency is enhanced than for the PMMA host, with values > 1. We can clearly observe that the polymer brush and chromophore C4 have the best poling efficiency (1.03), followed by C3 (1.28) and lastly C2 (1.37). For PMMA values were always below < 1. Chromophore C4 yielded 0.70, C3; 0.63 and C2; 0.51. Clearly the optimum chromophore is C4, which is a consequence of the much higher hyperpolarizability of the structure. Furthermore in all cases the P3 chromophore combinations were greatly enhanced compared to the benchmark PMMA.

4.4 Conclusions

A norbornene-dicarboximide derived polymer brush (**P3**) was prepared from a bi-functional monomer (**1**) capable of both ROMP and ATRP. Initially a norbornene-dicarboximide macro-initiator was synthesized by the ROMP of NDI monomer (**1**) using **G1** in chloroform at room temperature. ATRP was then used to grow the cylindrical polymer brush (**P3**), whilst also incorporating a DR1-MA associative chromophore for enhanced bi-chromophore miscibility. This polymer brush (**P3**) was used as an EO-host for our high hyperpolarizability chromophore (**C2**, **C3** and **C4**) guests. Measurement of the r_{33} using in-situ poling *via* the Teng-Man reflection technique showed that polymer brush (**P3**) and chromophore **C4** exhibited a maximum r_{33} of 94 pm/V as compared to 74 pm/V for the PMMA standard. The poling efficiency

of this optimal system was 1.37 as compared to 0.70 for PMMA. This is a consequence of the optimized chromophore structure (**C4**) incorporating as strongly donating tert-butyldiphenylsilane moiety which enhances β and an excellent compatibility with our polymer brush (**P3**). Such sophisticated polymer brush / bi-chromophore host-guest systems are a recent development in the field of electro-optics. Here we present the preliminary investigations of this effective system, further optimization may lead to a greatly enhanced r_{33} after a careful tuning of the brush characteristics.

4.5 References

[1] J. Luo, S. Huang, Z. Shi, B. M. Polishak, X.-H. Zhou, A. K-Y. Jen. *J*. Chem. Mater. 23 (2010) 544.

[2] N. S. Allen, Photochemistry and Photophysics of Polymer Materials. John Wiley & Sons: New York, 2010

[3] M. Hochberg, T. Baehr-Jones, G. Wang, M. Shearn, K. Harvard, J. Luo, B. Chen, Z. Shi, R. Lawson, P. Sullivan, A. K. Y. Jen, L. Dalton, A. Scherer. *J*. Nat Mater 5 (2006) 703.

[4] X. Piao, S. Inoue, S. Yokoyama. *J*. Thin Solid Films. 518 (2009) 481-484.

[5] X. Piao, X. Zhang, Y. Mori, M. Koishi, A. Nakaya, S. Inoue, I. Aoki, A. Otomo, S. Yokoyama. *J*. Polym. Sci., Part A: Polym. Chem. 49 (2011) 47.

[6] D. Briers, G. Koeckelberghs, I. Picard, T. Verbiest, A. Persoons, C. Samyn. *J*. Macromol. Rapid Commun. 24 (2003) 841.

[7] D. Briers, G. Koeckelberghs, I. Picard, T. Verbiest, A. Persoons, C. Samyn. *J*. Macromol. Rapid Commun. 24 (2003) 841.

[8] A. Scarpaci, C. Cabanetos, E. Blart, V. Montembault, L. Fontaine, V. Rodriguez, F. Odobel. *J*. J. Polym. Sci., Part A: Polym. Chem. 47 (2009) 5652.

[9] S. S. Sheiko, B. S. Sumerlin, K. Matyjaszewski. *J*. Prog. Polym. Sci. 33 (2008) 759.

[10] M. Zhang, A. H. E. Müller. *J*. J. Polym. Sci., Part A: Polym. Chem. 43 (2005) 3461.

[11] Y. Chen, X. Xiong. *J*. The Royal Society of Chemistry. 46 (2010) 5049.

[12] W. Zhang, Y. Li, L. Liu, Q. Sun, X. Shuai, W. Zhu, Y. Chen. *J*. Biomacromolecules 11(2010) 1331.

[13] H. Zhu, G. Deng, Y. Chen. *J*. Polymer 49 (2008) 405.

[14] P. A. Sullivan, J. Luo, L. R.Dalton. *J*. Acc. Chem. Res. 43 (2010) 10.

[15] P. A. Sullivan, J. Luo, L. R.Dalton. *J*. Acc. Chem. Res. 43 (2010) 10.

[16] A. J. D. Magenau, Y. Kwak, K. Matyjaszewski. *J*. Macromolecules 43 (2010) 9682-9689.

[17] G. Cheng, A. Boker, M. Zhang, G. Krausch, and A.E. Muller. *J*. Macromolecules. 34 (2001) 6883.

[18] K.F. Castner, N. Calderon. *J*. Journal of Molecular Catalysis. 15 (1982) 47-59.

[19] A. P. Contreras, A. M. Cerda, M. A. Tlenkopatchev. *J*. Macromo. Chem. Phys. 203 (2002) 1811-1818.

[20] M. Lanier, D. Schade, E. Willems, M. Tsuda, S. Spiering, J. Kalisiak, M. Mercola, J. R. Cashman. *J*. Journal of Medicinal Chemistry. 55 (2012) 697-708.

[21] A. P. Contreras, A. M. Cerda, M. A. Tlenkopatchev. *J*. Macromol. Chem. Phys. 203 (2002) 1811.

Chapter 5 Nonlinear Optical Properties of Norbornene derived Polymer Brushes with appended Azobenzene Dyes

5.1 Introduction

When an electric field (*E*) is applied across an organic electro-optic (EO) material the result is a change in the refractive index (Δn). The extent of the change is dependent upon the materials EO coefficient (r_{33}) as described by the equation: $\Delta n = -1/2(n^3 r_{33} E)$ [1]. As of late, EO polymeric materials have been utilized in applications such as telecommunications, THz generators and digital signal processing because of a broad bandwidth and a low drive voltage [2][3][4]. After the development by chemists of organic EO materials capable of attaining an r_{33} (> 100 pm/V) at telecommunications wavelengths, numerous publications have been forthcoming. From a practical perspective, a larger r_{33} is considered favorable, as it will lower the operating voltage (V_π) of any prospective device. This important property may be defined according to; $V_\pi = \lambda d/(2n^3 r_{33} L\Gamma)$, where λ, d, n, L and Γ are the working wavelength, electrode gap, refractive index, interaction length and overlap integral factor, respectively [5].

One of the simplest and most practically amenable EO-polymer approaches for device fabrication is the guest-host, as it is chemically simple and easy to scale. In this approach a high molecular hyperpolarizability chromophore serves as the active guest, this is mixed in intimately with a passive host polymer with a high Tg. When an

optimum chromophore loading is found, the EO response is greatly amplified by the polymer medium. Although, if the chromophore loading is increased beyond a certain threshold, the result is a reduction in the EO effect, because of strong intermolecular electrostatic interactions leading to localized chromophore aggregation. Therefore the limiting factor in host-guest dispersions is the maximum chromophore loading is somewhat low. An alternative approach, which can avoid this limitation is the side chain-type EO polymer [6]. Here a chromophore molecule is modified and attached directly to a passive polymer backbone. Unfortunately, the fragile nature of chromophore molecules towards many chemical transformations makes the direct attachment to monomers prior to polymerization problematic. Post polymerization functionalization therefore is often utilized [7]. However it is often challenging to control the polymer structure precisely by post polymerization functionalization, leading to a high polydispersity, poor solubility and difficulty in controlling the exact chromophore loading. An attractive means of avoiding this is to change the design of the polymer host, thus enabling higher chromophore loading and little aggregation in host-guest systems. In the rational design of an alternative polymer host we must prepare a material with a high chromophore miscibility, good optical transparency, thermal stability, and a high Tg [8].

Polymer brushes with a high density structure [9], a high chromophore miscibility and a well controlled synthetic route make them ideal EO chromophore hosts. A cylindrical or “bottle brush” class of polymer brush, incorporates a long polymer

backbone, which has been densely grafted with many shorter oligomeric side chains. The associated steric repulsion between these side chains is especially large, yielding a greatly extended main chain. Three main approaches have been used in brush synthesis; grafting through, grafting onto and grafting from [10].

In this investigation we have prepared and characterized a selection of poly(norbornene-*exo*-dicarboximide) polymer brushes containing three different substituted azobenzene dyes (methoxy, nitro and cyano) in the side chains with various laoding. In general, we would expect the addition of the azobenzene dye to have numerous beneficial effects on the polymer brush host, such as increasing the Tg, Td and interacting strongly with the FTC chromophore (**C3**) used the guest *via* intermolecular electrostatic forces. The poly(norbornene-*exo*-dicarboximide) backbone was prepared by the ROMP of an NDI monomer using the Grubbs 1st generation initiator [11]. The resulting macro-initiator then underwent ATRP with the substituted azobenzene dye and MMA to prepare the EO polymer brush as our host [12]. The FTC chromophore (**C3**) was prepared according to the established literature procedures [13][14]. This chromophore was mixed with the EO polymer brushes (25 wt%) in cyclopentanone with the concentration being kept constant over all samples.

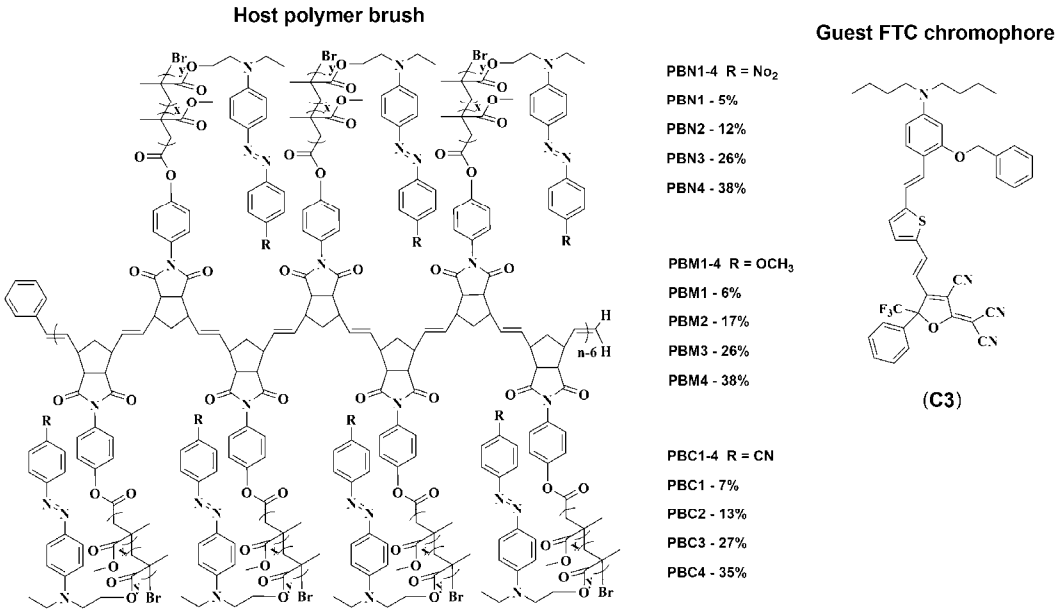

Fig. 5-1 Azobenzene dye containing polymer brush and chromophore (**C3**) structures investigated in this paper. Concentration of four for each substituents nitro, methoxy, cyano azobenzene dye were indicated.

5.2 Experimental details

5.2.1 Materials

Anisole, chloroform ($CHCl_3$), tetrahydrofuran (THF) and methylmethacrylate (MMA) were dried over calcium hydride and distilled. N,N,N',N'',N''-Pentamethyldiethylenetriamine (PMDETA) was obtained from Tokyo Chemical Industry Co and used as received. **G1** was purchased from Sigma Aldrich. Copper (I) bromide was purified according to literature procedure [15]. Unfunctionalized azobenzene chromophore was obtained from Alfa-Asar and used without further purification.

5.2.2 Techniques

Thermogravametric analysis (TGA) and differential scanning calorimetry (DSC) were performed using an SII-TG/DTA 6200 instrument under a nitrogen atmosphere at a heating rate of 5 ^{o}C /min. DSC was performed using a SII-DSC 6220 under a nitrogen atmosphere at a heating rate of 5 ^{o}C /min. The molecular weights (Mw) and polydispersity (PDI) of the polymers were determined by size-exclusion chromatography (SEC) using a Shodex GPC K-804L column on a JASCO LC2000 liquid chromatography system with $CHCl_3$ as the eluent. This system was calibrated using narrow PDI Shodex SM-105 polystyrene standards. UV absorption spectra were recorded using a Shimadzu UV–vis spectrometer 1240.

5.2.3 Synthesis

The NDI monomer (**1**) was prepared according to a modification of literature procedure [16]. Macro-initiator (**2**) synthesis; The NDI monomer (**1**) was dissolved in anhydrous chloroform and stirred for 10 minutes. The initiator (**G1**) was transferred to a separate vessel and also dissolved in anhydrous chloroform. The initiator solution was transferred quickly to the reaction vessel *via* syringe and the polymerization was allowed to proceed at room temperature for 60 minutes. After this period, quenching was achieved by the addition of an excess of ethyl vinyl ether. After stirring for 30 minutes the desired polymer was isolated by precipitation into methanol. Polymer brushes (**3**) synthesis; The macro-initiator (**2**) N, N, N′,N′,N″-Pentamethyldiethylene

triamine (PMDETA), methyl methacrylate (MMA), azobenzene chromophore (Az), and anisole were transferred to a Schlenk tube. The materials were degassed, after which copper(I) bromide was added. The polymerization to yield polymer brushes (**3**) were then carried out at 50 ^{o}C for 4 hours. The crude material was purified by passing through a neutral alumina plug and the obtained solution was precipitated into methanol.

5.2.4 Thin films preparation

The FTC chromophore (C3) was mixed with the host polymer brushes (**3**) at 25 wt% in cyclopentanone and stirred at room temperature for 12 hours. After this dispersion phase, the resulting solution was filtered through a 0.2 μm filter and spin coated onto an indium tin oxide (ITO) glass substrate, to produce thin films. After a short pre-baking (20 min) on a hotplate at 90 ^{o}C and then under vacuum at 85 ^{o}C (2 days) to remove the residual solvent, the measured thickness was 3.2 μm (Surface profiler - DEKTAK3). A thin gold layer (~ 50 nm) was sputtered directly onto the film to act as the electrode. The circular electrode area was a diameter of 5 mm and the r_{33} measurement was performed using the Teng-Man reflection method [17] at 1310 nm.

5.3 Results and discussion

5.3.1 Synthesis and characterization

The NDI monomer (**1**), macro-initiator (**2**) and polymer-brushes (**3**) were prepared according to the **Scheme 5-1**.

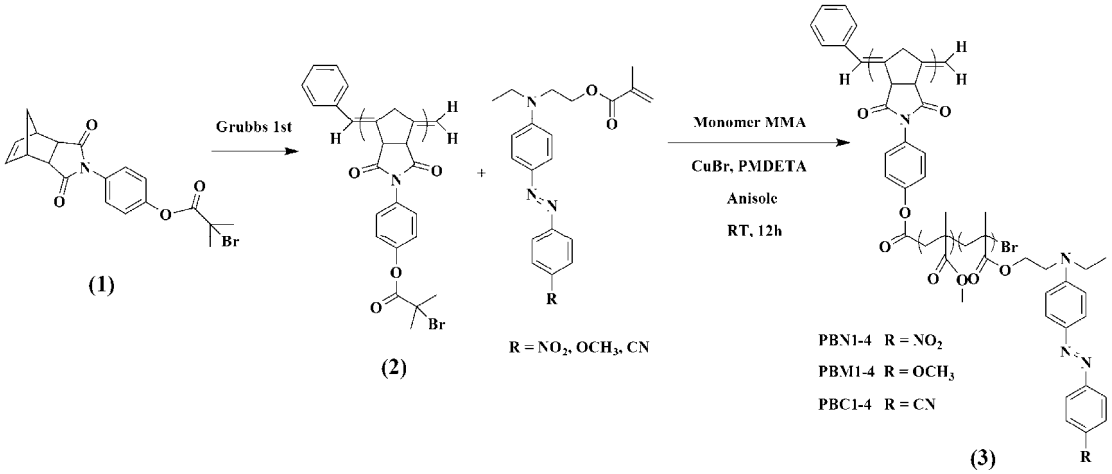

Scheme 5-1 Synthetic route of polymer brush

NDI monomer (**1**) was synthesized *via* an N-phenol-norbornene-*exo*-dicarboximide precursor prepared according to the literature [18]. The hydroxyl group of this compound was transformed using 2-bromoisobutyryl bromide to yield the desired NDI monomer (**1**). This monomer was subsequently polymerized *via* ROMP using the **G1** initiator at room temperature in chloroform for 60 minutes. The living polymerization was quenched by the addition of an excess of ethyl vinyl ether. Macro-initiator (**2**) was obtained by filtration and multiple precipitations from chloroform into methanol. In order to prepare the polymer brushes (**3**), the macro-initiator (**1**), PMDETA, MMA and azobenzene chromophore (Az) were

dissolved in anisole. The addition of a small quantity of CuBr facilitated the ATRP at 50 °C for 4 hours. Polymer-brushes (**3**) had an excellent solubility in a wide range of organic solvents such as THF, DMSO and chloroform. The chemical structure of the macro-initiator (**2**) and polymer-brushes (**3**) were confirmed by ^{1}H-NMR spectroscopy. Twelve polymer brushes were synthesized, four from each of the three different substituents, methoxy, nitro and cyano. Brushes derived from nitro (**PBN1-4**), were prepared with varying concentrations of 5 wt%, 12 wt%, 25 wt%, 38 wt%. Brushes derived from methoxy (**PBM1-4**), were prepared with the four concentrations, 6 wt%, 17 wt%, 25 wt%, 38 wt% and brushes derived from cyano (**PBC1-4**) were prepared with 7 wt%, 13 wt%, 27 wt%, 35 wt%, respectively.

Successful brush preparation in each case was confirmed by the SEC measured Mw always increasing from that of the parent macro-initiator (**2**), 175k to an average for the twelve polymer brushes of around 1 million. Similarly the PDIs also increased as was expected from 1.1 of the macro-initiator (**2**) to approximately 1.4 for the twelve brushes, shown in Table 5-1.

The measured Tg and Td of the macro initiator were 121 ^{o}C and 263 ^{o}C respectively. The Tgs of the brushes exhibited a small increase to on average 125 ^{o}C, while the Tds were elevated to around 300 ^{o}C.

Table 5-1 Physical properties of polymer brushes

	Mn (k) [a]	Mw (k) [a]	Mz (k) [a]	PDI [a]	Tg (^{o}C) [b]	Td (^{o}C) [b]
PBN1	175	219	251	1.24	125.3	307.4

PBN2	164	194	129	1.45	121.1	276.8
PBN3	154	187	124	1.49	103.6	265.4
PBN4	127	142	158	1.11	104.1	259.9
PBM1	179	254	326	1.42	111.2	263.9
PBM2	117	137	156	1.16	118.2	276.1
PBM3	109	153	187	1.40	115.4	286.7
PBM4	97	122	146	1.25	120.3	283.4
PBC1	159	222	306	1.39	110.4	280.9
PBC2	152	177	198	1.47	117.5	287.3
PBC3	103	128	153	1.34	113.1	272.6
PBC4	75	101	128	1.24	110.7	249.7

[a] The molecular weights (Mw) and polydispersity (PDI) of the polymers were determined by size-exclusion chromatography (SEC) using a Shodex GPC K-804L column on a JASCO LC2000 liquid chromatography system with $CHCl_3$ as the eluent. This system was calibrated using a narrow PDI Shodex SM-105 polystyrene standards.

[b] Thermogravametric analysis (TGA) and differential scanning calorimetry (DSC) were performed using an SII-TG/DTA 6200 instrument under a nitrogen atmosphere at a heating rate of 5 °C /min.

The precise content of the azobenzene chromophore (Az) incorporated into the polymer-brushes was evaluated by the absorption spectra, calculated against pure standards of a known concentration, shown in Figure 5-5 ~ Figure 5-7. TGA analysis (10% loss) showed that the polymer brushes (**3**) all did not undergo significant decomposition below 300 °C, therefore poling at temperature ranges of the Tg (~120 ^{o}C) should not have any adverse effect on the host.

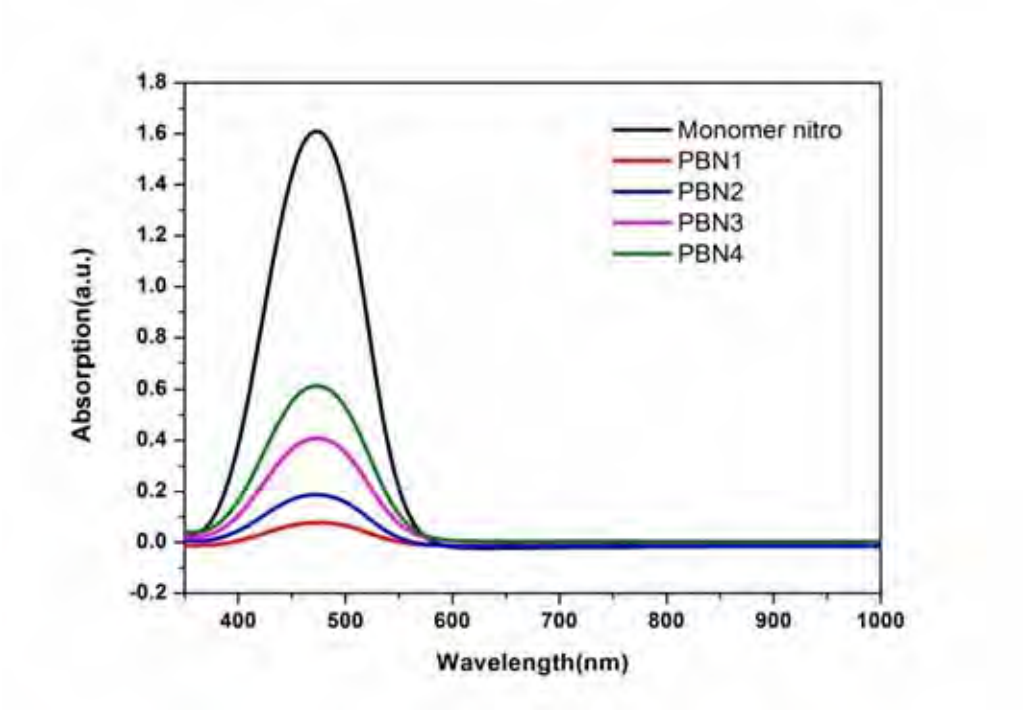

Fig. 5-2 UV absorption of Monomer nitro substituent pigment and polymer brushes PBN1-PBN4, in chloroform solvent.

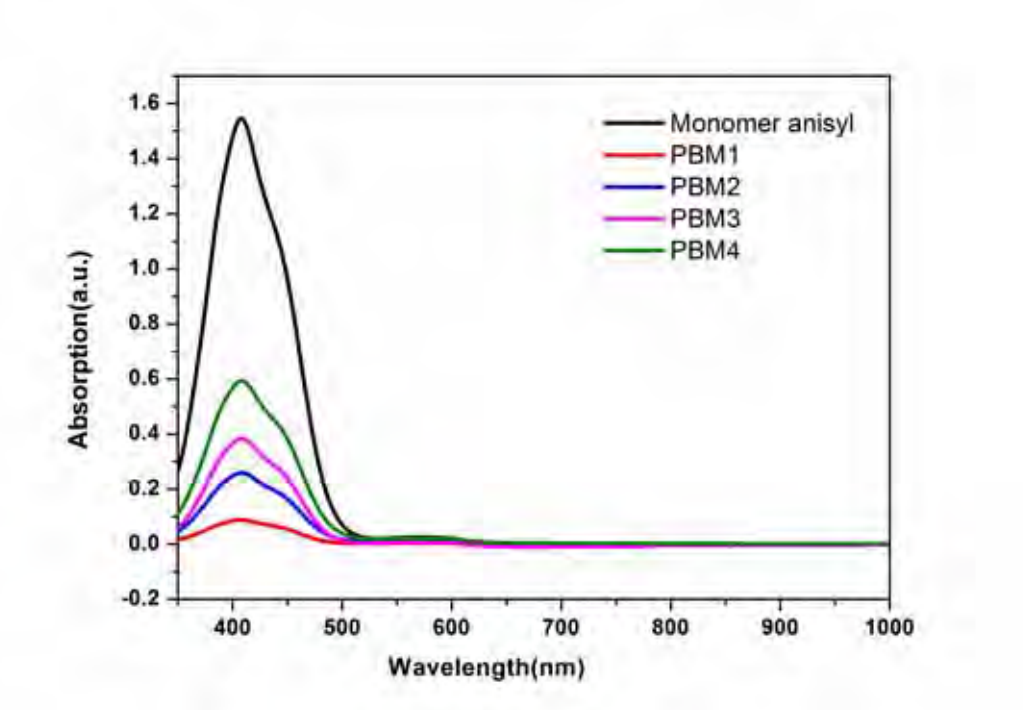

Fig. 5-3 UV absorption of Monomer methoxyl substituent pigment and polymer brushes PBA1-PBA4, in chloroform solvent.

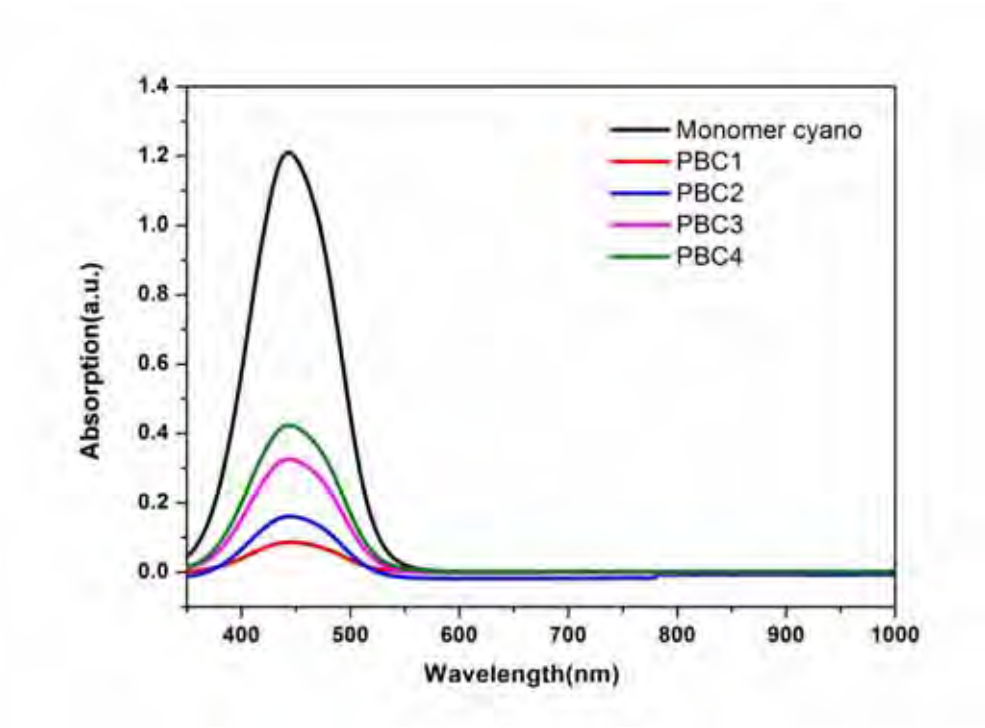

Fig. 5-4 UV absorption of Monomer cyano substituent pigment and polymer brushes PBC1-PBC4, in chloroform solvent.

5.3.2 NLO properties

From previous trial and error experiments in our research group, we have found that the optimum FTC chromophore (C3) loading density in a simple PMMA host is approximately 25 wt%. This can also be expressed as approximately 10^{20} (molecules / cm^3). Therefore the polymer-brushes (**3**) were also evaluated at this optimized concentration. After preparing thin films and devices, contact poling was utilized to evaluate the EO performance. An electric field of 100-130 V/μm was applied across the top and bottom of the device at an elevated temperature, near to that of the brushes Tg. The circular electrode area was a diameter of 5 mm and the r_{33} measurement was performed using the Teng-Man reflection method at 1310 nm with a modulation

frequency of 1000 Hz.

Using TGA, we have established that chromophore (C3) decomposition under nitrogen occurs at temperatures above 220 ^{o}C. The $\boldsymbol{\lambda_{max}}$ of the chromophore was measured in film at 776 nm. Transmission spectra were recorded for the twelve polymer brushes with 25% FTC chromophore (C3). The azobenzene moiety exhibits a peak at 408 nm, whilst the guest FTC chromophore (C3) displayed a peak at 803 nm. As can be seen in the spectra in **Figure 5-8 ~ Figure5-10**, between the wavelengths of 1200 to 2000 nm there is almost 100% transmittance, which makes the materials ideal candidates for polymer waveguides. For the polymer brushes containing nitro (**PBN1-4**) and cyano (**PBM1-4**) a similar property was observed with near 100% transmittance in the region of interest. Host nitro azobenzene pigment λ_{max} in **PBN1** and **PBN4** are all 478 nm, λ_{max} of guest chromophore C in **PBN1** is 794 nm, and λ_{max} of guest chromophore in **PBN4** is 851 nm. Host methoxyl azobenzene pigment λ_{max} in **PBM1** and **PBM4** are all 409 nm, λ_{max} of guest chromophore C in **PBM1** is 798 nm, and λ_{max} of guest chromophore in **PBM4** is 836 nm. Host cyano azobenzene pigment λ_{max} in **PBC1** and **PBC4** are all 447 nm, λ_{max} of guest chromophore C in **PBC1** is 792 nm, and λ_{max} of guest chromophore in **PBC4** is 818 nm. Introduce azobenzene chromophore cyano have the smallest wavelength move.

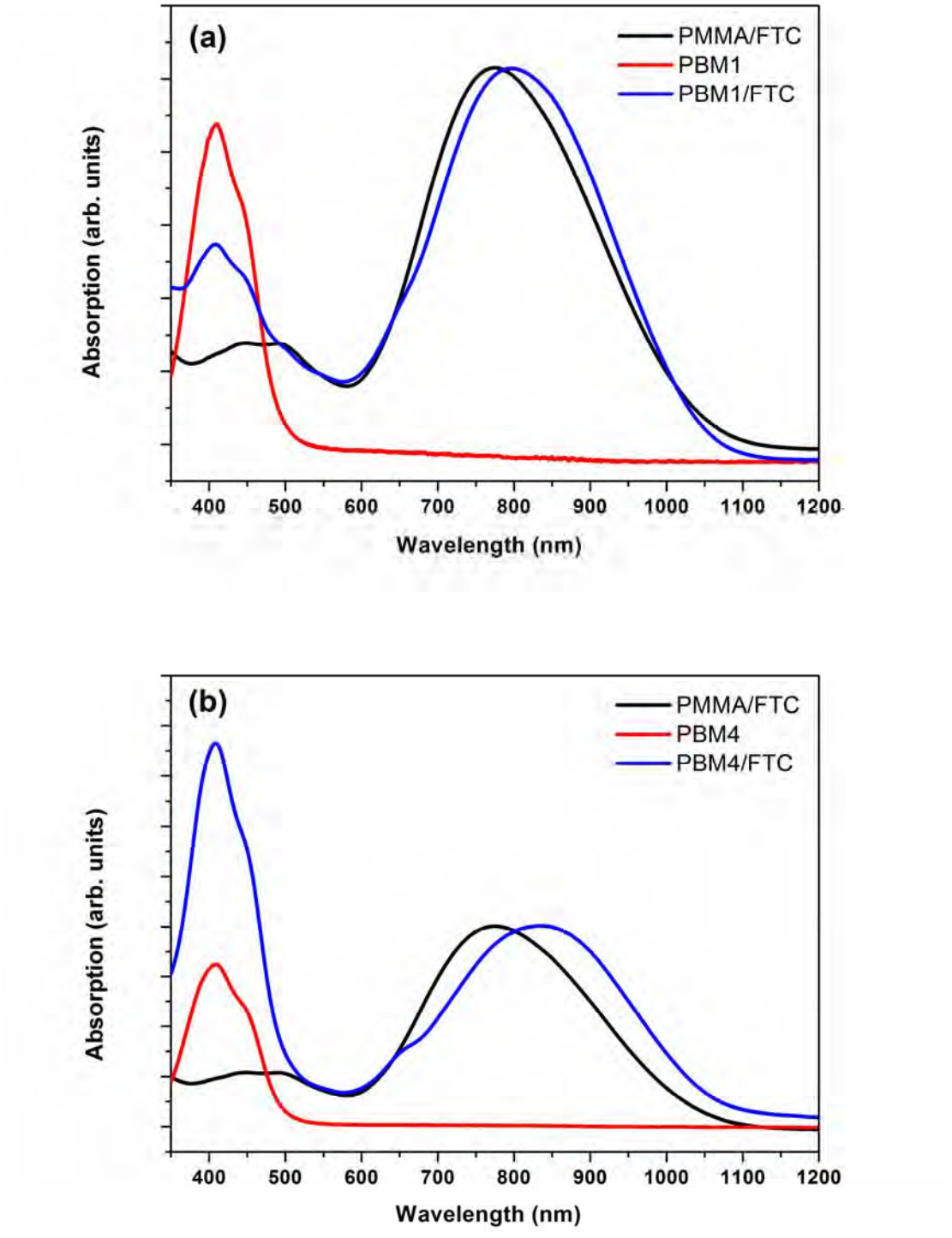

Fig. 5-5 UV absorption spectra of thin films consisting of the polymer-brushes (**PBM1** and **PBM4**) mixed with the FTC chromophore (C3) at a concentration of 25 wt%.

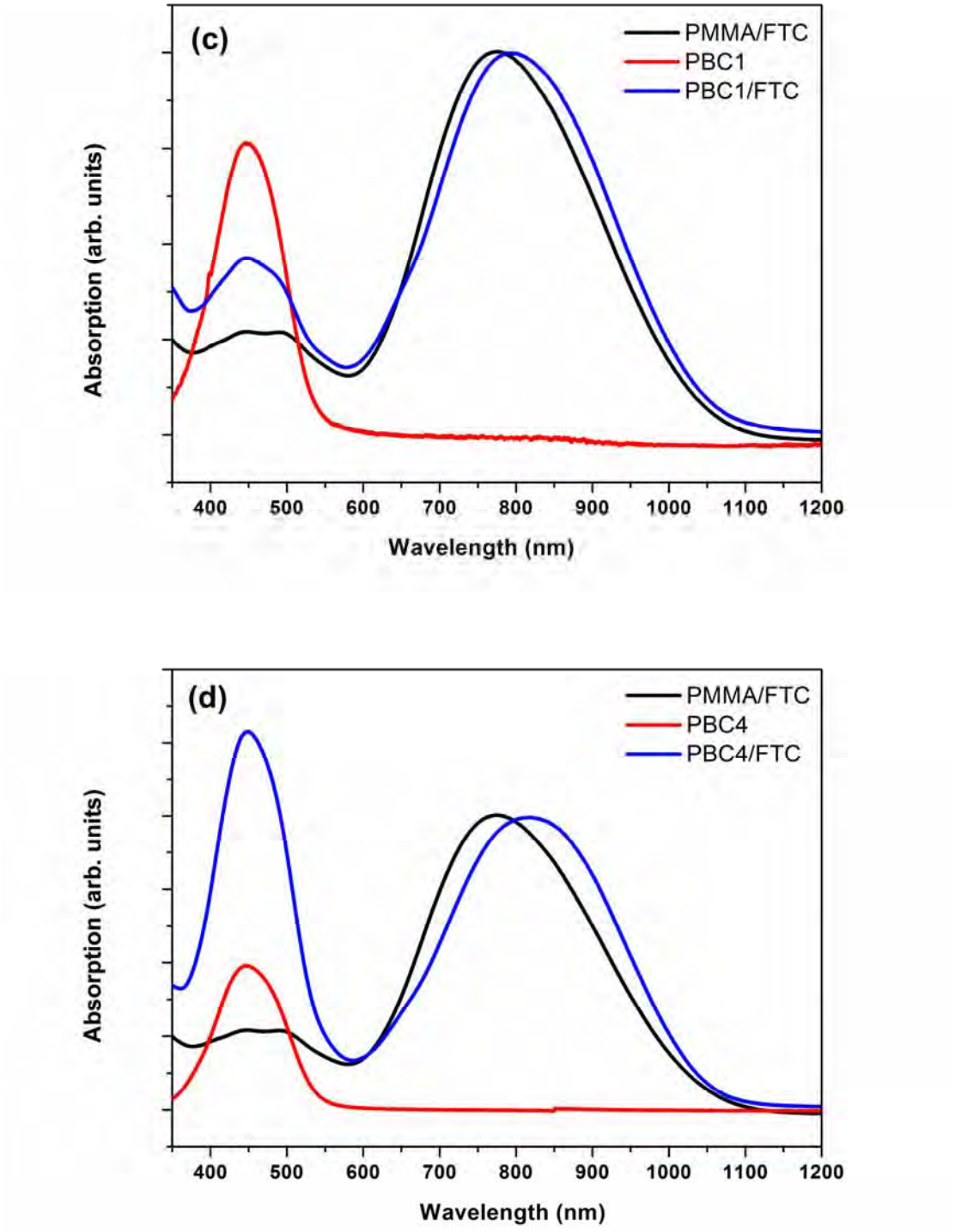

Fig. 5-6 UV absorption spectra of thin films consisting of the polymer-brushes (**PBC1** and **PBC4**) mixed with the FTC chromophore (C3) at a concentration of 25 wt%.

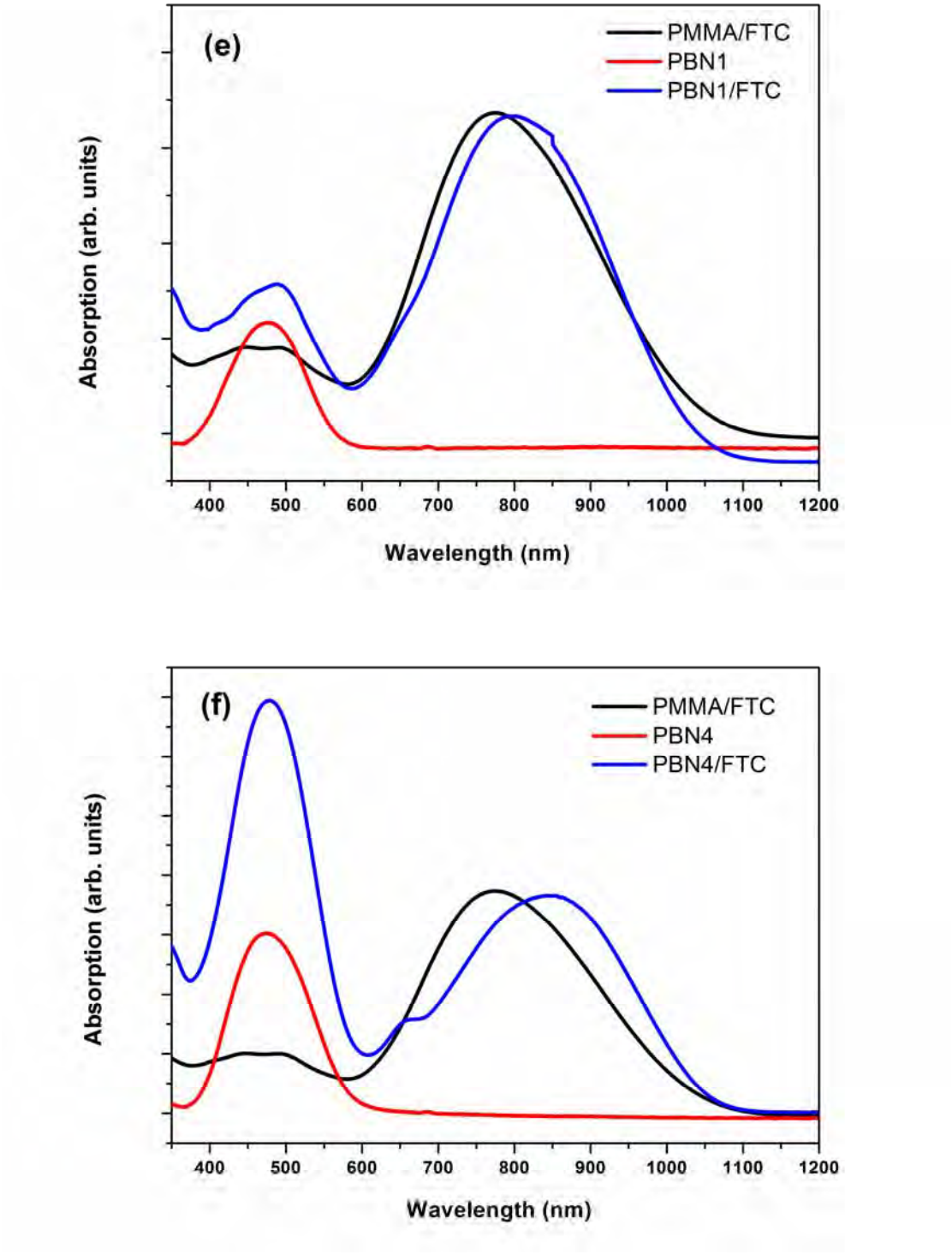

Fig. 5-7 UV absorption spectra of thin films consisting of the polymer-brushes (**PBN1** and **PBN4**) mixed with the FTC chromophore (C3) at a concentration of 25 wt%.

The refractive index against the azobenzene chromophore (**Ac**) concentration at 1310 nm and 1550 nm can be inspected in **Figure 5-11 ~ Figure 5-13**. As can be observed at both high and low concentrations the brushes with cyano substituents (**PBC1-4**) show the highest RI at both wavelengths, 1.6232 to 1.6789 at 1310 nm and 1.6067 to 1.6525 at 1550 nm. Brushes containing methoxy substituents (**PBM1-4**) have lower RIs than cyano (**PBC1-4**), but higher than nitro (**PBN1-4**). The methoxy brushes exhibited RIs from 1.5885 to 1.6651 at 1310 nm and 1.5797 to 1.6422 at 1550 nm respectively. Finally the brushes with nitro substituents on the azobenzene moiety had the lowest RIs, at both wavelengths from, 1.5525 to 1.6537 at 1310 nm and 1.5364 to 1.6258 at 1550 nm respectively. Therefore regardless of substituent we are able to manipulate the RI by increasing the azobenzene moiety (Az) content, which in turn increases the RI. Such a fine control may prove useful in the development of polymer / sol-gel waveguides.

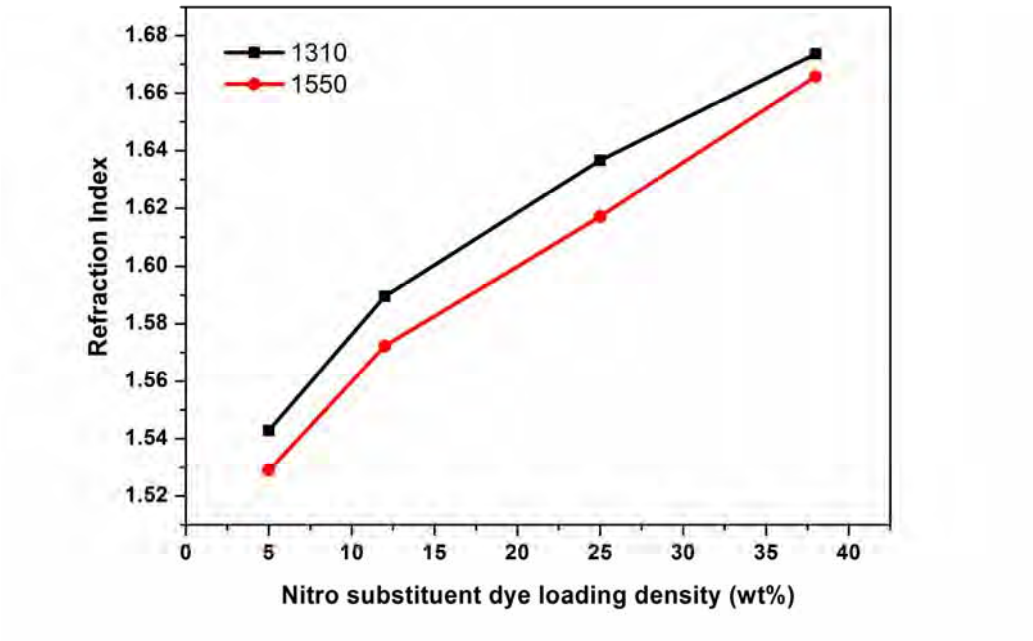

Fig. 5-8 A plot of the measured refractive index against the azobenzene moiety (Az) concentration at 1310 nm (a) and 1550 nm (b).

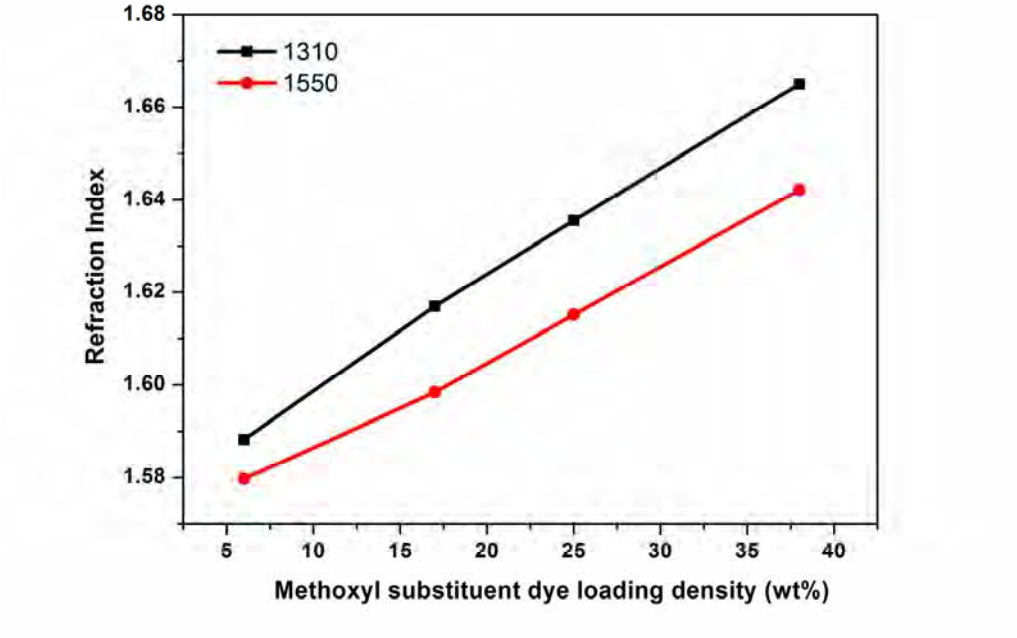

Fig. 5-9 A plot of the measured refractive index against the azobenzene moiety (Az) concentration at 1310 nm (a) and 1550 nm (b)

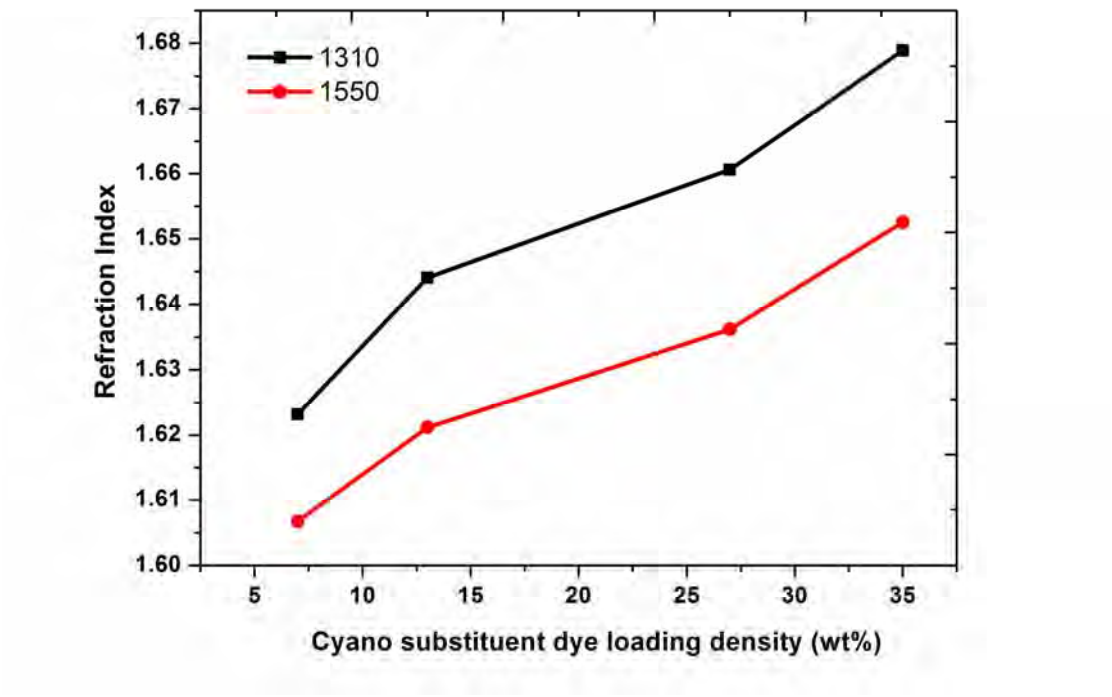

Fig. 5-10 A plot of the measured refractive index against the azobenzene moiety (Az) concentration at 1310 nm (a) and 1550 nm (b).

The relative r_{33} is evaluated with respect to the azobenzene moiety (**Az**) concentration as well as the substituent affect in **Figure 5-14 ~ Figure 5-16**. In all the EO measurements, FTC chromophore (C3) was mixed into the polymer brushes at 25 wt% as described earlier. For the brushes containing cyano substituents (**PBC1-4**) all display r_{33} lower than both the methoxy and nitro. In this substituent the r_{33} was measured at 54 pm/V at 7%, this then reaches a peak value at 63 pm/V at a concentration of 13%. The value then begins to decrease to 57 pm/V as the concentration is increased further to 27% and at 35% the r_{33} is reduced to 49 pm/V. In the case of the methoxy substituted polymer brushes (**PBM1-4**), we observed an initial r_{33} of 77 pm/V at 6%, this then increased to 84 pm/V at 17% and finally peaked

at 95 pm/V at 25 wt%. After this peak, a further increase in the azobenzene (**Az**) % to 38 reduced the r_{33} to 78 pm/V. Finally, for the nitro substituted polymer brushes (**PBN1-4**), the initial % of 5 generated the highest r_{33} (83 pm/V) at this low azobenzene concnetration of all the brush systems. The r_{33} then increased to 87 pm/V at 12%, however this upwards trend did not continue as the % was raised to 25. In fact the r_{33} was reduced to 77 pm/V. Furthermore increasing the % to 38, reduced the r_{33} to 68 pm/V.

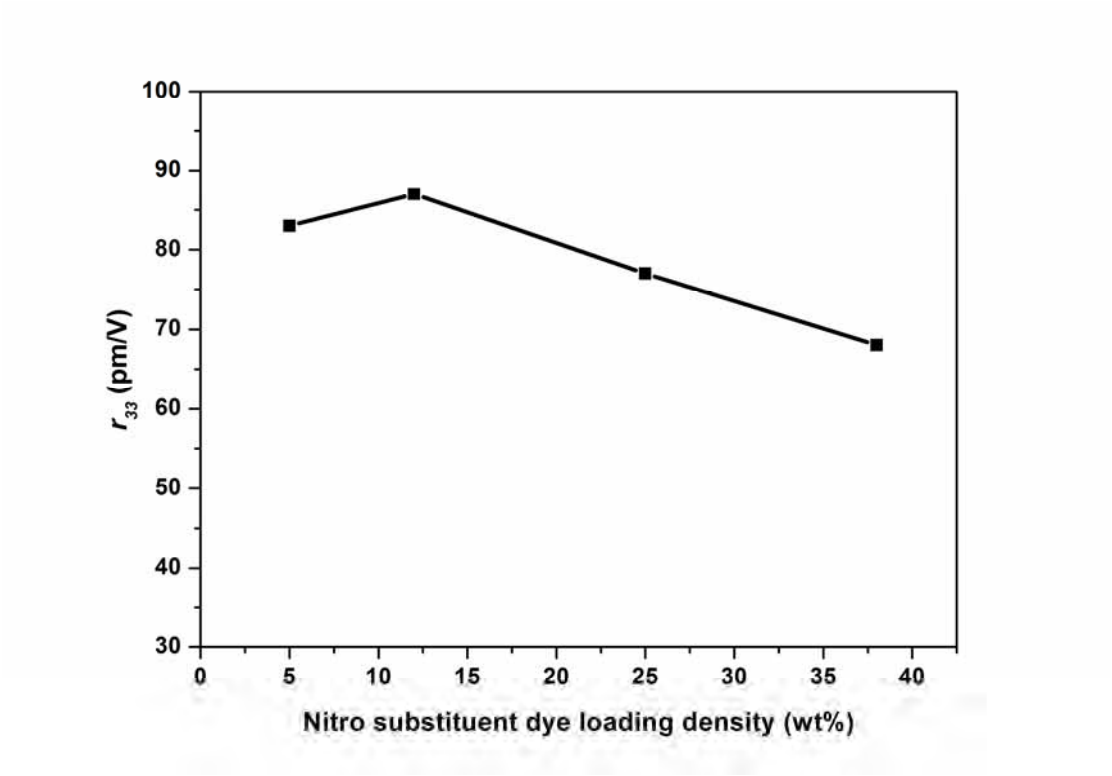

Fig. 5-11 The r_{33} of the polymer-brushes and chromophore (C3) combinations against the % of the azobenzene moiety as well as the effect of the substituent.

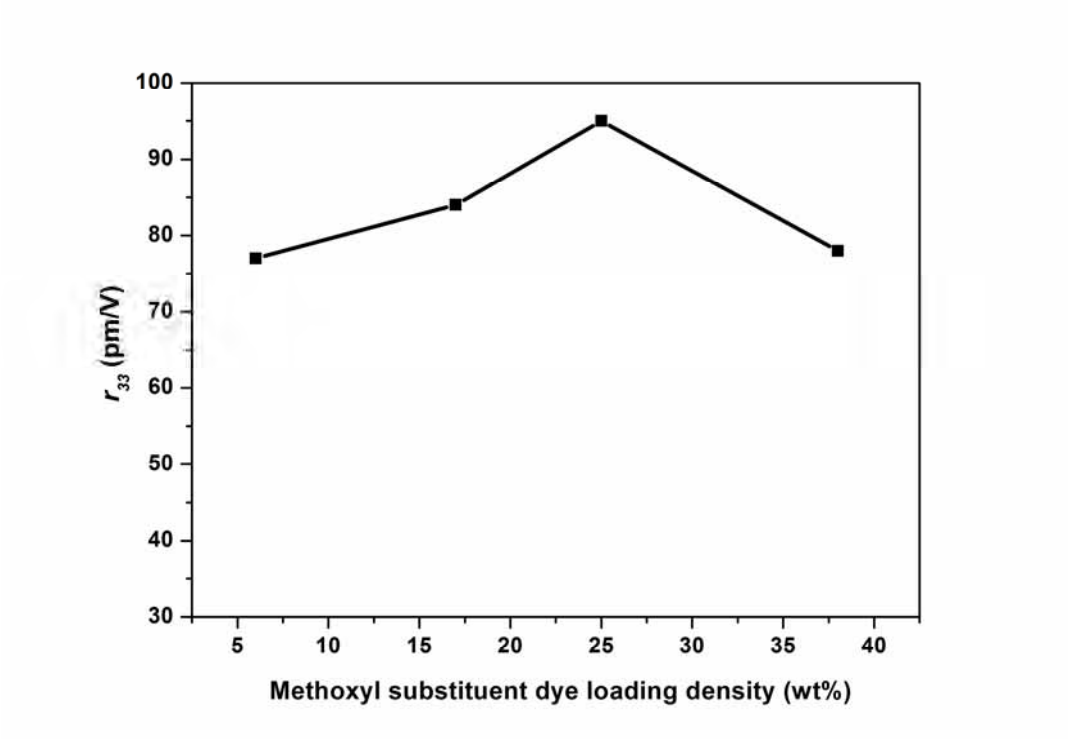

Fig. 5-12 The r_{33} of the polymer-brushes and chromophore (C3) combinations against the % of the azobenzene moiety as well as the effect of the substituent.

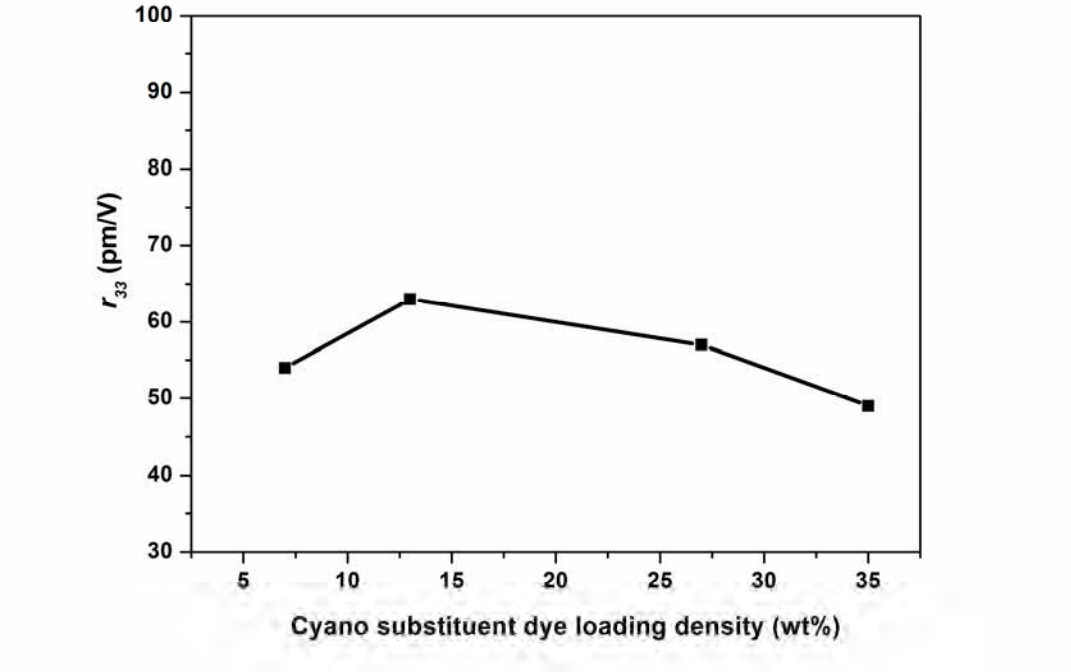

Fig. 5-13 The r_{33} of the polymer-brushes and chromophore (C3) combinations against the % of the azobenzene moiety as well as the effect of the substituent.

5.4 Conclusions

In this manuscript we have prepared a selection of twelve polymer brushes containing three different pendent azobenzene moieties. We have varied the substituent of this moiety to include three different groups, methoxy, cyano and nitro. Also we have manipulated the concentration of this azobenzene unit in order to maximize the EO response. The refractive index of the materials was measured at both 1310 and 1550 nm with a view to their utilization in current EO waveguide applications.

We have found that an optimum polymer brush system contained a methoxy substituent on the azobenzene moiety and furthermore that the r_{33} was maximized by incorporation of 25% of this moiety into the brush. In this ideal system a high r_{33} of 95 pm/V was achieved.

5.5 Reference

[1] J. Luo, S. Huang, Z. Shi, B. M. Polishak, X.-H. Zhou, A. K-Y. Jen. *J*. Chem. Mater. 23 (2010) 544.

[2] Y. Enami, C. T. Derose, D. Mathine, C. Loychik, C. Greenlee, N. Peyghambarian. *J*. Nature Photonics. 25 (2007) 180-185.

[3] F. Qiu, T. Narusawa. *J*. Jpn. J. Appl. Phys. 49 (2010) 092503-1-092503-3.

[4] F. Qiu, A. M. Spring, F. Yu, S. Yokoyama. *J*. Applied Physic Letters. 102 (2013) 051106/1-051106/3.

[5] X. Piao, S. Inoue, S. Yokoyama. *J*. Thin Solid Films. 518 (2009) 481-484.

[6] S. Allen: Photochemistry and Photophysics of Polymer Materials (Wiley, NewYork, 2010) p.148.

[7] H. Denis, N. Seuyep, A. G. Luinstraa, T. Patrick. *J*. Polym. Chem.. 4 (2013) 2724.

[8] Y. Mori, K. Nakaya, X. Piao, K. Yamamoto, A. Otomo, S. Yokoyama. *J*. Journal of Polymer Science, Part A: Polymer Chemistry. 50 (2012) 1254-1260.

[9] S. S. Sheiko, B. S. Sumerlin, K. Matyjaszewski. *J*. Prog. Polym. Sci. 33 (2008) 759.

[10] M. Zhang, A. H. E. Muller. *J*. Journal of Polymer Science, Part A: Polymer Chemistry. 43 (2005) 3461.

[11] F. Yu, A. M. Spring, L. Li, F. Qiu, K. Yamamoto, D. Maeda, M. Ozawa, K. Odoi. *J*. Journal of Polymer Science. 51 (2013) 1278-1284.

[12] W. Zhang, Y. Li, L. Liu, Q. Sun, X. Shuai, W. Zhu. Y. Chen. *J*. Biomacromolecules. 11 (2010) 1331.

[13] X. Piao, X. Zhang, S. Inoue, S. Yokoyama, I. Aoki, H. Miki, A. Otomo, H. Tazawa. *J*. Org. Electron. 12 (2011) 1093.

[14] X. Zhang, I. Aoki, X. Piao, S. Inoue, H. Tazawa, S. Yokoyama, A. Otomo. *J*. Tetrahedron Letters. 51 (2010) 5873.

[15] G. Cheng, A. Boker, M. Zhang, G. Krausch, and A.E. Muller. *J*. Macromolecules. 34 (2001) 6883.

[16] M. Lanier, D. Schade, E. Willems, M. Tsuda, S. Spiering, J. Kalisiak, M. Mercola, J. R. Cashman. *J*. Med. Chem. 55 (2011) 697.

[17] C. C. Teng, H. T. Man. *J*. Appl. Phys. Lett. 56 (1990) 1734.

[18] A. P. Contreras, A. M. Cerda, M. A. Tlenkopatchev. *J*. Macromol. Chem. Phys. 203 (2002) 1811.

Chapter 6 General Conclusions

6.1 Summary of the thesis

Organic electro-optic (EO) materials have been widely applied in ultra-fast communication, EO devices and polymer technologies. It is challengeable to develop EO material in synthesizing high β chromophore, exploiting particular polymer matrix, raising the chromophore loading density and at the same time maintaining the high poling efficiency. Synthesis polymer matrix as the main element strategy in organic EO materials seems urgent on the high β chromophore existence. In this thesis, the second to the fifth chapter, various EO polymer matrix attached dyes in the backbone were made through different synthesis routes and applied in binary chromophore EO material systems. The major conclusions of the thesis are summarized as below:

In **Chapter 2**, free radical polymerization was utilized in preparing polymers containing dye in the side chain, then these polymers were used in host-guest system to form binary chromophore EO materials. After synthesis these side chain polymer, optimization synthesis route was taken, and RAFT was applied during synthesizing to control the PDI and molecular weight. Nine azobenzene side chain polymers were prepared through free radical polymerization (FRP) which containing three different pendent azobenzene moieties, nitro, cyano, methoxy. The chemical structures of the nine azobenzene derivatives were confirmed by ^{1}H NMR, UV absorption and the GPC

traces. These polymers displayed a large molecular weight Mw 20 k, PDI 1.3 ~ 1.7, and glass transition temperature of nearly 110 ^{o}C. The macroscopic EO coefficient of these polymer were measured using Teng-Man measurement at 1310nm. We have found that an optimum PMMA-co-CABPMA$_5$ contained a 5 mol% cyano substituent on the azobenzene moiety and furthermore that the r_{33} was maximized by incorporation of 15 wt% guest chromophore **C1** into the polymer PMMA-co-CABPM$_5$. In this ideal system a high r_{33} of 63 pm/V was achieved.

Three different substituent group side-chain azobenzene polymers, including nitro, cyano, methoxyl substituent, were all optimized through RAFT. Size-exclusion chromatography (SEC) trace shows Mw 14k, PDI under 1.3 with THF as the eluent. From the polymer itself have been optimized on controlling the molecular weight and PDI, but the physical properties didn't change much through this way, Tg and Td are 110 ^{o}C and 260 ^{o}C similar as the side chain polymer getting from FRP. Cyano substituent side chain polymer making from RAFT accomplished with 15 wt% **C1** got the best result, the maximum r_{33} is 120 pm/V, final r_{33} is 65 pm/V.

In **Chapter 3**, Azobenzene polymer brushes PB-A, PB-B, PB-C, PB-D were prepared by atom transfer radical polymerization (ATRP) grafting MMA and disperse red 1 methacrylate (DR1-MA) from a macro initiator Poly(2-(2-bromoisobutyryloxy)ethyl methacrylate) (PBIEM$_{450}$) which bears bromoisobutyryl species. The reactivity ratios of the two monomers MMA and DR1-MA were determined to be close during the reaction, and monomer pigment

DR1-MA without decomposition. polymer brush PB-C with 15 wt% **C4** got the best result, the maximum r_{33} is 77 pm/V, final r_{33} is 58 pm/V. This result may be important for developing various well-controlled chromophore containing polymer brushes and to prepare EO polymer matrix objects.

In **Chapter 4**, to enhance the polymer brush physical properties, a special macro initiators norbornene dicarboximide (NDI) will be selected and synthesized. Then use this macro initiators to prepare polymer brush. A norbornene-dicarboximide derived polymer brush (**P3**) was prepared from a bi-functional monomer (**1**) capable of both ROMP and ATRP. Initially a norbornene-dicarboximide macro-initiator was synthesized by the ring opening metathesis polymerization (ROMP) of NDI monomer (**1**) using **G1** in chloroform at room temperature. ATRP was then used to grow the cylindrical polymer brush (**P3**), whilst also incorporating a DR1-MA associative chromophore for enhanced bi-chromophore miscibility. This polymer brush (**P3**) was used as an EO-host for our high hyperpolarizability chromophore (**C2**, **C3** and **C4**) guests. Measurement of the r_{33} using in-situ poling *via* the Teng-Man reflection technique showed that polymer brush (**P3**) and chromophore **C4** exhibited a maximum r_{33} of 94 pm/V as compared to 74 pm/V for the PMMA standard. The poling efficiency of this optimal system was 1.37 as compared to 0.70 for PMMA. This is a consequence of the optimized chromophore structure (**C4**) incorporating as strongly donating tert-butyldiphenylsilane moiety which enhances β and an excellent compatibility with our polymer brush (**P3**). Such sophisticated polymer brush / bi-chromophore host-guest

systems are a recent development in the field of EO. Here we present the preliminary investigations of this effective system, further optimization may lead to a greatly enhanced r_{33} after a careful tuning of the brush characteristics.

In **Chapter 5**, to investigate the application of the polymer brush using in EO materials, a serious polymer brush were prepared and employed in EO materials. In this chapter we have prepared a selection of twelve polymer brushes containing three different pendent azobenzene moieties. We have varied the substituent of this moiety to include three different groups, methoxy, cyano and nitro. Also we have manipulated the concentration of this azobenzene unit in order to maximize the EO response. The refractive index of the materials was measured at both 1310 and 1550 nm with a view to their utilization in current EO waveguide applications.

We have found that an optimum polymer brush system contained a methoxy substituent on the azobenzene moiety and furthermore that the r_{33} was maximized by incorporation of 25% of this moiety into the brush. In this ideal system a high r_{33} of 95 pm/V was achieved.

6.2 Future prospects

Binary chromophore systems represent a new and very promising class of organic second-order nonlinear optical (NLO) materials, where favorable intermolecular electrostatic interactions lead to significantly enhanced EO coefficients and other favorable physical properties such as low optical loss and high stability.

Polymer matrix using in these binary chromophore system always have dyes in their own structure and exhibit high glass transition temperature (Tg), the thermal and chemical stability and stability of longer-time polarization.

Let the materials meet the requirements of the device, the electro-optic polymer materials for future research work, will be improved or enhanced from the following aspects:

1. Making use of high β value chromophores, react with polymer, in order to achieve large macroscopic nonlinear optical effects, at the same time should enhance the thermal and chemical stability and lower the optical loss of the system.

2. Design and synthesis of polymers with comprehensive performance, and compatible with the chromophore. To ensure the considerable EO activity and the stability of longer-time polarization.

3. Strengthen the study of polymer structure and property, find out the model or equation so as to get bigger EO effect, provide a theoretical foundation for optimization design.

Appendices

FTC Chromophores list

	Mw (g/mol)	mp (°C) [a]	λ_{max} (nm) [b]	λ_{max} (nm) [c]	β (10^{-30}esu) [d]
Chromophore 1	606	191	814	711	2073
Chromophore 2	638	204	780	698	1828
Chromophore 3	744	196	823	731	2068
Chromophore 4	893	199	839	736	2287

[a] Thermogravametric analysis (TGA) and differential scanning calorimetry (DSC) were performed using an SII-TG/DTA 6200 instrument under a nitrogen atmosphere at a heating rate of 5 °C/min.

[b] UV absorption spectra were recorded using a Shimadzu UV–vis spectrometer 1240, in chloroform.

[b] UV absorption spectra were recorded using a Shimadzu UV–vis spectrometer 1240, in dioxane.

[d] β were measured at 1.91 nm.

Chromophore 1

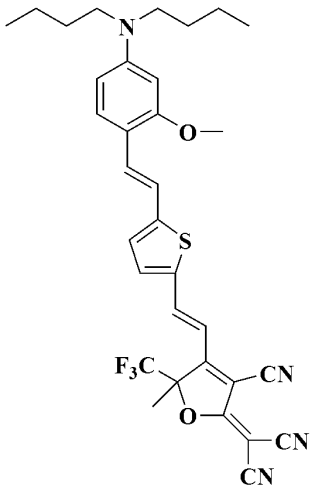

Chromophore 2

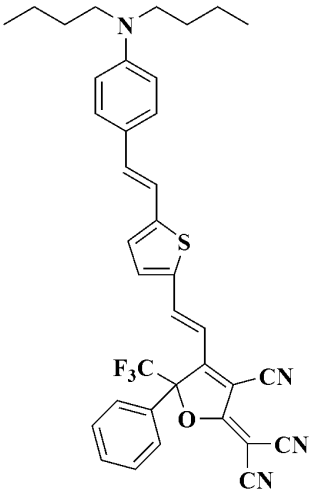

Chromophore 3

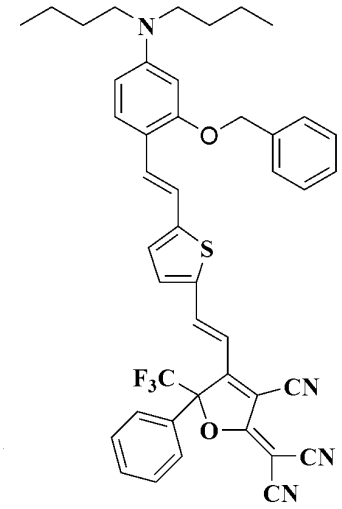

Chromophore 4

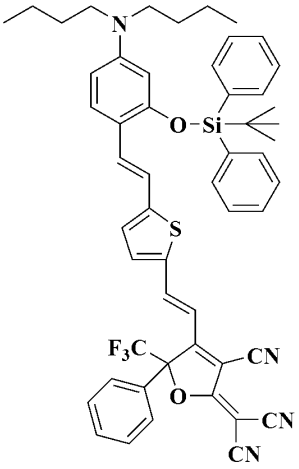

Publication Lists

1. Yue Jia, Andrew M. Spring, Feng Yu, Kazuhiro Yamamoto, Isao Aoki, Akira Otomo and Shiyoshi Yokoyama. "A Norbornene Polymer Brush for Electro-Optic Applications". Thin Solid Films. (Accept)

2. Yue Jia, Andrew M. Spring, Feng Qiu, Feng Yu, Kazuhiro Yamamoto, Isao Aoki, Akira Otomo and Shiyoshi Yokoyama. "Electro-optic Properties of Norbornene Derived Brush-type Polymers with Appended Azobenzene Dyes as Hosts". Japanese Journal of Applied Physics. (Accept)

3. Yue Jia and Shiyoshi Yokoyama. "The Synthesis and Characterization of Electro-Optic Material Based on Novel Polymer Brush", The 13th Cross Straits Symposium on Materials, Energy and Environmental Engineering (CSS13), Fukuoka, Japan, 2011/11

Presentation List

1. Yue Jia, Andrew M. Spring, Feng Yu, Kazuhiro Yamamoto and Shiyoshi Yokoyama. "Nonlinear Optical Properties of Norbornene Polymer Brush containing Azobenzene Chromophore", Seventh Internaional Conference on Molecular Electronics and Bioelectronics, Fukuoka, Japan, 2013/03.

2. Yue Jia, Andrew M. Spring, Feng Yu, Kazuhiro Yamamoto and Shiyoshi Yokoyama. "A Norbornene Polymer Brush for Electro-Optic Applications", The 10th International Conference on Nano-Molecular Electronics, Awaji, Japan, 2012/12.

3. Yue Jia and Shiyoshi Yokoyama. "Optimize Azobenzene Side-Chain Electro-Optic Polymer Host via RAFT(Reversible Addition-Fragmentation Chain Transfer Polymerization)", The 9th International Symposium on Novel Carbon Resource Sciences, Fukuoka, Japan, 2012/12.

4. Yue Jia and Shiyoshi Yokoyama. "Enhanced Electro-Optic Properties of Binary Chromophore System Using Novel Polymer Brush as Host", The 61th SPSJ Annual Meeting, Yokohama, Japan, 2012/05

5. Yue Jia and Shiyoshi Yokoyama. "The Synthesis and Characterization of Electro-Optic Material Based on Novel Polymer Brush", The 13th Cross Straits Symposium on Materials, Energy and Environmental Engineering (CSS13), Fukuoka, Japan, 2011/11

6. Yue Jia and Shiyoshi Yokoyama. "Synthesis of azobenzene sidechain polymer and application in binary chromophore EO materials", The Seventh International Symposium on Novel Carbon Resource Sciences: Green Materials for Sustainable Society, Seoul, South Korea, 2011/06

Acknowledgements

First and foremost, I would like to express my deepest appreciation to my supervisor, Professor Shiyoshi Yokoyama of Institute for Materials Chemistry and Engineering, Kyushu University, for his superb guidance and constant encouragement throughout the present work. My sincerely appreciation also to Assistance Professor Kazuhiro Yamamoto, for his precious comments and suggestions on the thesis. The great thanks also belong to Keiko James, without her help and encouragement this thesis cannot be finished. My gratitude is also to Dr. Andrew M. Spring, Dr. Feng Qiu and Dr. Feng Yu for their generosity, beneficial discussions and gracious advice. I would like to thank to secretary Ms. Yoko Shingai for her patient and careful assistance. I wish to express my thanks to Mr. Yuichi Mori, Mr. Akinari Nakaya, Keisuke Koyama and all other contemporaneity graduated students in Yokoyama Laboratory for their kind help and generous assistance. My thanks also to Mr. Arata Miki, Ms. Junko Yamamoto, Mr. Hiroki Miura, Mr. Naoyuki Hayashi, and all other students in Yokoyama laboratory for their generous help, useful advice and friendship.

I would like to express my gratitude to Professor Yongming Chen and research members in Institute of Chemistry Chinese Academy of Sciences, for their continuous support and encouragement.

I gratefully acknowledge Financial support was provided by the Global COE program, Novel Carbon Resource Sciences (NCRS) Foundation, Kyushu University and Mitsubishi UFJ foundation Scholarship for the award of Doctoral Fellowship.

Finally, my sincerely thanks also to family, for their love, faith and encouragement.

September, 2013